Aus dem Institut für Transfusionsmedizin und Immunologie
der Medizinischen Fakultät Mannheim
(Direktor: Prof. Dr. med. Harald Klüter)

Epigenetic regulation of S100A9 and S100A12 expression in monocyte-macrophage system in hyperglycemic conditions

Inauguraldissertation
zur Erlangung des Doctor scientiarum humanarum (Dr. sc. Hum.)
der
Medizinischen Fakultät Mannheim
der Ruprecht-Karls-Universität
zu
Heidelberg

vorgelegt von
Dieuwertje Marije Mossel

aus
Groningen, NL
2019

Dekan: Herr Prof. Dr. med. Sergij Goerdt
Referentin: Frau Prof. Dr. rer. nat. Julia Kzhyshkowska

TABLE OF CONTENTS

ABBREVIATIONS

2-NBDG - 2-(N-(7-Nitrobenz-2-oxa-1,3-diazol-4-yl)Amino)-2-Deoxyglucose
AGM - aorta-gonads-mesopnephros
AKT- Protein Kinase B
ALOX15- Arachidonate 15-lipoxygenase
ANOVA - Analysis of variance
AP1 - Activated protein-1
APS - Ammonium persulfate
ARRDC4 - Arrestin Domain Containing
BHQ1 - Black Hole Quencher-1
BMDM - Bone-marrow-derived macrophage
BMI – Body mass index
BSA - Bovine serum albumine
C2H2 – Zinc finger-SET histone methyltransferase
CBP - CREB-binding protein
CCL - C-C Motif Chemokine Ligand
CD – Cluster of differentiation
CGI - CG-islands CGI
ChIP – Chromatin immunoprecipitation
CNS - Central nervous system
CO2 - Carbon dioxide
COPD - Chronic obstructive pulmonary disease
COX – Cyclooxygenase
CSF1/M-CSF - Colony stimulating factor
CVD – Cardiovascular disease
DAMP - Damage-associated molecular patterns
DAPI - 4′,6-diamidino-2-phenylindole
DMSO - Dimethylsulfoxide
DNA – Deoxyribonucleic acid
DNMT – DNA methylase
dNTP - Deoxynucleotide
EDTA - Ethylenediaminetetraacetic acid
ELISA - Enzyme-Linked Immuno Sorbent Assay
ENCODE - Encyclopedia of DNA Coding Elements
ER – Endoplasmatic reticulum
ERK - Extracellular-signal-regulated kinase
FACS - Fluorescence-activated cell sorting
FAM - Fluorescein amidite
FCS - Fetal bovine serum
FFA – Free fatty acid
FG – Fasting glucose
FPN1 - Solute carrier family 40 protein
Fru-2,6-P2 - Fructose-2,6-biphosphate
GLO1 - Glyoxalase I
GLUT - Glucose transporter
GR - galactose receptor
GSK – Glycogen synthase kinase
H2O – Hydrogen

H3 – Histone 3
HAT – Histone acetyltransferase
HbA1c - Hemoglobine A 1c
HDAC – Histone deacetylase
HDL - High-density-lipoproteïne
HDM – Histone demethylases
hESCs - Human embryonic stem cells
HG – Hyperglycemia
HIF - Hypoxia-inducible factor
HLA - Human leukocyte antigens
HMGB1 - High mobility group box 1
HMT - Histone methyltransferases
HO-1 - Heme oxygenase-1
HSCs - Hematopoietic cells
IDH - Isocitrate dehydrogenase
IFN – Interferon
IFNAR – Interferon-α/β receptor
IKK - IκB kinase
IL – Interleukin
iPSCs - Induced pluripotent stem cells
IR – Insulin resistance
IRF - Interferon regulatory factors
JMJD - Jumonji domain-containing
KEGG - Kyoto Encyclopedia of Genes and Genomes
KLF - Krüppel-like factor 4
LDL - Low-density lipoprotein
LDTFs - lineage-determining factors
LOX-1 – Lectin-type oxidized LDL receptor 1
LPS – Lipopolysaccharide
MAPK - Mitogen-activated protein kinase
MCP-1 - Monocyte chemoattractant protein 1
MLL – mixed-lineage leukemia
MMP - Matrix metalloproteinases
mPGES - PGE synthase
NADPH - Nicotinamide adenine dinucleotide phosphate
NF-kB - Nuclear factor kappa-light-chain-enhancer of activated B cells
NLRP3 - pYRIN domain-containing 3
NO - Nitric oxide
NOS – Nitric oxide synthase
OXPHOS - oxidative phosphorylation
PA - Palmitic Acid
PBMCs - Peripheral blood mononuclear cell
PBS - Phosphate-buffered saline
PCAF – P300/CBP-associated factor
PCR - Polymerase chain reaction
PFA - Paraformaldehyde
PFK - 6-Phosphofructo-2-kinase
PI3K – Phosphatidylinositol 3-kinase
PKC – Protein kinase C
PKM2 - Pyruvate kinase M2
PMA - Phorbol 12-myristate 13-acetate

PPAR - Proliferator-activated receptor
PRC - Polycomb regulatory complexes
PRDM9 - PRDI-BF1 and RIZ homology domain containing
RAGE - Receptor for Advanced Glycation Endproducts
RANTES – Regulated upon Activation, Normal T cell Expressed, and Secreted (CCL5)
RNA - Ribonucleic acid
RNApII – RNA polymerase 2
ROS – Reactive oxygen species
SAM - S-Adenosyl Methionine
SDS - Sodium dodecyl sulfate
SDTFs - Signal-dependent transcription factors
SET – SET domain containing
SFM – Serum free medium
SMYD – SET and MYND domain-containing protein
SOCS - Suppressor of cytokine signalling
SOD2 - Superoxide dismutase 2
STAT - Signal transducer and activator of transcription
SWI/SNF - SWItch/Sucrose Non-Fermentable
T1D – Type 1 Diabetes
T2D – Type 2 Diabetes
TAE - Tris-acetate-EDTA
TCA cycle – Tricarboxylic acid cycle
TET – Ten-eleven Translocation Enzymes
TF - Transcription factor
TGF - Transforming growth factor
THP-1 – Human acute monocytic leukemia cell line
TLR - Toll-like receptor
TNF – Tumor necrosis factor
TSS - Transcription start site
TXNIP - Thioredoxin interacting protein
UCP1 – Uncoupling protein 1
UDP-GlcNAc - UDP-N-acetyl-alpha-D-glucosamine
VEGF - Vascular endothelial growth factor
WDR5 - WD repeat-containing protein 5
YS – Yolk sac

1 INTRODUCTION

1.1 Diabetic pathology, vascular complications and macrophages

Diabetes confers to about two-fold higher risk for a wide range of vascular diseases, independently from age, sex, smoking, systolic blood pressure, and BMI (Mathers and Loncar 2006, Collaboration 2010, The Emerging Risk Factors 2010). Hyperglycaemia concerns the increases of glucose in the blood plasma. Chronic hyperglycemia can vary depending on an individual renal threshold of glucose and glucose tolerance, the renal threshold, being the point at which glucose is excreted in the urine (DeFronzo, Hompesch et al. 2013). The diagnosis of diabetes is made after measuring blood glucose in either fasting state of 2 hours post glucose challenge. The majority of patients with Type 1 Diabetes (T1D) develop complications later in life (Katsarou, Gudbjörnsdottir et al. 2017) and higher HbA1c levels, glycated haemoglobin which reflects blood glucose over time, is associated with all-cause mortality (Orchard, Nathan et al. 2015). Diabetic retinopathy is an important cause of blindness (Bourne, Stevens et al. 2013) while diabetic nephropathy is one of the most serious complications of diabetes as well as leading cause of end-stage renal disease (Gillespie, Morgenstern et al. 2015). In T1D a genetically determined susceptibility may explain why not all individuals with very high blood glucose levels or vice versa some individuals with only slightly elevated levels develop complications (Reichard 1995). In case of Type 2 Diabetes (T2D) the patient is often diagnosed only at advanced disease stage and long-term complications may be already present at the time of diagnosis. The lack of insulin (T1D) or lack of insulin responsiveness (T2D) causes metabolic changes such as hyperglycemia which contributes to the pathology of diabetes. Hyperglycemia undesirably and unnecessarily activates immune responses and thus supports inflammation (Donath and Shoelson 2011, Chang and Yang 2016). Macrophages are essential regulators of inflammation and play a critical role in diabetic microvascular complications. In diabetic retinopathy activated resident macrophages produce inflammatory and neurotoxic mediators leading to vascular degradation break down (Altmann and Schmidt 2018). Macrophage recruitment and activation contribute to diabetic nephropathy (Tesch 2010) and neuropathy (Sandireddy, Yerra et al. 2014). Lastly, loss of plasticity of macrophages has been hypothesized to mediate delayed wound healing seen in diabetic patients (Boniakowski, Kimball et al. 2017). Therefore, diabetic complications result from an abnormal metabolic environment laundered by chronic hyperglycemia.

1.2 Diversity and plasticity of macrophages

Macrophages are the first line of defence against pathogens and essential for the control of tissue homeostasis. Their broad range of functions and prevalence probably contribute to the fact that they are involved in wide range of pathologies and makes it essential to understand how macrophages sense and respond to environmental cues (Asmis 2016).

The general dogma was that proliferating promonocytes, the bone marrow progenitor cells, give rise to circulating monocytes that extravasate into the tissue and maturate there into macrophages. Now it seems that, tissue resident macrophages are derived from the circulating monocytes as well as monocyte-independent systems (Ginhoux and Jung 2014). Haematopoiesis is characterised by two phases, primitive and definitive. Where the primitive phase takes place in the yolk sac (YS) through which erythrocytes and macrophages are being generated, the definite includes the generation of hematopoietic cells (HSCs) which give rise to the major blood cell lineages (Orkin and Zon 2008). The definite phase of haematopoiesis takes place in the aorta-gonads-mesopnephros (AGM) in the embryo. From there the cells relocate to various tissues e.g. the liver, spleen and bone-marrow where they reside throughout adult life. The anatomical sites and phases of haematopoiesis are depicted on Fig.1.

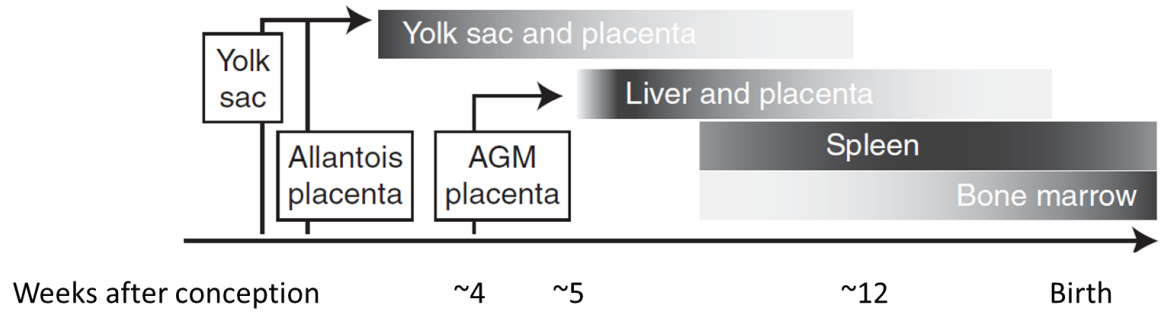

Figure 1. HSC generation, maintenance, and expansion during embryonic development in humans. The first HSCs are made outside of the embryo (YS, allantois, placenta) and finally in the AGM region and placenta. After that they migrate and expand into the different tissues. Cold Spring Harb Perspect Biol 2012;4:a008250, with copyright to Cold Spring Harbor Laboratory Press Rieger and Schroeder 2012.

Lineage definition and tracing in mice revealed certain pathways regulating distinct functions of embryonic and adult macrophages. For example, microglia are mostly derived from YS, e.g. primitive instead of definite haematopoiesis, and for their self-renewal do not depend on monocytes (Ajami, Bennett et al. 2007), whereas macrophages in the intestine, marginal zone of the spleen and uterus rely on constant inflow of monocytes. At the same time, macrophages at other locations including lung, liver and epidermis display a mixture of HSCs from both

origins (Yona, Kim et al. 2013). Tissue-resident macrophages although derived from common lineage still greatly vary in function and phenotype (Haldar and Murphy 2014). For example, the red pulp macrophages in the spleen are responsible for phagocytosis of old and damaged erythrocytes, iron recycling as well as clearance of B cells and immune surveillance. The alveolar macrophages in the lung control surfactant homeostasis and modulate dendritic cells in preventing allergic reactions and lastly, microglia in the central nervous system (CNS) promotes normal neuronal development and function (Haldar and Murphy 2014).

The hematopoietic system is identified as highly responsive to the physiological demands of the whole body e.g. development, homeostasis and repair (Okabe and Medzhitov 2015). At the same time, tissue-resident macrophages employ their local homeostatic mechanisms in order to maintain the number of cells i.e. by proliferating or recruitment of precursor cells (Haldar and Murphy 2014). The terminal differentiation and phenotype of the various types of resident macrophages likely depends on tissue-specific signals e.g. 'identity' signals as well as signals that mediate local functional demands (Okabe and Medzhitov 2015).

The phenotypes and transcriptional programs of macrophages are defined by a combination of differentiation and polarisation. Differentiation of macrophages is the stable irreversible conversion of progenitor cells by promotion of distinct differentiation paths, whereas polarisation is the stable and reversible programming on a specific demand in space and time (Okabe and Medzhitov 2015, Murray 2017). Activation of macrophages is broadly grouped in two activation phenotypes which occur during exposure with polarized CD4+ Th1/Th2 cells. M1 macrophages develop during inflammatory settings and activation usually occurs through Toll-like receptor (TLR) and interferon signalling, for example in response to bacteria and other pathogens. M2 activation in contrast, is associated with immune response during asthma and allergies (Biswas, Chittezhath et al. 2012, Murray 2017). For simplicity, cost effectiveness and time sake, in cell culture survival cytokines and polarizing agents are being used to study M1 and M2 macrophages. For M1 polarisation IFNγ and/or TLR agonist such as LPS, versus stimulation with IL-4, IL-10, IL-13, immune complexes, or glucocorticoids for the generation of M2 polarised macrophages (Fraternale, Brundu et al. 2015). The stimuli induce unique inflammatory profiles i.e. IFNγ polarized macrophages showed an autocrine feedback induction of cytokines and LPS induced macrophages higher secretion of IL-8, TNF-α, RANTES and IL-1β (Tarique, Logan et al. 2015). M1- and M2- polarisation states are presented schematically (Fig. 2 derived from (Biswas, Chittezhath et al. 2012).

The change in macrophage phenotype as a consequence of pathogenic or environmental signals show the great functional versatility of the cells and their ability to tailor the

appropriate response (Biswas, Chittezhath et al. 2012). Functional diversity of macrophage include triggering of inflammation, immune-regulation by secretion of anti-inflammatory factors such as IL-10 and TGF-β, but also phagocytosis of pathogens, clearance of debris and dead cells, and tissue remodelling through secretion of VEGF, CSF1, IL-8, MMP9 and polyamines that promote angiogenesis and fibrosis (Biswas, Chittezhath et al. 2012).

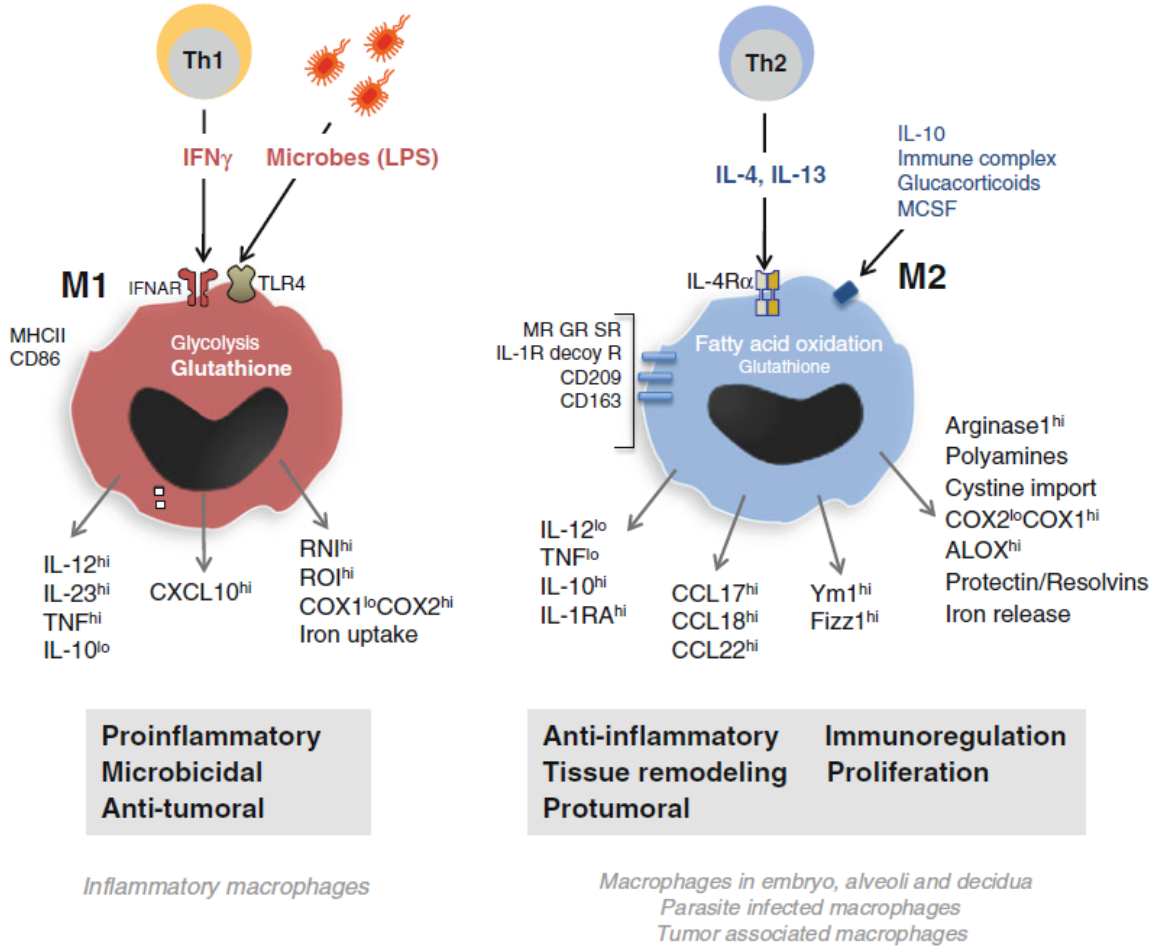

Figure 2. Schematic representation of the macrophage M1- and M2- polarisation states. Reprinted from Immunologic Research 53(1). Macrophage polarization and plasticity in health and disease. Biswas, S. K., M. Chittezhath, I. N. Shalova and J.-Y. Lim. 2012. with permission Springer Nature. SR scavenging receptor, MR mannose receptor, GR galactose receptor.

In vitro studies confirm the reversibility of polarisation states i.e. in cytokine deficient medium; both M1 and M2 polarized cells lost their phenotype after 6 days. Authors were also able to demonstrate repolarisation; after LPS + IFNγ treatment previous M2 cells exhibited CD64 and CD80, M1 like surface markers whereas previous M1 cells upon exposure with IL-13 showed upregulation of CD11 and CD209 but not CD1a, -b and CD200R (Tarique, Logan et al. 2015). Another study also reported that M2 polarizing stimuli abrogate all IFN-associated pathways, though it seems that macrophages respond differently to different types of M2-polarizing stimuli. For example, IL-4 and IL-10 lead to opposite responses compared

to LPS in repolarized human macrophages (Gharib, McMahan et al. 2019). Notably, other scientist report failure to repolarise M1 into M2 which depended on dampened mitochondrial oxidative respiration by nitric oxide (NO). Repolarisation then was successful after inhibition of NO production (Van den Bossche, Baardman et al. 2016).

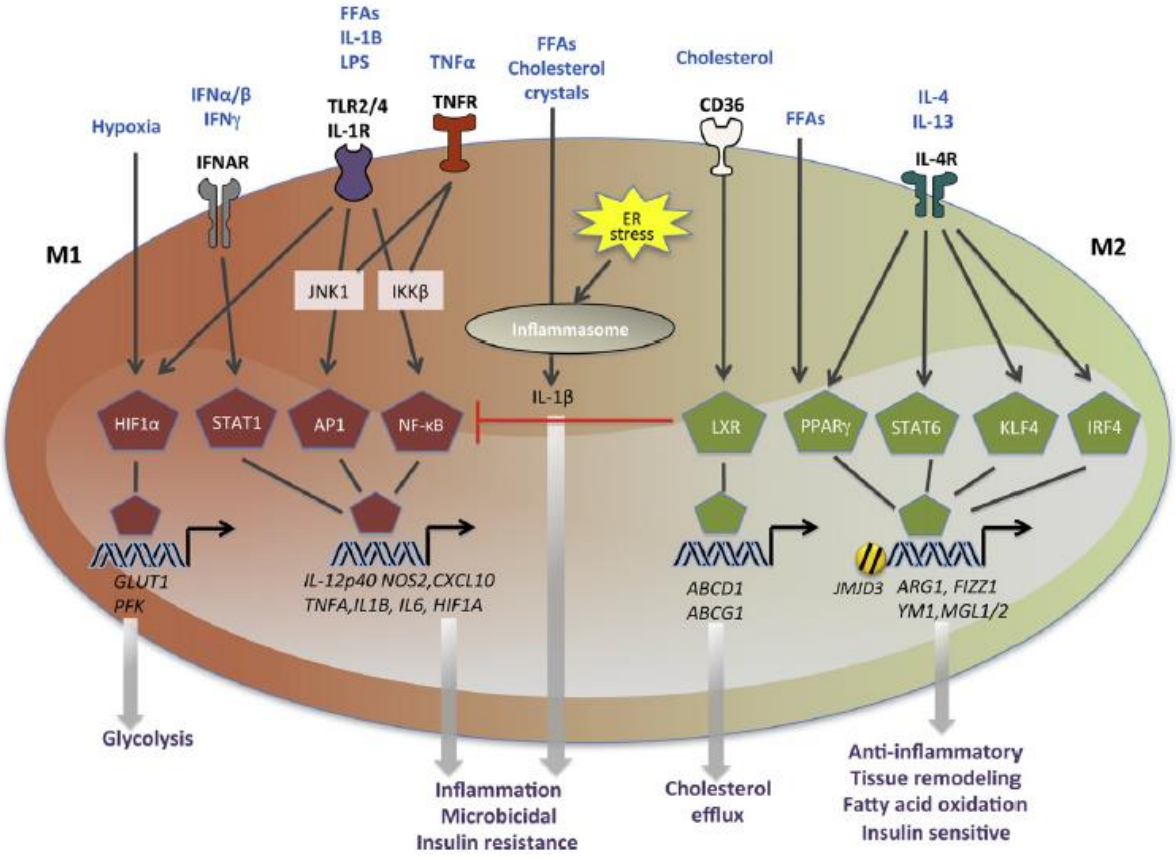

Figure 3. Signalling pathways involved in macrophage polarization. Reprinted from Cell Metabolism, 15(6), Subhra K. Biswas,Alberto Mantovani. Orchestration of Metabolism by Macrophages, 432-437, Apr 4, 2012 with permission from Elsevier.

In vivo, during the course of inflammation and its resolution, cells undergo transition from an M1 to M2 phenotype like macrophage. The huge role of macrophage plasticity in different disease settings, such as tissue regeneration, tumorigenesis, fibrosis and fat metabolism has increased the importance of understanding its regulation and opportunities to modulate (Biswas, Chittezhath et al. 2012, Helm, Held-Feindt et al. 2014, Pan, Liu et al. 2015, Alvarez, Liu et al. 2016, Chistiakov, Myasoedova et al. 2018).

The regulation of macrophage plasticity occurs on the level of signalling, through transcription factors, at epigenetic level and by miRNA's (paragraph 1.5, this thesis) and aforementioned microenvironmental signals. The effect of hypoxia is the mediated by transcription factor hypoxia-inducible factor (HIF) 1α and 2 (Fang, Hughes et al. 2009).

Signalling pathways involved in macrophage polarization are depicted in Fig. 3 derived from (Biswas and Mantovani 2012). INFγ and LPS signal through IFNAR1 and TLR4 thereby activating the transcription factors NF-kB (via IKKb), AP1, IRF3, and STAT1 which eventually leads to the transcription of M1 genes. In contrast, IL-4 and IL-13 act via IL-4 receptor to activate STAT6 and regulate the expression of M2 genes. The nuclear receptor peroxisome proliferator-activated receptor-γ (PPARγ) and Krüppel-like factor 4 (KLF4) and IRF4 transcription factors are also linked to M2 macrophage polarization as well as the histone demethylase Jumonji domain-containing 3 (JMJD3) (Biswas and Mantovani 2012). The polarisation states are linked to their functional metabolic outcomes (Fig. 3). Macrophages are important in homeostasis of metabolism of tissues as well as whole body metabolism whereas on the other side, the intrinsic metabolism of the cell shapes its activation state, (Biswas and Mantovani 2012). There is growing interest in understanding macrophage polarization under physiological and pathophysiological conditions and the relationship between metabolism and macrophage polarization. Metabolic regulators then could be used as modulators or switches between polarisation states (Murray 2017). Therefore, the regulation of macrophage polarisation at cell metabolism level will be discussed in the following paragraph.

1.3 Metabolism in differentially activated macrophages

Polarisation of macrophages greatly depends on biochemical pathways. For example, glutamine, fatty acid uptake, CD36 metabolism and mitochondrial oxidative phosphorylation are essential for the development of M2 macrophages (Huang, Everts et al. 2014) whereas M1 macrophages rely on glycolysis for their energy supply (O'Neill and Pearce 2016). Therefore, the major metabolic pathways will be described here.

Glucose metabolism: typically differentiated cells have low rates of glycolysis. During glycolysis glucose is converted into pyruvate. Pyruvate subsequently is oxidized in the TCA cycle in order to generate ATP. M1 and M2 polarized macrophages are fuelled from different energy sources. IFNγ/LPS trigger in macrophages an increased rate of glycolysis followed by lactic acid fermentation. This is due to concomitant increased expression of 6-Phosphofructo-2-kinase (PFK2) isoforms from the liver-type PFK2 (L-PFK2) to the more active and ubiquitous PFK2 isoform (uPFK2), which ultimately results in higher levels of Fructose-2,6-biphosphate (Saha, Shalova et al. 2017). The conversion of glucose into lactate however yields only two ATP per glucose molecule compared to 32 when following complete oxidation into CO2 and H2O. Lactate is normally produced under low oxygen conditions, in the presence of oxygen this process will be called aerobic glycolysis and the shift from mitochondrial oxidation towards aerobic glycolysis the Warburg effect which is mediated via the NF‐κB/HIF‐1α pathway (Odegaard and Chawla 2011, Saha, Shalova et al. 2017). Though, in M1 macrophages the TCA cycle is fragmented at two steps; after isocitrate dehydrogenase (IDH) and after succinate the cycle is broken leading to accumulation of citrate and succinate (O'Neill 2015, Saha, Shalova et al. 2017). In contrast, IL-4 activated M2 macrophages display an intact TCA cycle and rely on fatty acid oxidation as metabolic pathway in order to fulfil their energy demand for their role in tissue remodelling, wound healing and repair (Odegaard and Chawla 2011). Also, M2 macrophages are characterized by, high amounts of amino-sugar and nucleotide sugar mark high level of UDP-N-acetyl-alpha-D-glucosamine (UDP-GlcNAc) and are needed for glycosylation of the lectin/mannose receptor in M2 macrophages. Glutamine also appeared to be essential for M2 macrophage differentiation (Sica and Mantovani 2012, Jha, Huang et al. 2015).

A changed *lipid metabolism* contributes to the macrophage activation; fatty acid uptake is suppressed in M1 compared to M2 macrophages the latter one showing increased fatty acid uptake and oxidation. The changes in lipid metabolism are associated with regulatory changes in transcriptional profile and lipid mediators and kinases (Martinez, Gordon et al. 2006,

Biswas and Mantovani 2012) and provides energy needed for phagocytosis but also membrane elasticity required. Genes related to arachidonate metabolism which are up regulated in M1 macrophages are COX2 and microsomal PGE synthase (mPGES) whereas M2 macrophages show up regulation of COX1 and arachidonate 15-lipoxygenase (Martinez, Gordon et al. 2006).

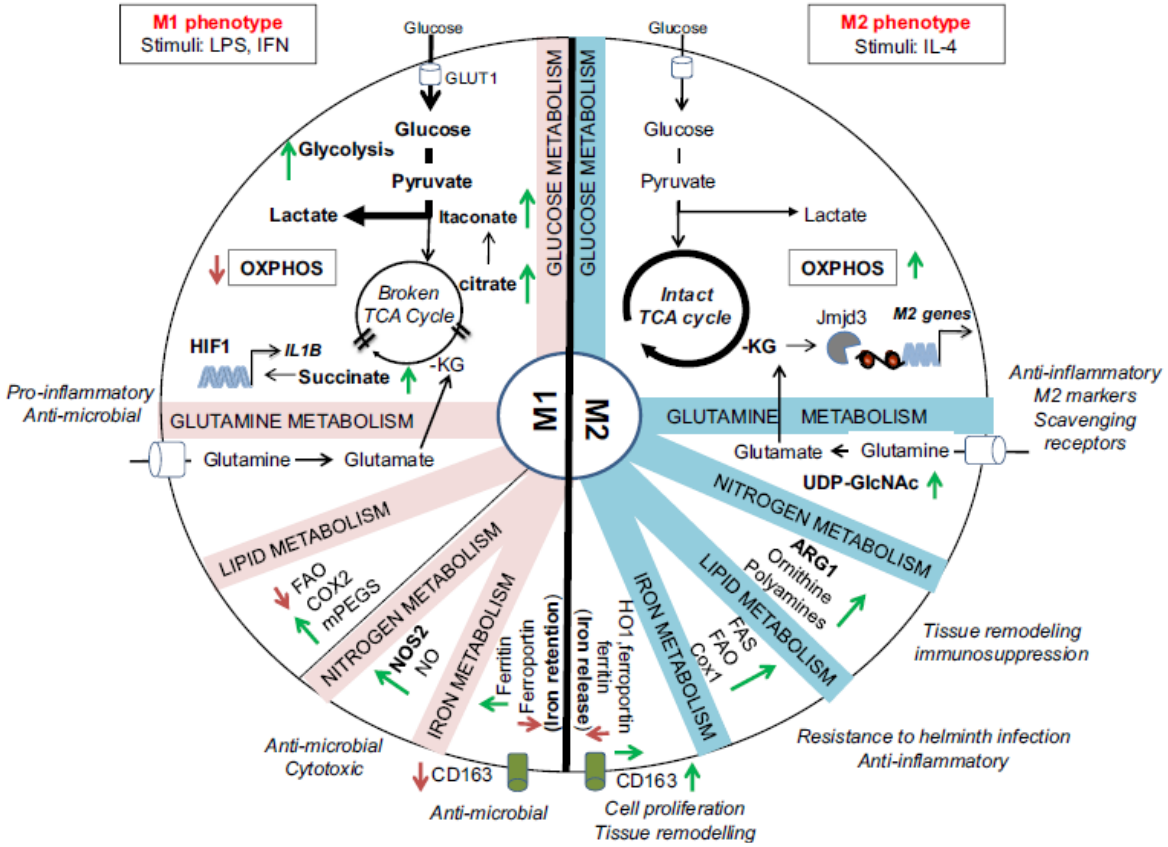

Figure 4. Intrinsic metabolism of M1 and M2 polarized macrophages. Figure derived from (Saha, Shalova et al. 2017) and reprinted with permission from John Wiley and Sons.

Amino acid metabolism Differences in arginine metabolism are used for long to distinguish M1 and M2 polarised macrophages. In M1 macrophages NOS2 expression is increased which converts L-arginine into NO and L-citrulline (Fig. 4) whereas in M2 macrophages arginase 1 is upregulated which metabolizes L-arginine into L-ornithine which serves as a precursor for polyamines used in collagen synthesis and cell proliferation during tissue remodelling (Biswas and Mantovani 2012, Saha, Shalova et al. 2017).

Iron metabolism By phagocytosis of red blood cells and setting iron free for erythropoiesis, macrophages contribute to iron homeostasis (Soares and Hamza 2016) and iron metabolism in M1 and M2 macrophages is dissimilar. The heme group of haemoglobin is catabolized by the heme oxygenase-1 (HO-1) enzyme and the iron produced via this process is either excreted

from macrophages via FPN1 (Solute carrier family 40 protein) or stored intracellularly by ferritin. M2 macrophages show HO-1 induction and high levels of CD163 and CD94, responsible for heme uptake and low levels of iron storage (Naito, Takagi et al. 2014). On the other side, M1 macrophages show iron retention, supported by low levels of CD163 (Cairo, Recalcati et al. 2011).

Glutathione and redox The intracellular redox status is characteristic for M1 and M2 macrophages. Reductive macrophages contain high levels of gluthatione and oxidative macrophages display low levels of gluthathione (Biswas and Mantovani 2012). In CD4+ T cells, a reductive phenotype coincided with production of IL-12 and NO and reduced IL-6 and IL-10. Therefore reductive phenotype may support Th1 differentiation (Murata, Shimamura et al. 2002).

In summary, metabolites itself and programming in response to change in the environment e.g. nutrients or oxygen, directly influence macrophage functions (O'Neill and Pearce 2016). Then, with diabetes pathology in mind, in the next paragraph the literature on the effect of hyperglycemia on monocytes/macrophages will be discussed.

1.4 Hyperglycemic effect on macrophages

Information on the effect of glucose on the activation of human primary macrophages is limited though animal and in vitro models suggest crucial changes in the biology of these immune cells. In THP-1 cells, a human monocytic cell line, high glucose led to increased expression of the receptor for oxidized LDL, LOX-1 as well as intracellular ROS and enhanced activation of NF-κB and activated protein-1 (AP-1) binding on the LOX-1 gene promotor. Overexpression of LOX-1 on monocyte-derived macrophage from T2D support the relevance of this gene in diabetic atherosclerosis (Li, Sawamura et al. 2004). Inflammatory effects of hyperglycemia are at least partly mediated via TLR activation as inhibition of high glucose induced TLR expression led to significant decreases in cytokine release in THP-1 cells as well as primary human monocytes. PKC signalling as well as p47Phox, essential component of the NADPH oxidase production, are proximal in HG-induced TLR2 and TLR4 activation (Dasu, Devaraj et al. 2008). Increased TLR mRNA and protein, and downstream MyD88 signalling has also been found in monocytes from T2D patients together with elevated proinflammatory mediators and TLR ligands in the serum compared to controls (Dasu, Devaraj et al. 2010). On a functional level, high glucose induced in THP-1 cells increased monocyte activation and transmigration (Nandy, Janardhanan et al. 2011). In primary human macrophages high glucose alone is rendering a mixed M1/M2 cytokine profile which can support progression of diabetic vascular complications (Moganti, Li et al. 2016). Acute but not long-term TNF-α as well as sustained IL-1β production was found in M1 macrophages. IL-1Ra normally released by M2, were produced in M0 and M1 in response to hyperglycemia (Moganti, Li et al. 2016). Consistent with in vitro results in monocytes of prediabetic people exhibited higher levels of inflammatory CD11c+ and lower content of CD206+ compared to controls. This was associated with obesity, IR, triglyceridemia and low serum levels of IL-10. Increased iNOS expression levels as well as Arg-1 reduction suggest that glucose alone is inducing M1 polarization (Torres-Castro, Arroyo-Camarena et al. 2016). Both studies suggest that glucose renders monocytes/macrophages pro-inflammatory.

FFAs, elevated glucose levels, and oligomers of islet amyloid polypeptide are reported to activate the NOD-like receptor family, pYRIN domain-containing 3 (NLRP3) inflammasome pathway (Masters et al., 2011). Activation of NLRP3 leads to caspase-1 expression and secretion of IL-1β, which mediate decreased insulin sensitivity. IL-1β blocks insulin signalling in target cells through activation of inflammatory signalling and the production of Suppressor of cytokine signalling (SOCS) proteins. In addition, IL-1β triggers cytotoxicity

and death of β cells in the pancreas. Mice genetically deficient for NLRP3, caspase-1, and IL-1β provided strong evidence for the role of the NLRP3 inflammasome pathway in the development of insulin resistance and diabetes (Masters et al., 2011).

Recently, we showed that in vitro hyperglycemia induces expression of pro-inflammatory chemokines and cytokines in primary human macrophages (Moganti, Li et al. 2017). This suggests that the negative impact of hyperglycemia on microvascular complications extents to its direct influence on immune cells too and thus on the interaction between ECs and monocytes. Hyperglycemia causes an immediate but transient production of TNF-α while it constitutively causes IL-1β release in human primary monocyte derived macrophages (Moganti, Li et al. 2017). In hyperglycemic conditions, macrophages had undergone M1-like polarisation.e. proinflammatory phenotype, with increased expression of CD11c and nitric oxide synthase while arginase-1 and interleukin IL-10 were down regulated (Torres-Castro, Arroyo-Camarena et al. 2016).

1.5 Epigenetic programming of macrophages

Epigenetic processes in monocytes and macrophages regulate transcriptional profile of the cells and their responses to stimuli and environmental changes. The epigenetic regulation without changing the DNA itself equips the cells with the plasticity they need for the diverse tasks in different tissues. Chromatin structure largely impacts the regulation of gene expression by altering accessibility to transcription factors, although it is not completely resolved how individual epigenetic marks are set up, maintained and influence chromatin structure. The major epigenetic mechanisms i.e. DNA-methylation, histone modifications and non-coding RNAs will be discussed here.

Dense DNA-methylation on cytosine's of CpG dinucleotides, predominantly concentrated in CG-islands (CGI), is associated with silencing of promoters (Deaton and Bird 2011). The level of DNA methylation is determined by the local activity of DNA methyltransferases (DNMT), DNA demethylases as well as the DNA replication rate (Jeltsch and Jurkowska 2014, van der Wijst, Venkiteswaran et al. 2015). DNA methylation is actively modified in different tissues during differentiation (Barres, Yan et al. 2012, Kirchner, Osler et al. 2013). Demethylation controls a specific fractions of genes involved in actin cytoskeleton regulation, innate immune system and phagocytosis in human monocytes (Wallner, Schröder et al. 2016). Methylated CpGs guide transcription factor binding for example transcription factor KLF2, -4, -5 bind in methylation dependent manner (Liu, Olanrewaju et al. 2014, Rothbart and Strahl 2014). An upregulation was observed of DNMT1 and 3a in M2 compared to M1 macrophages which directed silencing of specific genes (Kittan, Allen et al. 2013). DNMT3b in ATMs stimulated was enhanced by stimulation with fatty acids, leading to DNA methylation at the PPARγ1 promoter (Yang, Wang et al. 2014) whereas a combined treatment of DNMT inhibitor 5-Aza 2-deoxycytidine and HDAC inhibitor Trichostatin A, in treatment of acute lung injury during sepsis, showed a protective effect by decreasing the number of M1 versus M2 macrophages in the lung tissue (Thangavel, Samanta et al. 2015). Still, little is known about active demethylation in macrophages. Ten-eleven Translocation (TET) enzymes are essential for DNA demethylation in primary monocytes (Klug, Schmidhofer et al. 2013) though this occurs very early during initial 6-18h of the differentiation process (Wallner, Schröder et al. 2016).

Many posttranslational modifications to distinct amino acids of the histone tail have been discovered of which methylation and acetylation are most studied. From other modifications i.e. citrullination, ubiquitination, sumoylation, ADP-ribosylation, proline isomerization and

phosphorylation at different residues among others, the associated function is not completely known yet (Rothbart and Strahl 2014). Besides direct physical effect such as positively charged lysine acetylation, histone code can mediate indirectly effect on chromatin structure by selective recruitment of facilitory proteins. The combination of histone modifications and/or cooperation with DNA methylation increase the diversity of histone function (Rothbart and Strahl 2014). Histone code is mediated by epigenetic regulators. Epigenetic regulators can be divided in three groups based on their function; *writers* and *erasers* that mediate and respectively remove the marks which are consequently read by *readers* thereby altering the epigenetic status of enhancers and promotor (Hoeksema and de Winther 2016). Histone methylation for example is controlled by histone methyltransferases (HMT) and demethylases (HDM), which consists of the LSD and JMJC family of enzymes. H3K4me at the transcription start site (TSS) is generally associated with transcriptional activation whereas H3K9me2/3 and H3K27me3 with gene silencing (Bannister and Kouzarides 2011). H3K4me3 and H3K27me3 at promoters of macrophage-differentiation related transcription factors controls monocyte to macrophage differentiation (Zheng, Wang et al. 2017). However combinations of repressive and active marks can exist next to each other and silence developmental genes keeping cells poised for activation (Bernstein, Mikkelsen et al. 2006). Enzymes that catalyse the addition of methyl groups either belong to the SET-domain containing family of proteins, DOT1-like proteins or N-methyltransferases which specifically methylate arginine residues (Greer and Shi 2012). HMTs involved in inflammatory signalling in macrophages include MLL1, MLL4, Ash11, SET7, SMyd2, Setdb2, Suv39h2, G9a Ezh1 and 2 and SMYD5. Also, HDMs modulate macrophage polarisation by removing repressive marks e.g. on the histone tails of H3K9, H3K36 and H3K27 (Kapellos and Iqbal 2016). The most extensively studied HDM being H3K27 specific demethylase JMJD3, which drives expression of inflammatory genes in response to LPS (De Santa, Narang et al. 2009) and drives IL-12 expression in M1 macrophages during diabetic wound healing (Gallagher, Joshi et al. 2015, Kapellos and Iqbal 2016). Another key histone modification to regulate gene expression is acetylation. Acetylation of histones is achieved by histone acetyltransferases (HATs) and histone deacetylases (HDACs). Acetylation, irrespective of the residue, is in general associated with open chromatin and active transcription (Barski, Cuddapah et al. 2007). Several members of HATs including p300, CBP and PCAF regulate NF-κB mediated gene expression in macrophages and their inhibition manifests in anti-inflammatory effects. HDACs in macrophages regulate TLR pathways and inflammatory cytokine production for example, by recruiting interferon regulator factor (IRF) and Rel family transcription factors to

TLR-target genes; HDAC inhibitor trichostatin A targeted LPS-inducible expression of IL-6 and IFNβ, but not IL-1β in human primary macrophages (Bode, Schroder et al. 2007). Therefore, histone code is inducible by the inflammatory factors including bacteria and cytokines.

miRNA are a class of 19–24 nucleotide long non-coding RNAs, that fine tune gene transcription i.e. by controlling the stability of targeted mRNAs and/or inhibiting their protein translation but also controlling transcription factor expression. Different miRNAs have been involved in polarisation of development, polarisation and function of macrophage (Roy 2016). Macrophages in turn secrete microvesicles containing miRNAs thereby exerting effects on target cells (Roy 2016). and RNAs which exclusively associate with certain argonaut proteins, have been shown to mediate epigenetic modifications of DNA and histones (Morris 2009, Loscalzo and Handy 2014). miRNA-seq profiling of primary mouse BMDM revealed 31 miRNAs that regulate macrophage polarization. High expression levels of miR-155, miR-9, miR-146a and miR-19 were found in M1- compared to miR-26a-2-3p and let-7c in M2-polarized macrophages whereas 29 of them specifically target C2H2 zinc-finger genes (Lu, McCurdy et al. 2016). Some have been used as therapeutic targets in the study of diabetes. For example, anta-miR155, a potent promoter of M1 polarization, delivered into macrophages via phagocytosis, reduced inflammation and restored the cardiac function in a mice model for diabetic cardiomyopathy (Jia, Chen et al. 2017). Also, anti-miR33 treatment, which negatively regulates reverse cholesterol transport factors ABCA1 and HDL, reduced M1-related genes *IL-1B, TNFA, NOS2* and increased anti-inflammatory M2 related genes *YM1*, *CD206* in atherosclerotic plaque macrophages of diabetic mice (Distel, Barrett et al. 2014). Deletion of microRNA-generating enzyme dicer in macrophages, accelerated atherosclerosis in Apoe-/- mice decreased the expression of genes that enhance mitochondrial function, fatty acid oxidation, and oxidative phosphorylation via miR-10a and let-7b and miR-195a, suggesting that dicer promotes metabolic reprogramming of AAMs (Wei, Corbalán-Campos et al. 2018).

Recent studies point out memory properties for not only the adaptive immune system but also for innate immune cells e.g. training vs tolerance (Netea 2013). The role of histone modifications involved in macrophage trained immunity was revealed recently (Saeed, Quintin et al. 2014). Endogenous stimuli from the diabetic environment, such as glucose and advanced glycation end products (AGEs), through epigenetic changes could contribute to reprogramming of monocytes/macrophages and this can already occur in the bone marrow (El-Osta 2012, van Diepen, Thiem et al. 2016). Current research about the role of glycemic

memory in development of diabetic complications later in life, has focused mostly on cells of the vascular system i.e. endothelial cells and/or mesengial cells (Brasacchio, Okabe et al. 2009). Therefore a relevant open question is the effect of hyperglycemia on the epigenetic programming of monocytes and macrophages leading to the expression of genes related to diabetes pathology.

1.6 The effect of hyperglycemia on the transcriptional profile of human primary macrophages and expression of S100 family

The effect of hyperglycemia on the transcriptional profile of human primary macrophages has been identified previously using Affymetrix gene expression profiling technology and was published elsewhere GSE86298 (Moganti 2017). GSEA/KEGG analysis was done to examine pathways enriched in gene sets with a significant difference in expression between hyperglycemic cells compared to controls. The Affymetrix gene expression profiling revealed that several members of the S100 family of proteins to be up regulated by culture under high glucose conditions. In M0 as well as M1 macrophages it was found that gene expression of *S100A9* and *S100A12* were highest up regulated in hyperglycemic condition in M1 macrophages and S100A8 in M0 macrophages (Table 1). *S100A8* and *S100A9* are part of the IL-17 signaling (KEGG) pathway. Other members of the pathway which are significantly up regulated include *MAPK3, CHUK, HSP90AB1, CASP8, CXCL3, LCN2* for M0 and *HSP90B1, MAPK3, IL1B, FOS, MAPK14, TRAF3, TNFAIP3, MAPK9, IL17F, MAPK13, RELA, CXCL5* for M1 macrophages.

Table 1. Differential expression of S100 family members identified by Affymetrix chip technology

GeneSymbol	Fold change NS	Fold change IFNγ	Fold change IL-4	Adjusted p-Value for Estimate of NS	Adjusted p-Value for Estimate of IFNγ	Adjusted p-Value for Estimate of IL-4
S100A12	1,309409	4,411155	1,055020	0,368051	0,000035*	0,973707
S100A10	1,080588	1,287492	1,157048	0,478160	0,008734*	0,421370
S100Z	1,132830	1,658848	1,089954	0,674781	0,024781*	0,929235
S100A4	1,051011	1,970927	1,017411	0,894199	0,004853*	0,993473
S100A9	1,435917	2,130770	1,019306	0,073179	0,000687*	0,990445
S100A16	1,954496	1,004997	2,022121	0,020164*	0,990636	0,088720
S100A7L2	1,106120	1,023489	1,049944	0,029907*	0,677327	0,644794
S100A8	3,193302	1,865075	1,380401	0,003648*	0,066537	0,728683

*Every comparison is between cells cultured in high glucose conditions versus cells cultured in normal glucose conditions

Plasma levels of inflammatory proteins revealed new markers for prediabetes as well as T2D. These included EN-RAGE (S100A12) as well as IL-17 (Mac-Marcjanek, Zieleniak et al. 2018). Macrophage are important in T1D onset and progression together with T and B lymphocytes (Kopan, Tucker et al. 2018). B-cells bind antigens directly whereas T cells need antigen presenting. Macrophages are weak APCs compared to dendritic cells but can sustain activation and differentiation of primed T lymphocytes (Geissmann, Gordon et al. 2010). After initial priming, polarizing cytokines determine T helper cell differentiation. S100 proteins can induce Th17 cells (Reinhardt, Foell et al. 2014), and IL-17 and Th17 cells do play an important role in pathogenesis of diabetes (Abdel-Moneim, Bakery et al. 2018). S100 genes are mainly expressed in myeloid cells (Donato, Cannon et al. 2013). They are differentially expressed in neutrophils compared to macrophages and dendritic cells (Averill, Barnhart et al. 2011). S100 proteins act upon changes in intracellular Ca^{2+} levels and are found to play a role in inflammatory diseases, where they are used as diagnostic marker, and cancer (Leach, Yang et al. 2007, Bresnick, Weber et al. 2015). Expression levels of S100A8, -A9 (Bouma, Coppens et al. 2005, Jin, Sharma et al. 2013) and circulating levels (Ortega, Sabater et al. 2012, Cotoi, Dunér et al. 2014) of S100A12 (ENRAGE) and soluble RAGE (Basta, Sironi et al. 2006, Dong, Shi et al. 2015) are positively related to diabetes pathology. Taking into account that they are pro-inflammatory molecules and can be significantly implicated in diabetes development and progression, we examined the regulation of expression of S100 proteins by glucose and glucose programming in human primary macrophages.

1.7 Aims

The goal of the study was to investigate the mechanisms of hyperglycemia-mediated programming of macrophage functions supporting diabetes progression. S100A9 and S100A12 have been selected as reference genes due to the role in the activation of endothelial cells and elevated expression levels in the circulation of diabetic patients.

The specific aims included:

- To investigate the regulation of S100A9 and S100A12 expression during the macrophage differentiation in normal and hyperglycemic conditions
- To analyse the expression of S100A9 and S100A12 in monocytes of diabetic patients

- To examine the effect of hyperglycemia on the histone code modifications on the promoters of S100A9 and S100A12 in human macrophages
- To examine the involvement of histone modifying enzymes in the regulation of S100A9 and S100A12 expression
- To examine potential memory for the expression of S100A9 and S100A12 compared to IL1□ and CCR2
- To examine whether hyperglycemia sensitizes macrophages to respond to pro-inflammatory exogenous and endogenous factors by induction of S100A9 and S100A12 gene expression

2 MATERIALS & METHODS

2.1 Chemicals, reagents and kits

Table 2. Chemicals, reagents and kits.

Product	Company
0.05% Trypsin/EDTA solution	Biochrom
10x Earle's Balanced Salt Solution (EBSS)	Sigma Aldrich
10x Incomplete PCR buffer	BIORON
30% Acrylamide/Bis Solution	Bio-rad
4',6-diamidino-2-phenylindole (DAPI)	Roche Diagnostics
50x Tris-Acetate EDTA (TAE) buffer	Eppendorf
Acetic acid	Merck
Agarose	Bioron
Amersham Hyperfilm ECL	GE Healthcare
Ammonium persulfate (APS)	Merck Millipore
Ampicillin	Sigma Aldrich
BL21-(DE3)-RIL-Codon-Plus E.coli	Stratagene
Bovine Serum Albumin (BSA)	Sigma Aldrich
BSA loading controls	Bio Rad
CD14 MicroBeads	Miltenyi Biotec
Dako Pen	Dako
Dako Fluorescent Mounting Medium	Dako
Deoxyribonucleotides (dNTPs) 10M	Fermentas
DEPC Water	Thermo Fisher Scientific
Dexamethasone	Sigma Aldrich
Dimethylsulfoxide (DMSO)	Sigma Aldrich
DMEM medium+Gluta MAX	Thermo Fisher Scientific
DMSO	Sigma Aldrich
DNA ladder	Thermo Fisher Scientific
DNA Loading Dye (6x)	Thermo Fisher Scientific
DNase Buffer (10x)	Thermo Fisher Scientific
DNase I RNase free 1U/μl solution	Fermentas
DRAQ5	Cell Signaling

EDTA	Invitrogen
EDTA-free Protease Inhibitor Cocktail Tablets	Roche
Ethanol	Roth
Fetal calf serum (FCS)	Biochrom
Gel Blue stain reagent	Pierce
Gel Red	Biotium
Glycerol	Sigma Aldrich
Isopropanol	Merck Millipore
Laemmli sample buffer	Bio Rad
Methanol	Merck
Nitrocellulose blotting membrane	GE Healthcare
Non-Fat Dry Milk	Bio Rad
Oligo(dt) primer	Thermo Fisher Scientific
Page Ruler Plus Prestained Protein Ladder (10-250 kD)	Thermo Fisher Scientific
Paraformaldehyde (PFA)	Sigma Aldrich
1X Phosphate buffered saline (D-PBS), sterile 1x	Biochrom
PCR primers	Eurofins MWG Operon
PCR probes	Eurofins MWG Operon
Penicillin/Streptomycin	Biochrom
Percoll	GE Healthcare Life Sciences
Ponceau S solution	Sigma Aldrich
Recombinant human MCP-1 (CCL2)	Prepotech
Recombinant Human IL-4	Peprotech
Recombinant human M-CSF	Peprotech
RPMI medium	Life Technologies
Sensimix II Probe Kit	Bioline
Sodium Chloride	Sigma Aldrich
Sodium dodecyl sulfate (SDS) 10%	Bio-Rad
TEMED	Roth
TGS (Tris/Glycine/SDS) buffer 10x	Bio-Rad
Tris-HCl buffer 0.5M, pH 8.8	Bio-Rad
Tris-HCl buffer 1.5M, pH 6.8	Bio-Rad
Triton X-100	Sigma Aldrich

Trypan blue solution	Sigma Aldrich
Tween 20	Sigma Aldrich
β-mercaptoethanol	Sigma Aldrich
Luminata Forte Western HRP substrate	Millipore

2.2 Consumables

Table 3. Consumables.

Product	Company
0.22 μm filter	Fisherbrand
22x22 mm coverslips	Marienfeld
3MM blotting papers	GE Healthcare
CASY cups	Omni Life Sciences
Cryovials	Nunc
Elisa plate sealers	R&D systems
Elisa Plates	R&D systems
GeneChip® Human Gene 2.0 ST Array	Affymetrix
Glass slides	Servoprax
LS columns	Miltenyi Biotec
Parafilm	American National Can
PCR tubes	Star Labs
Petri dishes	Nunc
Pipettes tips	Eppendorf
Pipettes	Eppendorf
Plastic wrap	Toppits
Western film	GE Healthcare
Safe-Lock Eppendorf Tubes, 1.5 ml	Eppendorf
Scalpel	Feather
Sterile pipette tips	Star Labs, Nerbeplus
Tubes	Falcon
Trans-well 5 μm	Corning
Medical X-ray film	Typon Röntgen-film GmbH

2.3 Equipment

Table 4. Equipment.

Product	Company
Agarose electrophoresis unit	VWR
Autoclave VX-95	Systec
Balance	Kern
Bioruptor	Diagenode
CASY Cell Counter	Schärfe System
Cell culture hood	Thermo Fisher Scientific
Cell culture incubator	Heraeus Instruments
Centrifuge 5415 D	Eppendorf
Centrifuge 5804 R	Eppendorf
Confocal laser scanning microscope SP8	Leica Microsystems
Electrophoresis comb	Peqlab
Electrophoresis power supply	Peqlab
FACS Canto II	BD Biosciences
Freezer (-20°C)	Liebherr
Freezer (-80°C)	Sanyo
Fridge (4°C)	Liebherr
Ice machine AF100	Scotsman
Inverted microscope	Leica Microsystems
LightCycler 480 Instrument	Roche Diagnostics
MACS manual cell separator	Miltenyi Biotec
Gel dryer model 583	Bio-Rad
Magnetic stirrer MR3000	Heidolph
Microwave oven	Sharp
Neubauer haemocytometer	Assistent
Pipette Controller	Accu Jet Pro, Brand
Roller	Ortho Diagnostic Systems
Rotator	Neolab
SDS-PAGE chamber	Peqlab
SDS-PAGE gel comb	Peqlab

SDS-PAGE power unit Power-Pac 200	Bio-Rad
SDS-PAGE unit	Biometra
Shaker KS 260 basic	IKA
Sorvall RC5C Plus ultracentrifuge	Thermo Fisher Scientific
Staining Dish	Neolab
Staining rack	Neolab
Tecan Infinite 200	Tecan
Thermomixer 5436	Eppendorf
Thermomixer comfort	Eppendorf
Tweezers	Neolab
Ultracentrifuge tubes 50 ml	Thermo Fisher Scientific
UV fluorescent light	Peqlab
Vortex Genie 2	Scientific Industries
Water bath	Memmert
Water bath VWB12	VWR
X-ray cassette	Kodak
X-ray film processor CAWOMEN 2000 IR	CAWO Solutions

2.4 Kits

Table 5. Kits used in the study.

Kit	Company
E.Z.N.A. Total RNA Kit I	Omega bio-tek
DNeasy Blood & Tissue Kit	Qiagen
QIAquick PCR Purification Kit	Qiagen
RevertAid H Minus First Strand Synthesis Kit	Fermentas
SimpleChIP® Enzymatic Chromatin IP Kit	Cell Signaling Technology
Pierce™ BCA Protein Assay Kit	Thermo Scientific

2.5 Cell culture

2.5.1 Monocyte isolation and generation of macrophages

Human monocytes were isolated from buffy coats from individual donors as described (Kzhyshkowska, Gratchev et al. 2004) with modifications. Buffy coats were provided by the

German Red Cross Blood Service Baden-Württemberg – Hessen. Buffy coats were obtained from healthy donors after informed consent. Buffy coats were diluted 1x with Ca2+- and Mg2+- free phosphate-buffered saline (PBS) (Biochrom). A volume of 25 ml then was layered on top of a 15 ml Ficoll gradient (Biochrom) in a 50 ml falcon tube. Peripheral blood mononuclear cells (PBMCs) were collected from the interphase and washed three times with PBS. PBMCs were further purified using a PercollTM gradient. Ficoll and Percoll gradients were centrifuged at 420 g for 30 minutes at RT without brakes. The cells obtained were subjected to CD14+ magnetic cells sorting (Milteny Biotech). For the culture, CD14+ Monocytes were resuspended in SFM serum-free medium supplemented with 5mM (normoglycemia, NG) or 25 mM glucose (hyperglycemia, HG) at a concentration of $1x10^6$ cells/ml. Cells were incubated with cytokines derived from TEBU Peprotech in the presence of 7.5% CO2 for 6 days. 5ng/ml MCSF and 100ng/ml interferon-gamma (IFNγ) was used to induce M1 macrophage polarization and MCF with 10ng/ml IL-4 to induce M2 macrophage polarization.

2.5.2 Collecting of conditioned medium

Conditioned medium as collected on day 1, day 3 and day 6. The samples were stored at -80°C until further use. Human S100A9 and S100A12 were detected using and ELISA kit (DY5578, and DY1052-05, R&D systems) according to the manufacturer's instructions. Concentration was calculated by regression analysis of a standard curve.

2.5.3 Viability Assay

Alamar blue solution (Life technologies, Germany) was added to the medium (10% of total volume) and the cells were incubated in the presence of 7.5% CO2 at 37°C for 3h. Fluorescence was measured in triplicates at 590 nm read by Tecan Infinite® 200. Fluorescence of pure Alamar Blue was used as a negative control.

2.5.4 Inhibition of histone modifying enzymes

Primary human derived macrophages were obtained as previously described. M1 macrophages which were cultured in the presence of MCSF and IFN-γ under normal and high glucose conditions were treated with inhibitors for SET7, SMYD3 and Mixed Lineage Leukemia (MLL) histone methyltransferases (HMTs). PFI-2 hydrochloride inhibitor for SET7 and EPZ031686 inhibitor of SMYD3 where obtained from MedChem Express (US). WDR5 0103 inhibitor of MLL HMTs was obtained from Bio-techne (US). The inhibitors dissolved in DMSO. Following stock concentration have been prepared; EPZ031686 1 mM, PFI-2 0.1 mM

and WDR5 0103 10 mM. Working concentrations are indicated. Corresponding amounts of DMSO were used as controls. Cells were treated with inhibitors from the time of isolation on up to 6 days followed by RNA isolation. The sets of donors used for application of different inhibitors partially overlap but are not identical due to technical reasons.

2.5.5 Immunofluorescence staining

Monocyte derived macrophages were stimulated with MCSF and INF-γ and cultured on cover glasses (Neolab, Germany) for 6 days under normal and high glucose conditions. All further procedures have been performed at RT. Cells were fixed using 2% PFA for 10 minutes, followed by incubation with 0.5 % TritonX-100/PBS 15 minutes for permeabilisation, and finally fixed with 4% PFA 10 minutes. Plates were washed 2 times with PBS for 5 minutes on shaker and one time with PBS 1x / 0.1% Tween20 for 30 seconds. Blocking was done with 3% BSA/PBS for 1 hour at RT. After washing one more time with PBS 1x /0.1% Tween20, 30 seconds primary antibodies were applied diluted in 1% BSA/PBS. Following antibodies were used: SET7/SET9 (#2813 - Cell Signaling, stock 35.3 µg/ml, used in 1:25 dilution) and Rabbit IgG #2729 - Cell Signaling, stock 1 mg/ml) used in same concentration as a negative control, were incubated for 1.5 hour in a humid chamber. Cells were washed 3 times with PBS for 5 minutes on shaker and one time with PBS 1x /0.1% Tween20, 30 seconds. Secondary antibodies diluted in 1% BSA/PBS Donkey-α Rabbit IgG Cy3 (#711-165-152 – Dianova, 1:400) and DRAQ5 (#4084L - Cell Signalling, 1:1000) for nuclear staining and incubated for 45 minutes After washing 4 times for 5 minutes with PBS, slides were mounted with Fluorescent mounting media (Dako) and kept at 4°C. Expression and localization was analysed using the Leica TCS SP8 confocal laser scanning microscope.

2.6 RNA-related methods

2.6.1 Isolation of total RNA

Cells were lysed in TRK lysis buffer, and RNA was isolated using E.Z.N.A. Total RNA kit according to the manufacturer's instructions (Omega Bio-tek). A working solution of TRK Lysis Buffer was made prior to starting by mixing 20 µl of ß-mercaptoethanol per 1 ml of TRK Lysis Buffer. $3x10^6$-$1x10^7$ cells were disrupted by adding 350 µl of TRK Lysis Buffer. The cells were homogenized by passing the lysate 10-15 times through a needle fitted with a syringe. An equal volume of 70% ethanol was added to the lysate. Each sample was vortexed and applied to a HiBind RNA spin column placed into a 2 ml collection tube. The column was centrifuged at 10,000 g for 1 minute. The flow-through was discarded, and the column was

washed once with 500 µl of RNA wash buffer I and two times with 500 µl of RNA wash buffer II. After the last centrifugation, the column was placed in a 1.5 ml RNAse-free Eppendorf tube. The RNA was eluted with 40 µl of RNase-free water preheated at 70°C at maximum speed for 1 minutes The concentration of isolated RNA was determined with a Tecan Infinite® 200. The quality of the obtained RNA samples was analysed on 1% agarose gel. Isolated samples were stored at -80°C until use.

2.6.2 cDNA synthesis

cDNA synthesis was performed using RevertAid RT Reverse Transcription Kit (Thermo Scientific) with oligo-dT primers according to the manufacturer's instructions. Shortly, 5 µl RNA was digested with 1 µl of DNase, 1 µl of DNase buffer 10X and 3µl of H_2O at 37°C for 40 min and followed by inactivation of the enzyme at 70°C. After digestion, 1 µl of Oligo dT primer and 1µl of H_2O was added to the above RNA sample. Annealing of the primer was done at 70°C for 5 minutes and the samples were placed on ice.

4 µl of Reaction Buffer 5x, 1µl Ribolock RNase inhibitor, 2µl of dNTP Mix(10M) and 1µl of Reverse transcriptase was added to the above sample and incubated at 42^{o}C for 1 hour and activity of the enzyme was stopped by an additional incubation at 70°C for 10 minutes. The obtained cDNA was diluted 1:10 with double distilled water and 1µl was used for RT-PCR.

2.6.3 Real-time PCR Taqman

Primers and probes were obtained from Eurofins (Germany). Dual-labelled probes were used containing FAM on the 5' end and a BHQ1 quencher at the 3' end of the sequence. A list of designed primers used in experiments is shown in Table 6. Primer sequences are shown from the 5' end to 3' end direction. For normalization 18SrRNA was used as a reference gene. Use of 18S was validated compared to other housekeeping genes (not shown). Taqman ready to use Human primers for S100A9 (Hs00610058_m1), S100A12 (Hs00942835_g1), ARRDC4 (Hs00411771_m1) and CCL24 (Hs00171082_m1) were obtained from ThermoFisher Scientific. Primers for IL1B, CCR2 and 18SRNA were designed.

Table 6. Primers used to determine mRNA expression by RT-PCR.

Gene	Primer	Sequence (written 5' - 3')
CCR2	Forward	GACCAGGAAAGAATGTGAAAGTGA
CCR2	Reverse	GCTCTGCCAATTGACTTTCCT
CCR2	Probe	CACAAGGACTCCTCGATGGTCGTGG

IL-1B	Forward	ACAGATGAAGTGCTCCTTCCA
IL-1B	Reverse	GTCGGAGATTCGTAGCTGGAT
IL-1B	Probe	CTCTGCCCTCTGGATGGCGG
18S rRNA	Forward	CCATTCGAACGTCTGCCCTAT
18S rRNA	Reverse	TCACCCGTGGTCACCATG
18S rRNA	Probe	ACTTTCGATGGTAGTCGCCGTGCCT

2.6.4 Primer design and optimization

GenScript Real-time PCR (TaqMan) online Primer Design tool was used to design primers and probes for your Real-time PCR experiments. PCR amplicon's size range of ideally 100-200bp and primer Tm (melting temperature) between 52-60°C and probe Tm 62-70°C and an optimum CG content of 50%. A primer matrix (Table 7) with the forward and reverse primers was used to determine the optimal primer concentrations for RT-PCR which gives the lowest threshold cycle (Ct) and maximum reporter minus baseline signal. Primer optimization was performed with a fixed probe concentration of 250 nM. After the primers were optimized, probe optimization was performed with the following concentrations: 50nM, 100nM, 150nM, 200nM and 250nM. The primer and probe combination that yielded optimal assay performance was chosen for further experiments.

Table 7. Matrix for primer concentrations.

Primer Design Matrix				
	Forward Primer (nM)			
		50	300	900
Reverse Primer (nM)	50	50/50	300/50	50/900
	300	50/300	300/300	300/900
	900	50/900	300/900	900/900

A PCR reaction mix was prepared as described (Table 8) and amplification was performed using PCR reaction program (Table 8) by LightCycler 480 (Roche).

Table 8. PCR reaction mix

Reagent	Volume for 1 PCR reaction (10 µl)
TaqMan Gene Expression Master Mix	5 µl
TaqMan primer mix (target)	0.5 µl
TaqMan primer mix (reference)	0.5 µl
cDNA	1 µl
Distilled water	3 µl

Table 9. PCR reaction program.

	Temperature	Time
a. Initial denaturation	95°C	3 minutes
b. Denature	95°C	10 seconds
c. Anneal and extension	60°C	30 seconds
d. Repeat steps a. and b. for a total of 50 cycles		

2.7 Protein techniques

2.7.1 Western blot

Whole cell lysates of macrophages were collected by plating the cells on ice and taking the medium to collect also the floating cell. 50 µl of 2x Laemmli buffer supplemented with 2% ß-mercaptoethanol was added per $1x10^6$ cells and cells were collected together with the cells in the medium. Protein concentrations were measured by Pierce™ BCA Protein Assay kit**.** Samples where heated for 2-3 minutes at 95^{o}C, and 10 µg of protein was used for loading on the gel.

A 15 % separation gel was prepared according to Table 10 and poured between the two glass plates to cover 80 % of the unit. Isopropanol was added on top and the separation gel was left to polymerize until it was solid. A stacking gel was prepared according to Table 10 and poured on top of the separation gel. A comb was inserted into the stacking gel to form loading wells. The gel was left to polymerize until it was solid. The gel casting unit was transferred to the electrophoresis unit and filled with 1x TGS running buffer. 5 µl of PageRuler™ Plus Prestained Protein Ladder (#26619, Thermo scientific) was pipetted into the first well. Electrophoresis was performed at a constant current of 20 mA for 1 gel and 40 mA for 2 gels.

The gel was placed in a plastic container filled with blotting buffer. Filter papers and a nitrocellulose membrane were cut to the gel size. The Western Blot cassette was arranged in

the following order: Spongy pad/ 2x Whatmanpaper / gel/ nitrocellulose blotting membrane 0.2 µm / 2x Whatmanpaper / Spongy pad. The cassette was placed in the blotting device, which filled with blotting buffer. The blotting was done at a constant current of 150 mA overnight. The membrane was washed in a plastic container with PBS and then stained with Ponceau S solution for 10 min to visualize the protein bands. The membrane was washed and replaced into blocking buffer 6% Blotting Grade Blocker non-fat dry milk in PBS and then incubated for 1 hour. The membrane was further incubated with primary antibody diluted in 1% non-fat milk/PBS on a shaker for 3 hours at RT or O/N at 4 degrees. The membrane was washed 4 times for 5 minutes with 0.1% Tween 20/PBS on a shaker. The membrane was then incubated with the secondary antibody diluted in 1% milk/PBS for 45 minutes at RT on a shaker. The membrane was washed 4 times for 10 minutes with 0.1% Tween 20/PBS on a shaker. 2 ml western HRP development solution was added to cover the membrane, and the membrane was incubated for 2 minutes The X-ray film was developed with the CAWOMAT 2000 IR film processor.

Table 10. Buffer preparation for Western Blotting.

Components	**Volume (ml)**
Lysis buffer	*For 100 ml with ddH2O*
1M Tris ph7,4	5
NaCl 5 M	3
10% NP-40 solution	10
10% Sodium Deoxycholate	2,5
0,5 M EDTA (Gibco)	0,2
Use fresh 10 ml lysis buffer + Protease inhibitor cocktail	
Blotting-buffer= „Towbin-Puffer“	*For 1L*
ddH_2O	700
Methanol	200
10x TGS	100

Table 11. Preparation of gels.

Components	Separation gel 15% For 25 ml	Stacking gel For 10 ml
H_2O	5,57	6,8
30% Acrylamide mix	12,5	1,7
1,5 M Tris (pH 8.8)	6,25	1,25
10% SDS	0,25	0,1
10% APS	0,25	0,1
TEMED	0,01	0,01

Table 12. Antibodies used for Western Blotting.

Antibody	Company	CatNr	Dilution
Anti-S100A8	R&D	MAB4570	1:250
Anti-S100A9	R&D	AF5578	1:1000
Anti-S100A12	R&D	AF1052	1:200
Anti-B-actin	Santa cruz	sc47778	1:500
Anti-mouse HRP	Amersham	NA931	1:2000
Anti-sheep HRP	R&D	HAF016	1:1000
Anti-goat HRP	R&D	HAF017	1:1000

2.7.2 Flow cytometry

Frozen PBMCs of healthy controls and diabetic individuals, were resurrected and plated in RPMI+10% FCS+1% P/S and incubated overnight at 37°C, with the diabetic group consisting of patients with severe complications, consisting of nephropathy and additional patients with nephropathy and cardiovascular disease. The next day, the cells were harvested and washed with PBS. Fixable viability dye (FVD, Thermofisher) was added to all unstained, IgG control and stained FACs tubes and incubated for 30 minutes at 4°C protected from light. Cells were washed twice with FACS Buffer (PBS +0.4% BSA +0.02 NaN3). 10 µl FcR Blocking Reagent (Miltenyi Biotec) was added to all tubes and incubated for 5 min at RT. Antibodies were added to stained tube and incubated 20 minutes at 4°C in the dark. Cells were washed twice with cellwash, resuspended cells in PBS and fixed with 3.5% Formaldehyde while vortexing. After 15 minutes at RT in the dark, cells were washed with PBS and resuspended in 0.1% Saponin (Roth) and left on ice for 15 minutes. Cells were centrifuged, resuspended in

0.1% Saponin. 10 µl FcR block was added and incubated for 5 minutes on ice. For intracellular staining antibodies or isotype controls for the critical colours were added to the respective tubes and incubated for 30 minutes on ice. Cells were washed twice with 0.1% Saponin, resuspended in FACS Buffer and analysed by BD FACS Canto II.

Antibodies for the following markers were used: HLA-DR, CD3, CD19, CD56, CD16, and CD14 (Biolegend). First, cells were selected that were positive for HLA-DR. All cells that were positive for CD3, CD19, and CD56 were excluded. Using a scatter plot of CD16 versus CD14 monocyte population were separated into classical (CD14+CD16-), non-classical with low CD14 expression (CD14-CD16+) and intermediate (CD14+CD16+) monocytes. These populations were analysed for the expression S100A9 and S100A12.

Table 13. Antibodies used for flow cytometry.

Marker	Conjugate	Control isotype-matched ab	Volume per assay (µl)
CD16	APC	Na	2,5
CD3	FITC	Na	1
CD19	FITC	Na	1
CD56	FITC	Na	1
CD14	PerCPCy5.5	Na	1
HLA-DR	PE Cy7	Na	0.5
S100A9	PE	IgG1, κ	0.5
S100A12	AF405	IgG2b	5

na: not applicable

2.7.3 Enzyme-Linked Immuno Sorbent Assay (ELISA)

Concentrations of secreted cytokines were analysed in the conditioned medium (also named supernatants) of M0, M1 and M2 macrophages cultured under normal and high glucose conditions using ELISA assays from R&D systems (Wiesbaden, Germany) according to the manufacturer's instructions. 96 well plates were coated with capture antibody at working concentration for overnight incubation. The next day these plates were washed with washing buffer (0.05% Tween® 20 in PBS pH: 7.2-7.4) and plates were blocked with Reagent Diluent (1% BSA in pH: 7.2-7.4) for 1 hour. After blocking, 50 µl of sample or 100 µl of standards in Reagent Diluent was added per well and incubated for 2 hours. After incubation, wells were washed 3 times with washing buffer, and 100 µl of detection antibody was added according to

the manufacturer's instructions and incubated for 2 hours. After incubation, wells were washed 3 times, and 100 µl of Streptavidin-HRP diluted in Reagent Diluent was added to each well and incubated for 20 minutes After incubation, wells were washed 3 times and substrate solution was added to each well and incubated for 20 minutes Blue colour development was controlled and 50 µl of stop solution (2N H2SO4) was added to stop the reaction. Optical density of each well was measured immediately, using a micro plate reader (Tecan Infinite® 200) at 450nm.

2.8 Glucose uptake assay

Glucose uptake was measured by Glucose uptake cell-based assay kit (Cayman chemical, USA). Cells were seeded in 96-well plate (black with clear bottom) $1x10^5$ per 100 µl. At day six the medium was changed to Zero glucose SFM and incubated at 37^o for 2 hours. Ten minutes before measurement, 2-NBDG (100-200µg/ml) and/or 100µM WZB117 GLUT1 inhibitor (Cayman chemical, USA) as a negative control, were added to the cells. Cells were kept in dark to prevent bleaching. Cells were washed once with PBS. 100 µl PBS was added and glucose uptake was analysed immediately using a micro plate reader (Tecan Infinite® 200) at a fluorescence intensity of 485/535nm.

2.9 Chromatin-Immunoprecipitation (ChIP)

2.9.1 Chromatin isolation.

ChIP is used to recognize relative abundance of chromatin fractions which contain a specific antigen. Specific antibodies are used which recognize a specific protein or histone modification of interest and its interaction at one or more locations in the genome.

ChIP assays were performed with SimpleChIP® Enzymatic Chromatin IP Kit (Cell Signaling Technology) according to the manufacturers' protocol. Cells were fixed and the antigen of interest is cross-linked to its chromatin binding site with 1% formaldehyde for 10 minutes at RT. Glycine was added for 5 minutes to quench the formaldehyde and terminate the cross-linking reaction. From every culture dish cells were washed twice with ice-cold PBS scraped and taken in 2 ml PBS + 10 µl PIC buffer.

2.9.2 Immunoprecipitation

One immunoprecipitation preparation (IP prep) was defined as 5×10^6 cells. Cells were washed once in buffer A and nuclei were pelleted and resuspended in buffer B. Chromatin was digested with micrococcal nuclease with an optimized ratio of 0.5 µl per IP prep and

sonicated 9 cycles with high intensity and ON-OFF intervals (Diagenode UCD-200TM-EX) to obtain fragments of 150 to 900 base pairs. For immunoprecipitation digested chromatin was diluted into ChIP buffer and 2 µg of DNA and 2 µg of primary antibody (Table 14) was used in a final volume of 0.5 ml and incubated at overnight at 4°C with rotation. Normal rabbit immunoglobulin G (IgG) was used as a negative control for the pull down and Anti-histone H3 (D2B12 antibody) was used as a positive controls.

Table 14. Antibodies used for ChiP assay.

Antibody	Company
Anti-H3K4me1	Abcam (#8895)
Anti-H3K4me3	Merck Millipore (#07-473)
Anti-Ace H3	Merck Millipore (#06-599)
Anti-rabbit IgG	Abcam (#27478)
Anti-Total H3	Cell Signaling (#4620)

2.9.3 Elution of chromatin, reversal of cross-links and DNA purification

Immune complexes were captured using 30 µl of ChIP Grade Protein G Magnetic Beads. The chromatin was eluted, and crosslinks were reversed by adding 6 µl 5M NaCl and 2 µl Proteinase K and incubation for 2 hours at 65°C. The DNA was purified using QIAquick PCR Purification Kit. The amount of precipitated genomic DNA concentration was measured with a Tecan Infinite® 200.

2.9.4 Quantification of DNA by PCR

Samples were subjected to RT-PCR using primers for different promoter regions of S100A9, S100A12, IL1B and CCR2 (Table 15). 1 µl of DNA was added to each well. PCR reactions included a 2% input sample, isotype and total H3 control and one well with no DNA to control for contamination. Signals obtained from each immunoprecipitation are expressed as a percent of total input chromatin. IP efficiency was calculated with the following equation: Percent Input = 2% x 2(C_T 2%Input Sample – C_T IP Sample). Big differences by inefficient washing or contamination result in high background of IgG, when IgG was lower than 0.1% of the input control, we considered variation as negligible. Anti-histone H3 (D2B12 antibody) was used as a positive control. C_T values of the Input-samples were compared between normal and high glucose samples. With normalizing to H3 the density of specific chromatin

modification to the amount of nucleosomes on promoter was normalised. 3,000 bp upstream of the transcription start site (TSS), defined by SwitchGear genomics tool in the Epigenomebrowser.org was used to scan for suitable ChIP primers.

Table 15. Primers used for ChIP on the different promoters.

Gene promoter	Region	Primer name	Sequence 5' - 3'
S100A9	P1	S100A9 (1) F	GCCTGGTGCTAAGACTTTGG
		S100A9 (1) R	GCATGACAATGAAGCAGGGT
		S100A9 (1) Pr	AGCAGGCAGCATCCCTGCCT
	P2	S100A9 (2) F	TGAGCTCTTCCCAACTTTCCA
		S100A9 (2) R	CTCACACTGCTGAGATGCAC
		S100A9 (2) Pr	ACTGCCTAAGGTCACACAGACAGTCTG
	P3	S100A9 (3) F	GCATTACCACACTGCTCACC
		S100A9 (3) R	GAGCCACACAGAGTGTTTGC
		S100A9 (3) Pr	TGGCCCTTTGGCCCTGTCTC
	P4	S100A9 (4) F	TCCGGGTGTCAGTTTCTTCA
		S100A9 (4) R	TGCCTGGCTCTGTGATACTTA
		S100A9 (4) Pr	TGCAAGAGGGTTGCCCACCTCT
	P5	S100A9 (5) F	GCTGTGTGCATAGGAGAAGG
		S100A9 (5) R	TCTGGCTCTCAACACTTGCT
		S100A9 (5) Pr	TGCCTCTGTCCAACAATTGGCTGTAGA
S10012	P1	S100A12 (1) F	ACAGCCTGAGTGTCTTGTTT
		S100A12 (1) R	ACTGATCCTCTGCTCCAGTG
		S100A12 (1) Pr	ACCTCCTCCTAAGTCGTTCTGGGATGC
	P2	S100A12 (2) F	CCCACACCTGTGAAGATAAGC
		S100A12 (2) R	CCCACCCAGGTTGGTTTCTA
		S100A12 (2) Pr	ACCAATCTCACAACTTGCCCACAAGGA
	P3	S100A12 (3) F	AGGGCTAAGATGAAGCCTGA
		S100A12 (3) R	ACCACCTAAGAACCCATCCA
		S100A12 (3) Pr	TGCCCTTCACCACTGCTGGC
	P4	S100A12 (4) F	GGGATGCAGGAGAACAGACA
		S100A12 (4) R	GGCAGTTTGTGTTTGGTGGT

	S100A12 (4) Pr	TGCTCCCACTGCCTGGTGCT
P5	S100A12 (5) F	CAATCAAGGCCATGCCAGAA
	S100A12 (5) R	CACATGGATCGGAGAGACAGA
	S100A12 (5) Pr	TGTGCCCACCGACCTCTCTGG

2.10 Statistical analysis

Statistical analysis was done by use of GraphPad Prism. Normality was tested before every assay. Bar graphs show mean ± SD, box & whiskers with 5-95% Confidence Intervals or data is shown as percentages where appropriate. The significance of the data was analysed using Student's t-test for parametric data and the Mann–Whitney test for nonparametric data, unless stated differently. The Pearson product-moment correlation was performed to measure the linear correlation between two variables X and Y. Two-way ANOVA was used for more than two groups followed by multiple comparisons tests. $P < 0.05$ was considered statistically significant, ns = non significant, $P > 0.05$*, $P \leq 0.05$**, $P \leq 0.01$ and ***$P \leq 0.001$.

3 RESULTS

3.1 Regulation of S100A9 and S100A12 expression

3.1.1 Hyperglycemia enhances the expression levels of S100A9, S100A12 among other genes in macrophages

To confirm results of Affymetrix chip analysis mRNA expression of *S100A9* and *S100A12*, were verified by RT-PCR and two other genes; *CCL24* - Chemokine binding to CCR3, eosinophil chemoattractant (Menzies-Gow, Ying et al. 2002) and *ARRDC4* - Adaptor protein with potential role in endocytosis of G protein-coupled receptors, which, when overexpressed, inhibits glucose uptake (Patwari, Chutkow et al. 2009).

S100A9 and *S100A12* were significantly higher expressed in M1 macrophages (P= 0.0155) and significantly lower expressed in M2 macrophages (P = 0.0194) under normal glucose conditions (Fig. 1). It was shown that hyperglycemia induces significantly higher levels of *S100A9* in M0 macrophages, up to 2.5-fold for individual donors (P = 0.0257) but mostly increased in M1 macrophages, which are stimulated with IFNγ, up to 4.4 fold increase (P = 0.0097) (Fig. 1). For *S100A12* a similar effect was seen; after six days hyperglycemia induced significantly higher levels of *S100A12* expression in M0 macrophages, up to 4.9 fold increase for individual donors (P = 0.0257) but mostly increased in M1 macrophages, up to 9.8 fold increase for individual donors (P = 0.0097) (Fig. 5).

Hyperglycemia also had an inducing effect on both *ARRDC4* and *CCL24* in different macrophage subtypes. Under normal glucose conditions *ARRDC4* was highest expressed in M2 compared to M0 macrophages (P = 0.0027). Glucose up regulated *ARRDC4* gene expression in all donors and in both M1 and M2 macrophages. We found the strongest increases for individual donors in M1 conditions; up to 12.9-fold increase. *CCL24* was not differentially expressed in M1 and M2 polarized macrophages under normal glucose conditions compared to M0 macrophages. Glucose increased the expression of *CCL24* in 7 out of 9 donors for M0 and 5 out of 9 donors for both M1 and M2 polarized macrophages. We find the highest *CCL24* expression and also the highest increase induced by glucose in individual donors in M1 polarized macrophages (Fig. 5).

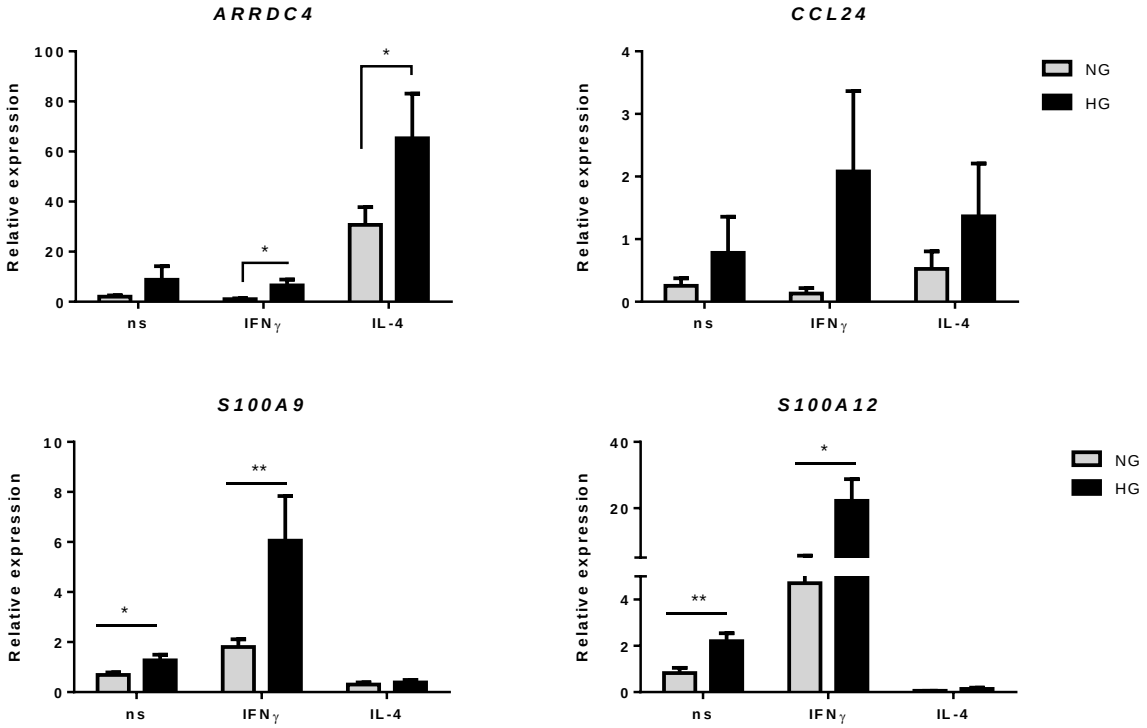

Figure 5. Analysis of the effect of hyperglycemia on the expression of ARRDC4, CCL24, S100A9 and S100A12. mRNA expression was analysed by RT-PCR in M0, M1 and M2 macrophages cultured for 6 days under normal (NG, 5mM) and high glucose (HG, 25mM) conditions. Data present mean ± SEM normalized to 18SrRNA expression levels. N=9 for *ARRDC4* and *CCL24*, n=6 for S100 genes. *p<0,05.

3.1.2 Cultivation in high glucose conditions does not change glucose uptake of M0 and M1 macrophages

The first step in glucose response is the entry of glucose into the cell. Since glucose metabolism determines immune cell activation and also long-term training of monocytes via the AKT–mTOR–HIF-1a pathway (Cheng, Quintin et al. 2014). Van Diepen et al. hypothesized that high circulating levels of glucose could program immune cells towards an inflammatory phenotype (van Diepen, Thiem et al. 2016). GLUT1 is the primary rate-limiting glucose transporter for proinflammatory macrophages (Freemerman, Johnson et al. 2014).

2-deoxc-2-[(7-nitro-2,1,3-benzoxadiazol-4-y)amino]-D-glucose or 2-NBDG was added to M0 and M1 macrophages which were on zero glucose medium for 2 hours. Uptake of the 2-NBDG was higher in M1 compared to M0 macrophages with 200 µg of 2-NBDG added. High glucose culture did not change the glucose uptake in M0 nor in M1 macrophages (Fig. 6).

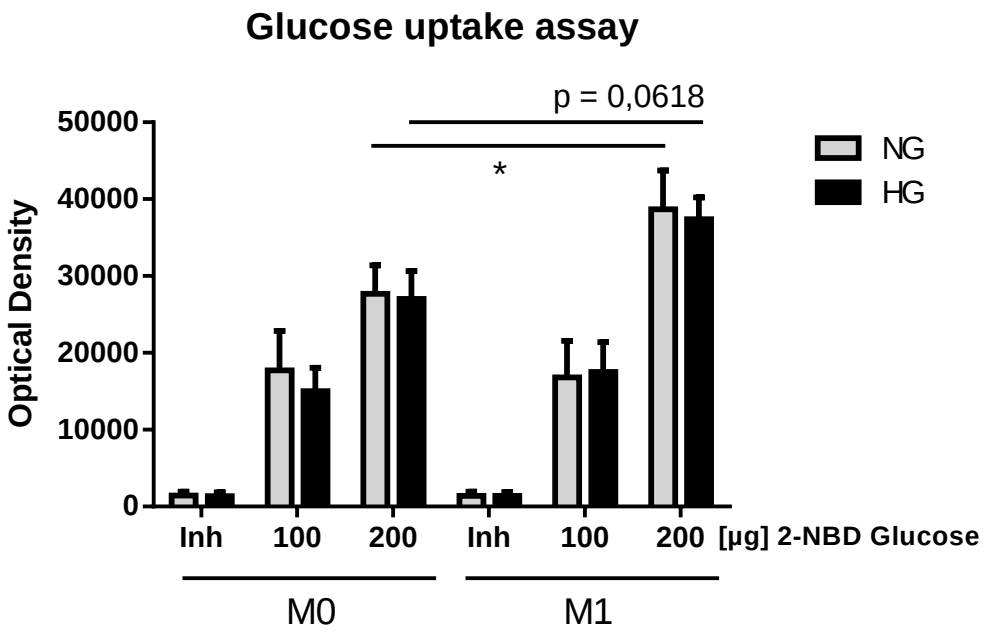

Figure 6. **Glucose uptake was not affected by hyperglycemic conditions.** M0 and M1 macrophages were cultured for 6d. Medium was changed to zero glucose medium and glucose uptake was measured after two hours by addition of 2-NBDG (100 and 200µg/ml) and control inhibitor of glucose uptake WZB (100µM). Statistical analysis was performed using paired two-tailed t-test. The difference was considered to be statistically significant in case of *p<0.05, n=4.

3.1.3 Hyperglycemia supports the expression of S100 genes during monocyte/macrophage differentiation under IFNγ stimulation

We determined the expression of *S100A9* and *S100A12* at different stages of maturation from monocytes into macrophage. It is known that *S100A8 and S100A9* mRNA levels decline during monocyte differentiation into macrophage (Averill, Barnhart et al. 2011). In our experiments, the expression of S100 mRNA drops during differentiation in all conditions (ns, IFNγ, IL-4). After *S100A9* is highest expressed in M1 macrophages compared to *S100A12* in M0 macrophages. Both genes were higher expressed in monocytes than macrophages and S100A12 was downregulated stronger during maturation into macrophages than *S100A9* (Fig. 7). But on the late stages of differentiation IFNγ again induces *S100A9* and *S100A12*. In addition, in high glucose conditions 9 out of 10 donors showed increased *S100A9* expression induced up to 4.9 fold (P= 0.0019) after 6 days, whereas 8 out of 10 donors showed increased *S100A12* expression induced by glucose up to 3-fold (P= 0.0155) after 6 days.

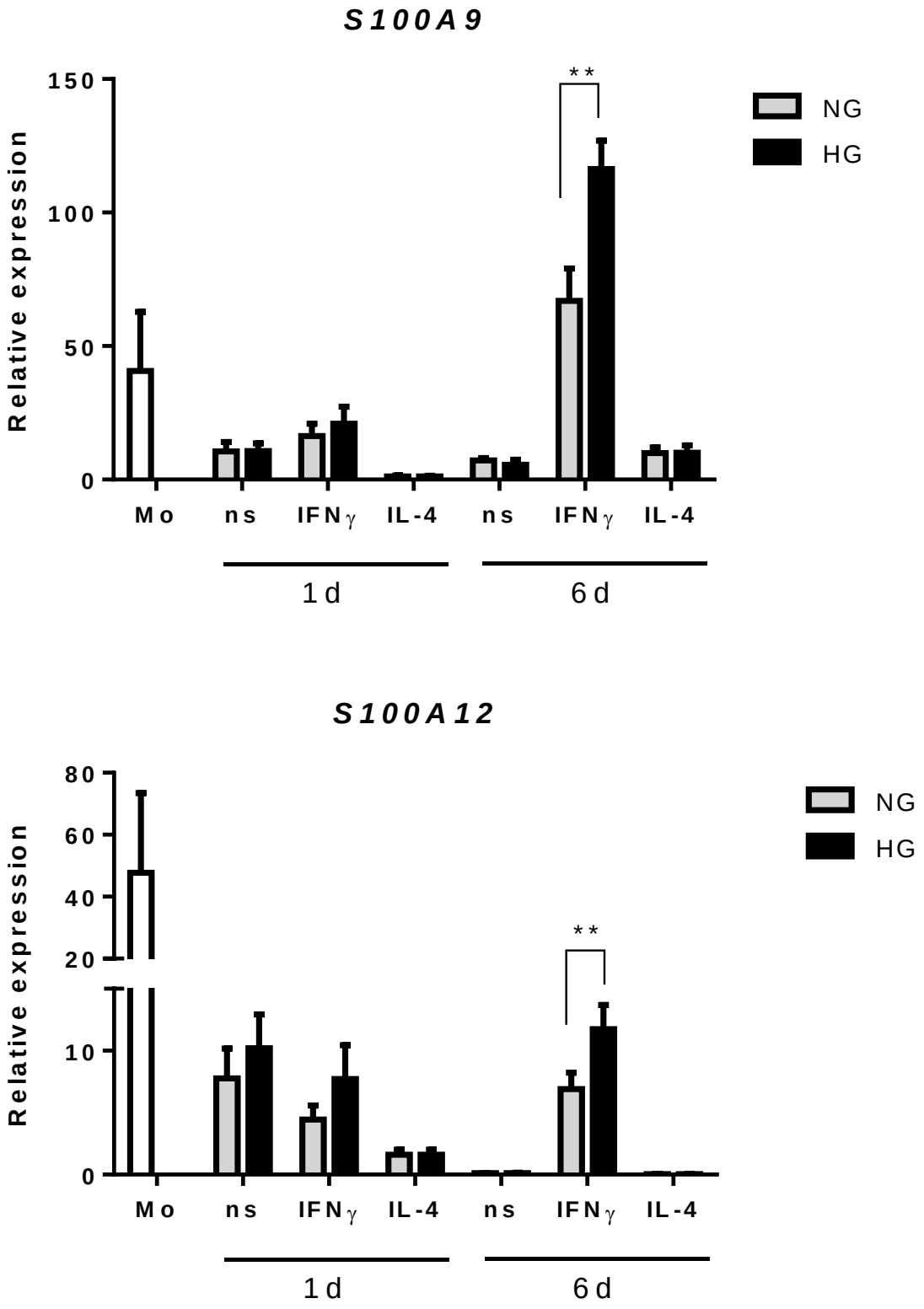

Figure 7. The expression levels of S100A9 and S100A12 are elevated by hyperglycemia in macrophages after 6 days. RT-PCR analysis of mRNA expression S100A9 and S100A12 in M0, M1 and M2 macrophages cultured under normal (NG) and high glucose (HG) conditions. Data present mean ± SD normalized to 18SrRNA expression levels. n = 9 and 8 respectively *p<0.05, **p<0.01

3.1.4 Hyperglycemia affects S100A9/A12 gene expression ratios

Since S100A9 is able to form heterodimers with S100A8 upon activation (Vogl, Gharibyan et al. 2012), we measured mRNA levels of *S100A8* in monocytes and macrophages from healthy donors. In contrast to *S100A9* and *S100A12* which are abundantly present in monocytes compared to matured macrophages we find that *S100A8* is present at mediate levels in monocytes compared to the maturated macrophages (data not shown). Under NG conditions the expression levels of *S100A8* and *S100A9* always significantly correlated whereas highest correlation was seen in M2 macrophages. Under HG conditions this correlation was even stronger, specifically in M0 and M2 macrophages (Table 16).

As analysis of calgranulin gene expression revealed higher levels of both *S100A9* and *S100A12* in macrophages cultured under high glucose conditions, it was examined whether there is a correlation between *S100A9* and *S100A12* expression levels in the different subtypes of macrophages. Under NG conditions the expression levels of *S100A9* and *S100A12* significantly correlated in M0 and M1 but not M2 macrophages. Under HG conditions this correlation between *S100A9* and *S100A12* expression decreased in favour of S100A9 (Table 16). In summary, S100A8 alone or as heterodimer with S100A9 seemed to be relevant in M2 macrophages as there almost linear correlation is found between *S100A8* and *–A9* expression levels. *S100A9* and *S100A12* expression are correlated in M0 and M1 macrophages, however under high glucose conditions this correlation decreased. The regulation of expression and ratio of the different S100 genes might provide more insight in the mechanism of inflammation.

Table 16. Linear regression analysis of S100 gene expression in human primary macrophages.

Gene			*NG*	*HG*
S100A8 / S100A9	M0	R^2	0,7603	0,8465
		p value	0,0235*	0,0093**
	M1	R^2	0,8275	0,833
		p value	0,0119*	0,0111*
	M2	R^2	0,7695	0,8924
		p value	0,0217*	0,0045**
S100A9 / S100A12	M0	R^2	0,519	0,05307
		p value	0,0286*	0,5831
	M1	R^2	0,9251	0,6
		p value	< 0,0001***	0,0085**
	M2	R^2	0,2859	0,405
		p value	0,138	0,0654

3.1.5 S100 Protein expression

We measured protein levels of S100A9 and S100A12 in monocytes and macrophages from healthy donors by Western blot. Similar as observed for mRNA expression, we find on protein level that S100A9 and S100A12 protein are more abundantly present in monocytes compared to matured macrophages (not shown). S100A9 is expressed in all types of macrophages. Both proteins were typically expressed in M1 macrophages (Fig. 8). During stimulation of cells with IL-4 S100A12 was deficient in some donors in M2 macrophage population, similar as seen on mRNA level before. Further differences in expression relate to different donor responses (Fig. 8). Thus, macrophages contain high levels of intracellular S100 proteins and protein expression had not changed significantly by stimulation with cytokines or culture under high glucose.

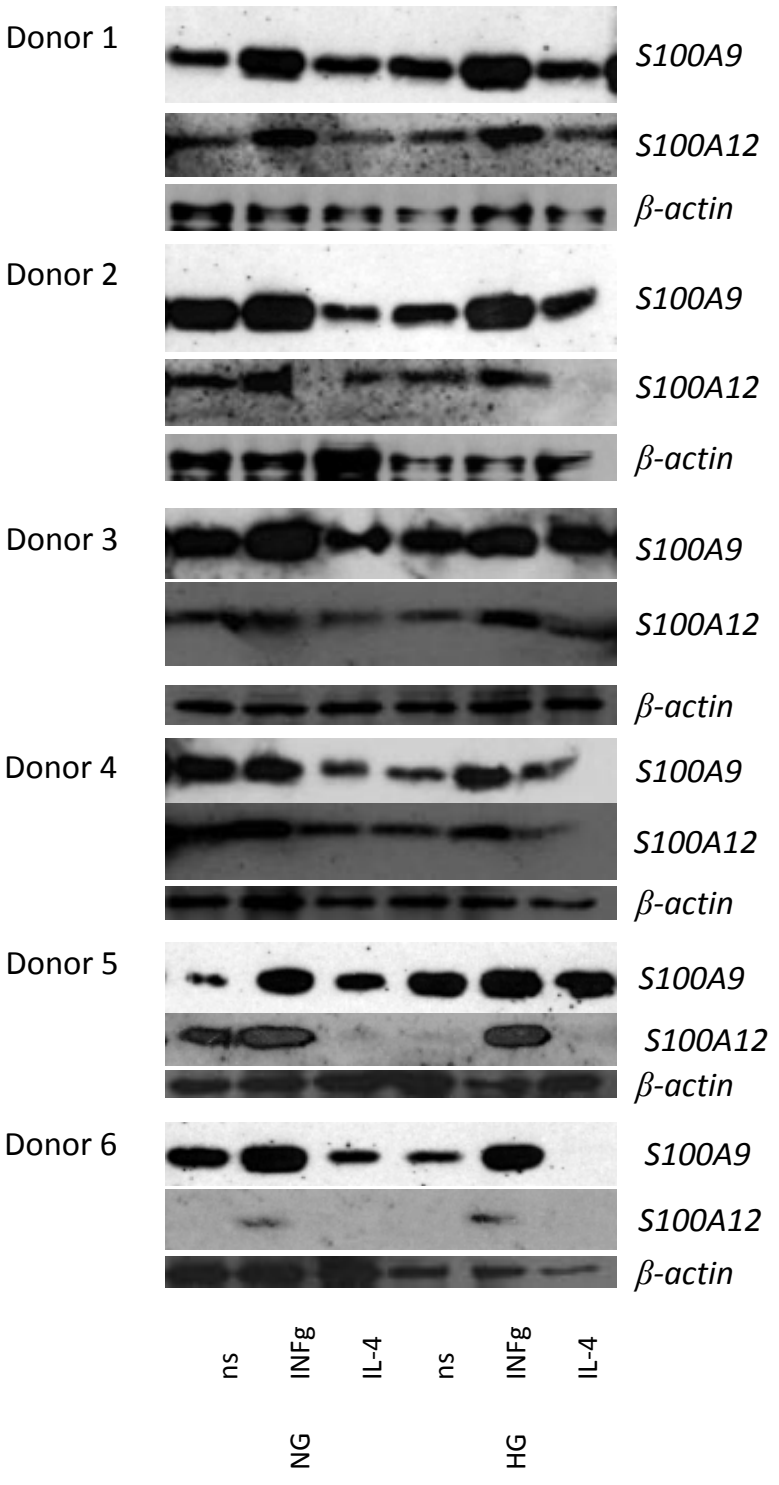

Figure 8. S100A9 and S100A12 protein expression in primary human macrophages. Western Blot analysis of protein expression S100A8, -A9 and S100A12 (n=6) in M0, M1 and M2 macrophages cultured for 6 days cultured under normal (NG) and high glucose (HG) conditions.

3.1.6 Secretion of S100A9 and S100A12

S100 proteins are either expressed intracellular or secreted into the extracellular space (Donato, Cannon et al. 2013). Secreted forms of S100A9 and S100A12 proteins were assessed by ELISA in different types of macrophages cultured in NG and HG conditions (Fig. 9). Secretion of S100A9 and S100A12 was measured at different time points; 6h, 24h and 6d after seeding the monocytes.

For S100A9 secretion, no significant effects were observed after 6 and 24 hours. After 6 days, there was a slight increase of secretion levels in M2 macrophages cultured in high glucose conditions compared to normal glucose ($P = 0.0361$ by student's t-test). The highest levels of S100A9 secretion we find in M1 macrophages with ranges between 990.7 ± 264.5 pg/ml under normal glucose conditions. HG medium tend increase to secretion of S100A9 in all types of macrophages but not to a significant level.

After 6 days, S100A12 secretion was lower in M2 macrophages compared to M0 macrophages under normal glucose conditions ($P=0.0248$). The highest levels of S100A12 secretion we find in M0 macrophages with ranges between 32997 ± 26615 pg/ml under normal glucose conditions. HG medium decreased secretion levels in M0 macrophages ($P=0.0006$). This effect was already seen after 24 hours already ($P = 0.0328$) (Fig. 9).

The data on secretion are much lower than serum levels seen in diabetic patients, seen from literature (Bouma, Lam-Tse et al. 2004, Nagareddy, Murphy et al. 2013, Ingels, Derese et al. 2015). It seems that macrophages cannot release the intracellular accumulated S100 protein, release only standard amount in cell culture or need an addition trigger from the *in vivo* microenvironment to be able to secrete the S100 protein e.g., cytokines, Fatty Acids (FA), AGEs or direct contact with activated endothelium or tend to have more intracellular functions.

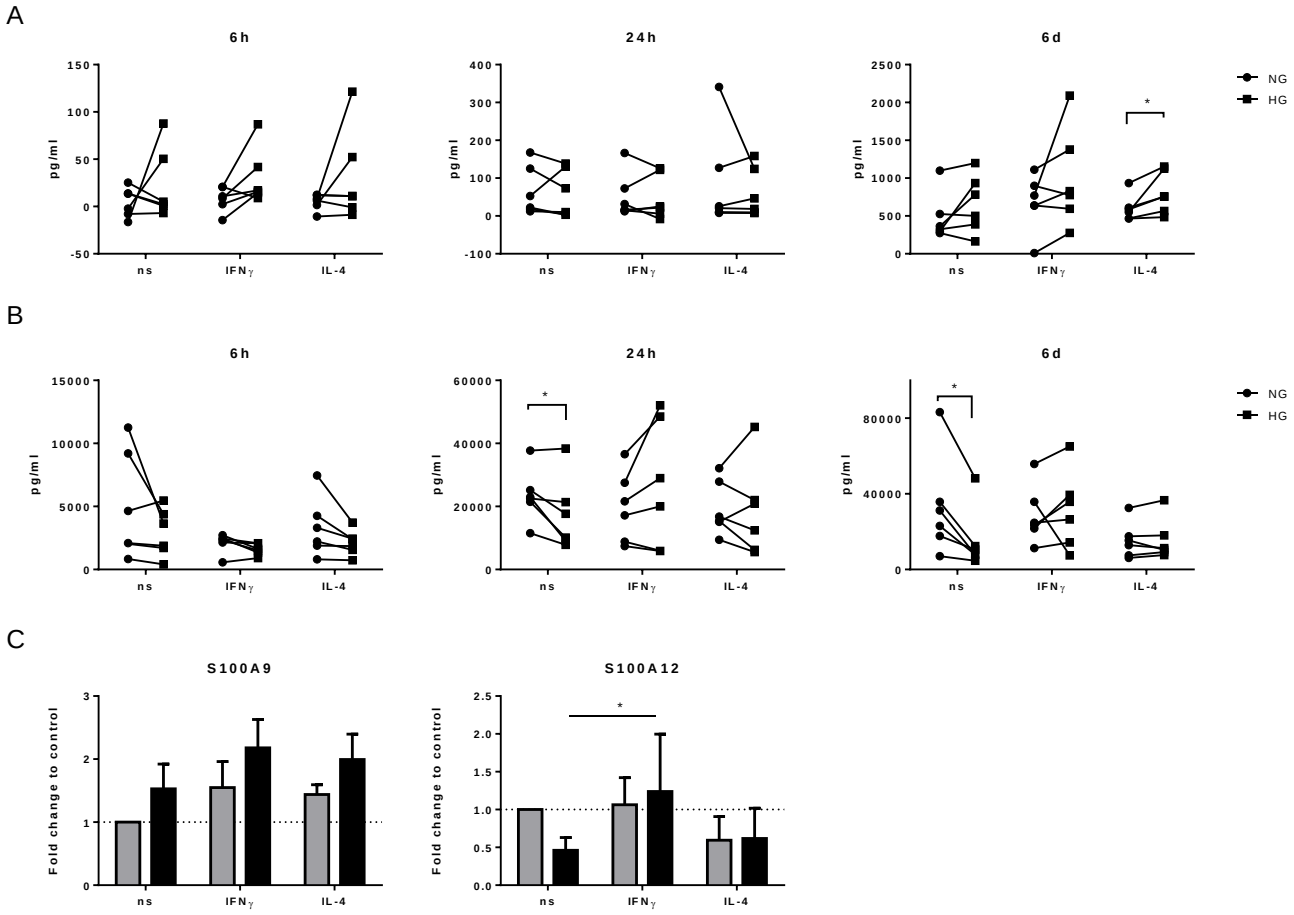

Figure 9. The effect of hyperglycemia on secretion of S100A9 (A) and S100A12 (B) in cultured M0, M1 and M2 macrophages after 6h, 24h and 6d (n=6). Data after 6d expressed as fold change increase compared to ns NG control (C). Student t-test and Two-way ANOVA for groups were used, n=6.

3.2 Expression of S100 proteins in diabetic patients

3.2.1 Gene expression in PBMCs of diabetic patients

Next we identified whether S100 genes are higher expressed and therefore relevant in prediabetic and diabetic patients. PBMCs of diabetic patients were kindly provided by Dr. Thomas Fleming (Department of Medicine I and Clinical Chemistry, Heidelberg-clinic). We measured gene expression of the individual genes in fractioned PBMC fractions and normalized to the expression of monocyte marker CD14. Within the group of T1D patients 75% of the subjects suffered from neuropathy, 37.5% retinopathy and 17.6% nephropathy in T1D. Also, patients with T2D diabetes suffered from polyneuropathy (76.2%) and nephropathy (52.4%) and showed albuminuria (Table 17).

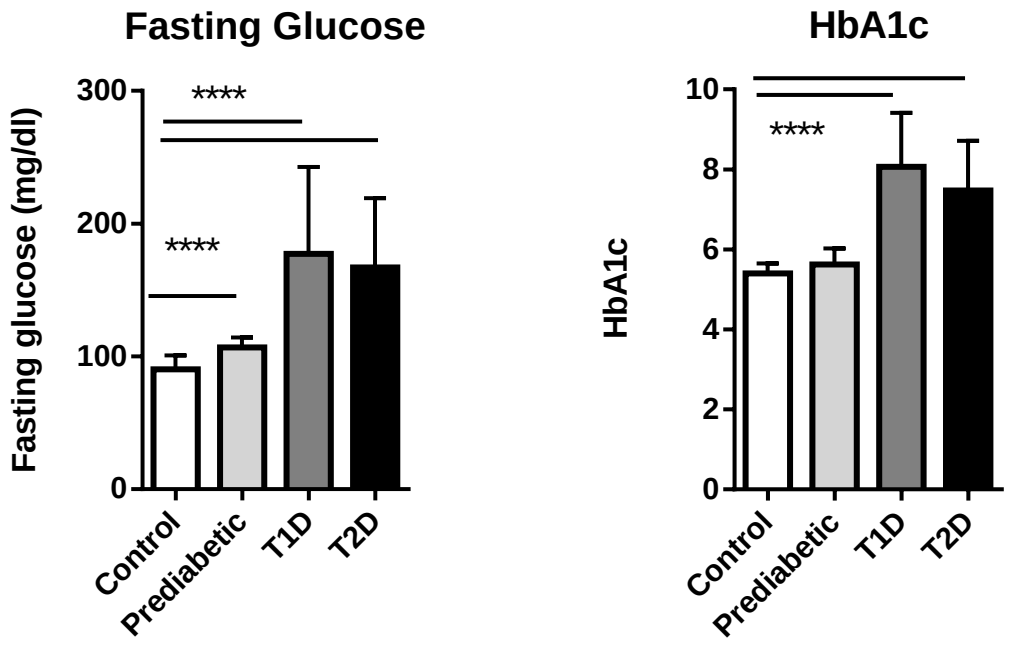

Figure 10. Fasting glucose and HbA1c levels in prediabetic individuals, diabetic patients and healthy controls. Pre-diabetic subjects were defined based on increased fasting glucose between 100-125mg/dl or an impaired glucose tolerance – with elevated blood glucose levels between 140-199mg/dl after intake of 75g glucose. Control (n=21), Prediabetic (n=19), T1D (n=19) and T2D (n=21).

Table 17. Characteristics according to patient diagnosis.

	T1D (n=19)	T2D (n=21)	Prediabetic (n=19)	Control (n=21)
Age (years)	50,2 ± 18,1	59,7 ± 6,1	59,1 ± 7,6	57,9 ± 7,4
Sex (women)	56%	48%	47,4%	57%
Diabetes duration (years)	31,1 ± 14,4	9,7 ± 6,0		
Size (cm)	172 ± 11	171 ± 10	171 ± 8	169 ± 10
Weight (kg)	79,8 ± 15,6	96,8 ± 19,6 *	97,8 ± 21,7 *	84,0 ± 18,2
BMI (kg/m2)	26,8 ± 4,3	31,4 ± 9,3	33,4 ± 7 *	29,2 ± 4,3
Smoking (%)	20,0	25,0	5,6	-
Retinopathy (%)	37,5 *	14,3	5,3	4,8
Polyneuropathy (%)	75,0 ***	76,2 ***	-	-
Fasting glucose (mg/dl)	177,2 ± 63,4 ***	167,0 ± 52,2 ***	106,7 ± 7,5 ***	90,2 ± 9,4
HbA1c	8,3 ± 1,6 ***	7,5 ± 1,2 ***	5,6 ± 0,4	5,5 ± 0,3
eGFR		95,6 ± 13,3	87,8 ± 11,9	92,9 ± 14,5
Urine Creatinine	91,9 ± 56,8	108,4 ± 63,3	130,5 ± 79,6	113,8 ± 57,2
Urine Albumin	39,9 ± 67,5	88,8 ± 137,8 *	13,9 ± 11,1	8,3 ± 4,0
U_ACR	16,0 ± 18,4	22,0 ± 27,4	2,9	
Nephropathy (%)	17,6 *	52,4 ***	11	-
NSS	4,0 ± 2,6	6,2 ± 2,5		
NDS	4,1 ± 3,0	4,5 ± 2,8		

Values represent mean ± SD or percentages (%). Control vs. other groups *p < 0.05, **p < 0.01 *** p < 0.001. BMI – Body Mass Index, eGFR - Estimated Glomerular Filtration Rate, ACR - albumin/creatinine ratio, NSS - Neuropathy Symptoms Score, NDS - Neuropathy Disability Score.

We measured gene expression levels in PBMCs and normalized to CD14. Data were not normally distributed therefore we presented the medians. We found *S100A9* tend to be higher expressed in T2D whereas *S100A12* was higher expressed in T1D patients (not significant by Kruskal-Wallis test) (Fig. 11). However, we found similarly that *S100A9* and *S100A12* expression are very tightly correlated in T1D, T2D and healthy controls (P = < 0.0001 for all three) but not in prediabetic individuals (Table 18).

Then, it was examined whether correlations found for are specific for S100 genes other inflammatory macrophage markers *IL-1B* and *CCR2*. We found *IL1B* tend to be higher expressed in T2D (not significant by Kruskal-Wallis test). The *CCR2* expression did not differ between the groups.

Table 18. Correlation between *S100A9* and *S100A12* expression in monocytes from healthy controls, prediabetic individuals and diabetic patients, normalized to CD14 expression.

Patient PBMCs normalized to CD14+

	Control	*Prediabetic*	*T1D*	*T2D*
R^2	0,8091	0,1403	0,878	0,9778
p value	< 0,0001***	0,169	< 0,0001***	< 0,0001***

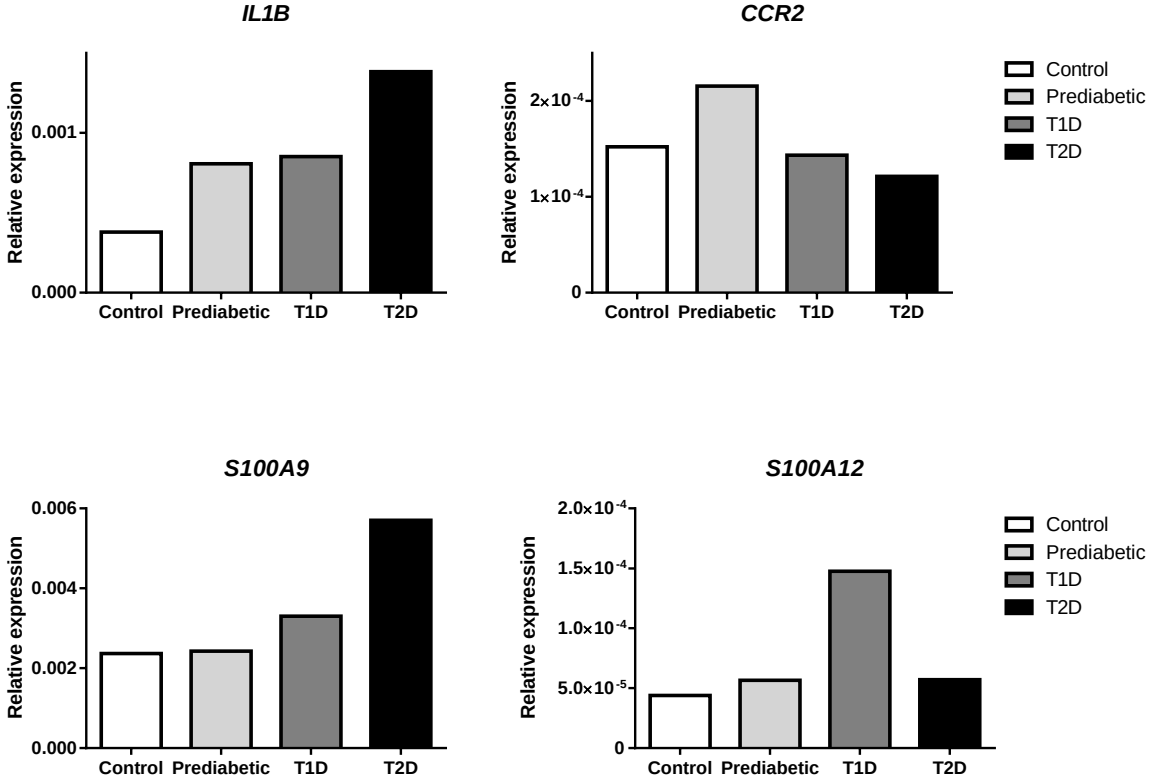

Figure 11. RT-PCR analysis of *IL-1B, CCR2, S100A9* and *S100A12* expression in PBMCs from prediabetic individuals, diabetic patients and healthy controls normalized to CD14 expression. Data present medians. Kruskal Wallis followed by Dunn's multiple comparisons test.

Regarding the variables age, weight, BMI, glucose and HbA1c the ANOVAs yielded significant results (Scheffe's post hoc test used for pairwise comparisons). According to descriptive statistics for the total group (n = 76), the distributions of the gene expressions are skewed and not normally distributed. Therefore, logarithmic transformation was used for statistic tests. Pearson correlation coefficients showed no significant correlation between inflammatory gene expression and fasting glucose levels in prediabetic individuals. Yet, diversity in expression resembles diversity in response but not the absence of response. Some individuals with high expression show high FG levels (Fig. 12). We did not observe a correlation between gene expression levels and HbA1c levels, BMI or weight as well (data not shown).

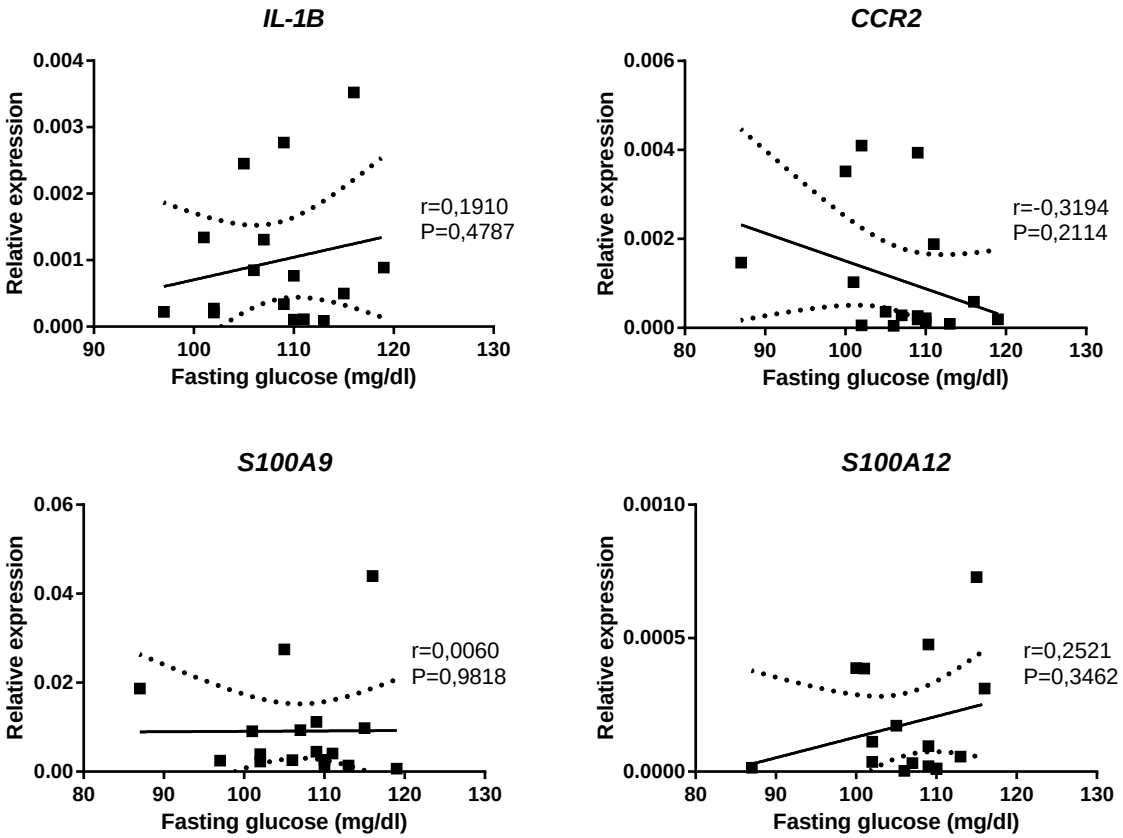

Figure 12. Correlation between *IL-1B* and *CCR2, S100A9* and *S100A12* expression and fasting glucose in pre-diabetic individuals. Number of XY Pairs = 16. Graphs show 95% confidence band of best-fit line. Correlation coefficient (r) and p-value are given in the graphs.

3.2.2 Protein expression in monocytes of diabetic patients

Since no significant changes in *S100A9* and *–A12* gene expression levels were found in diabetic patients we sought to investigate protein levels in PBMCs of patients with microvascular complications. Plasma levels of S100 proteins have been assessed in diabetic patients but not protein expression in blood cells (Basta, Sironi et al. 2006, Pedersen, Nybo et al. 2014, Dong, Shi et al. 2015). To this end, intracellular expression levels of S100A9, S100A12 were assessed in monocytes form T2D with cardiovascular disease and/nephropathy. First, changes in different monocyte subsets were characterised; designated as classical (CD14+ CD16-), intermediate (CD14+ CD16+) and non-classical monocytes with low CD14 expression (CD14- CD16+).

Table 19. Clinical characteristics of the patients and control individuals.

Variable	Healthy controls (n=5)	T2D with complications (n=12)
Age (years)	54,0 ± 12,1	67,4 ± 10,8
Sex (%female)	100%	42%
BMI (kg/m2)	25,1 ± 2,4	31,5 ± 6,1
Waist circumference (cm)	85,4 ± 3,4	111,6 ± 14,2
Current smoke (%)	20%	16%
Hypertension	0%	83%
Cardiovascular disease (%)	0%	67%
Cholesterol (mg/dl) (mmol/l)	200,0 ± 46,0	196,2 ± 60,2
HDL (mg/dl) (mmol/l)	71,2 ± 29,6	44,5 ± 10,3
LDL (mg/dl) (mmol/l)	114,8 ± 26,4	107,8 ± 49,4
Triglycerides (mg/dl) (mmol/l)	70,6 ± 39,0	304,2 ±389,1
Glucose (mg/dl) (mmol/l)	89,8 ± 7,4	192,9 ± 101,4
HbA1c (%) (mmol/l)	5,4 ± 0,1	7,9 ± 1,4

Values represent mean ± SD or percentages (%). Control vs. other groups *p < 0.05, **p < 0.01 *** p < 0.001. BMI – Body Mass Index, HDL - High-density-lipoprotein, LDL – Low-density-lipoprotein, HbA1c - Hemoglobine A1c

First, we evaluated whether the distribution of the different monocyte populations had changed in T2D compared to healthy controls. We found that the most abundant were classical monocyte population, which encompassed 10.5 ± 7.8% of the total monocyte population for healthy individuals compared to 12.4 ± 7.8% of T2D patients with cell counts between 2252 and 41899 (Fig. 13A).

In the diabetic subgroups healthy control group showed the least and T2D with cardiovascular complications (CVD) the relative highest number of classical CD14+ monocytes, whereas T2D+CVD with additional nephropathy (N) showed the highest number of intermediate monocytes CD14+, CD16+ (Fig. 13B).

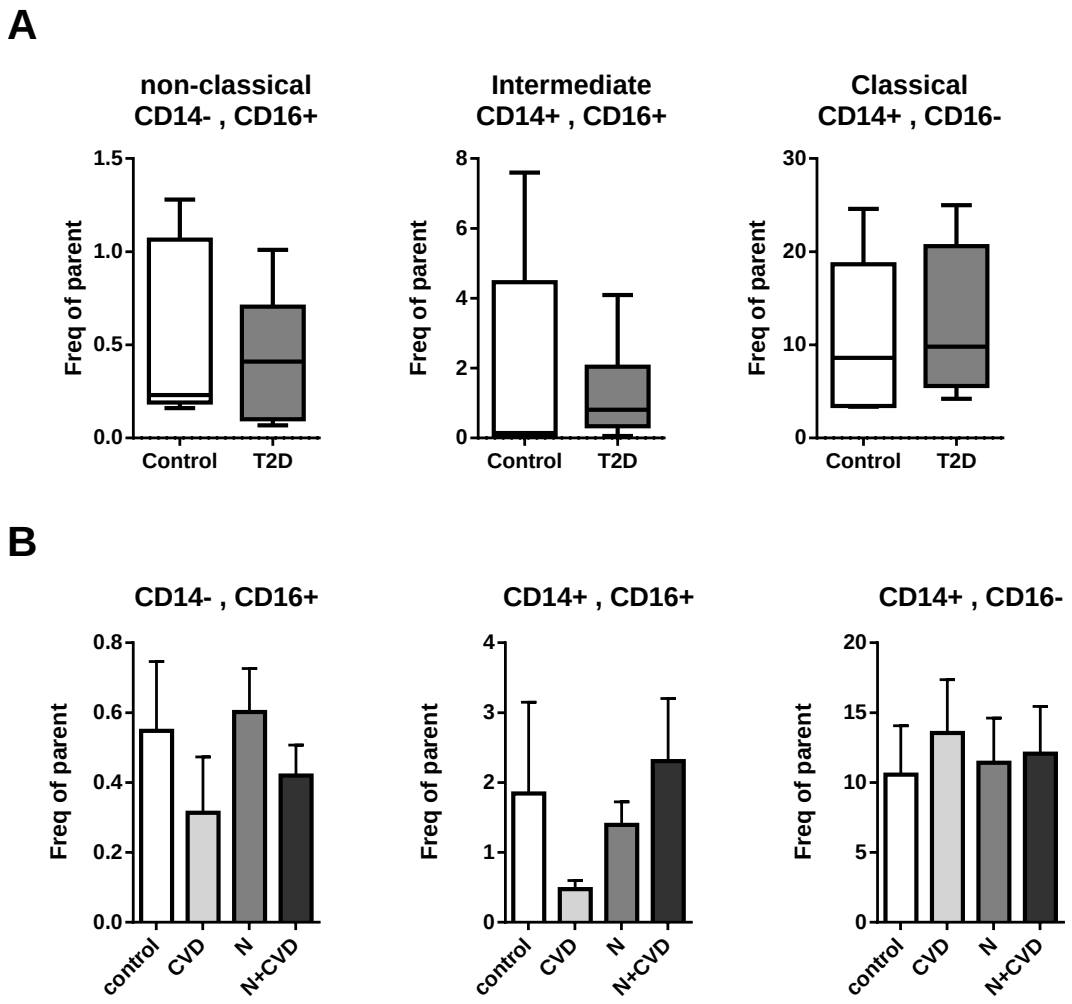

Figure 13. Classical, intermediate and non-classical monocytes subsets from T2D patients with microvascular complications were analysed based on CD14+ and CD16+ expression by FACs. Cells positive for HLA-DR were selected and all cells expressing CD3, CD19 and CD56 were excluded. A) Monocyte subsets in total T2D group compared to healthy controls. B) Monocyte subsets in T2D patients with different vascular complications compared to healthy controls. Cardiovascular disease (CVD), nephropathy (N) and both, compared to healthy controls. Mann Whitney test (A) and One-way ANOVA with Dunnett's multiple comparisons test (B) were used.

Next, expression of S100A9 was analysed in the different monocyte populations as its expression has been shown to vary between the monocyte populations of healthy donors (Yang, Anholts et al. 2018). The median fluorescence intensity (MFI) of S100A9 in classical monocytes was 1.18 times (12703 MFI units), higher compared to 4.08-fold (5193 MFI units) in non-classical monocytes and 1.39 times (35085 MFI units) fold in intermediate monocytes (Fig 14). Thus, for T2D patients with microvascular complications highest absolute increase in S100A9 expression was observed in the intermediate monocytes.

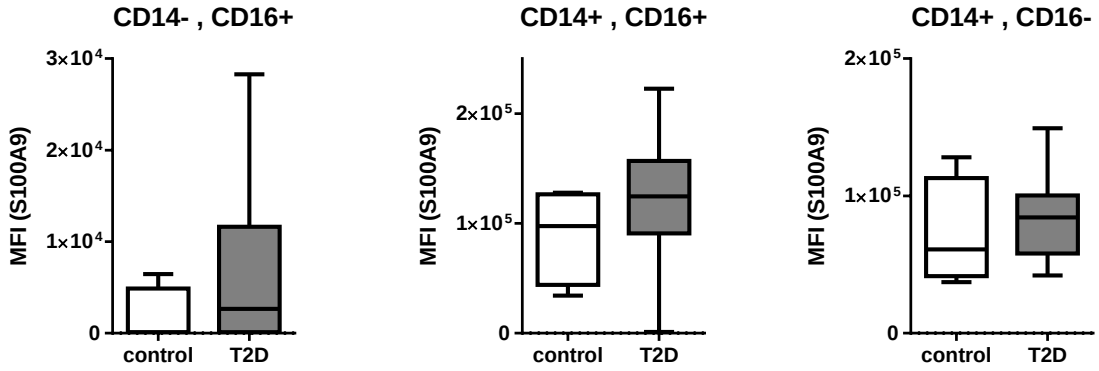

Figure 14. Intracellular S100A9 expression in different monocyte populations. Protein expression was analysed by FACS in cells positive for HLA-DR negative for CD3, CD19, CD56 were excluded. T2D patients with microvascular complications, cardiovascular disease (CVD), nephropathy (N) and both (n=21) compared to healthy controls (n=5).

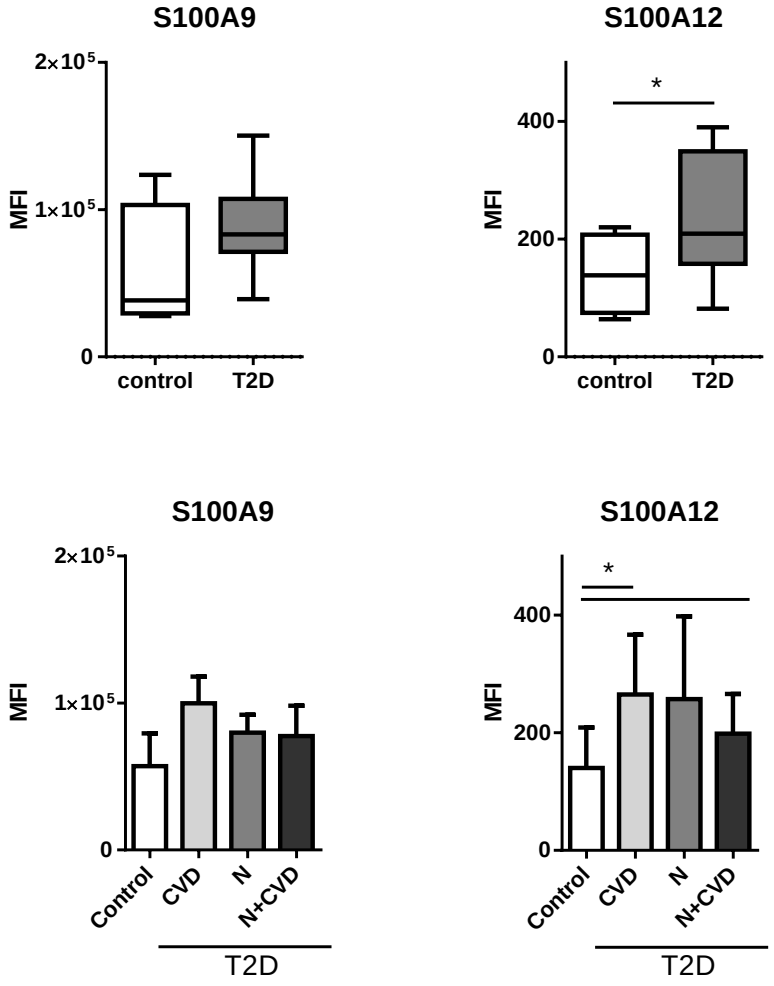

Figure 15. Intracellular expression levels of S100A9, S100A12 in CD14+ monocytes from T2D patients with microvascular complications and healthy controls. Protein expression was analysed by FACS in cells positive for HLA-DR negative for CD3, CD19, CD56 were excluded. T2D patients with microvascular complications, cardiovascular disease (CVD), nephropathy (N) and both (n=21), compared to healthy controls (n=5).

When evaluating S100A9 and S100A12 expression in all CD14+ positive cells and within the different T2D subgroups according microvascular complications, protein expression of S100A12 has increased significantly in T2D compared to controls ($P<0.05$). When evaluating the different subgroups with complications, it was observed that S100A9 and S100A12 levels were increased in T2D + CVD patients whereas this was statistically significant for S100A12 (Fig. 15).

No correlations of S100A9, S100A12 protein expression were found with HbA1c. Also, there were no correlation of frequency of the different monocyte populations with HbA1c levels (Fig. 16). Further no correlations were found between S100A9, S100A12 protein expression

and other metabolic factors (BMI, HDL or fasting glucose). Only, S100A9 expression in non-classical CD14-CD16+ cells were correlated with BMI, P = 0.0345 (data not shown).

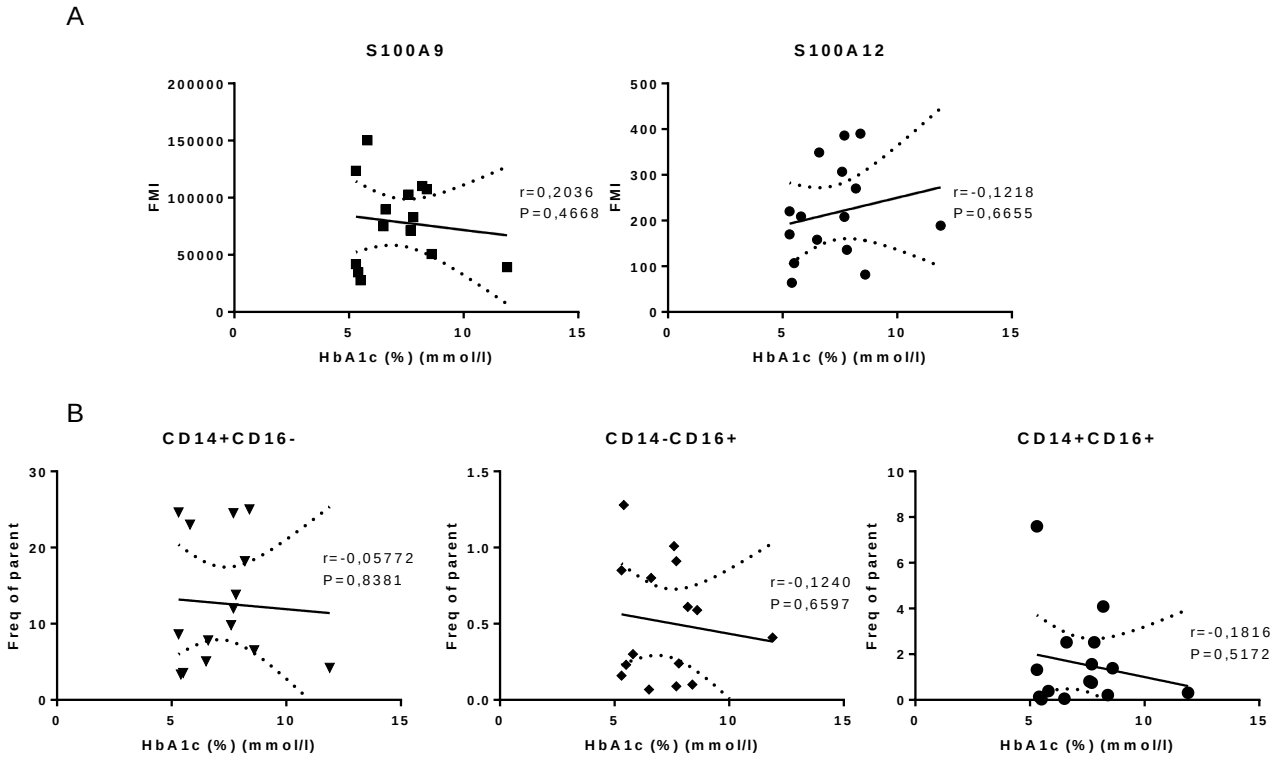

Figure 16. Correlation of protein expression levels of S100A9, S100A12 (A) and monocyte populations (B) with HbA1c level in T2D patients with microvascular complications (n=15). Correlation was analysed using Pearson's r coefficient, showing 95% confidence band of the best-fit line.

3.3 Chromatin Immunoprecipitation (ChIP)

3.3.1 Design of ChIP primers and optimization of ChIP

We examined the promoters of *S100A9* and *S100A12* genes for activating and repressive histone marks in order to design primers for ChIP analysis by RT-PCR. The UCSC genome browser provides the histone modifications for cell lines included in the Encyclopedia of DNA Coding Elements (ENCODE) and was used for experimental design in order to define the histone marks to be analysed by ChIP. The use of specific primers for each histone mark within a promoter increases the sensitivity of the assays. Within the UCSC Genome Browser on Human Feb. 2009 (GRCh37/hg19), we used the ENCODE Histone Modification Tracks which displays Histone Modifications by ChIP-seq from ENCODE/Broad Institute and from the subtracks by antibody and cell line we selected Monocytes CD14+ RO01746 (Tier 2). In UCSC we selected S100A9, S100A12 genes and used up to 3000bp upstream of the TSS to scan for suitable ChIP primers (Fig. 17).

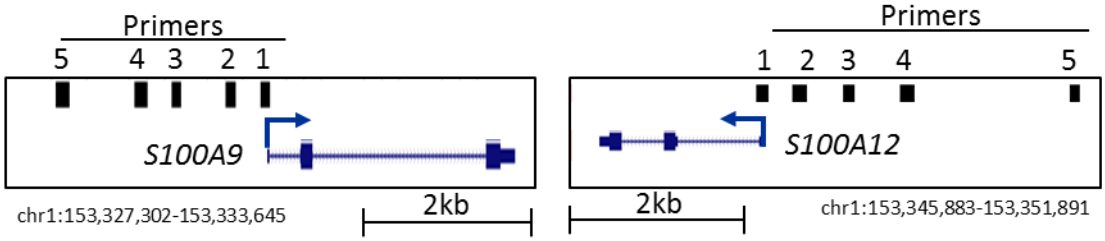

Figure 17. Different promoter regions for which qRT-PCR primers were designed. Regions were chosen based on UCSC genome browser available Chipseq data for monocytes for the histone modifications H3K4me1, H3K4me3 *S100A9* promoter (left), *S100A12* promoter (right).

3.3.2 Optimization of ChIP

ChIP is a valuable tool to compare transcription factors or modifications of DNA-bound proteins to specific genes across the genome. Macrophages were formaldehyde-crosslinked, and chromatin was prepared and digested by Micrococcal Nuclease. Optimal duration and concentration of micrococcal nuclease were determined for digestion. The digestion by enzyme has been very stable between the different experiments and we obtained fragment sizes between 150 and 1000bp (Fig. 18).

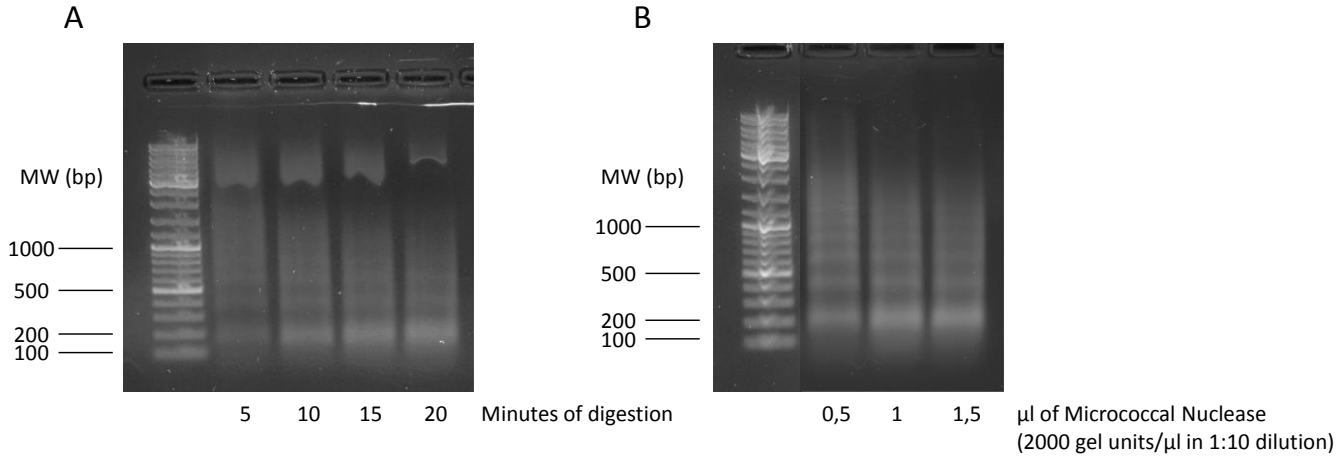

Figure 18. Agarose gel for varying digestion by Micrococcal Nuclease. For ChIP approximately 5 X 10^6 cells for each IP prep were considered optimal. For determination of the optimal digestion conditions different time (A) and different volume of Micrococcal Nuclease (B) were added per 100 µl nuclei preparation.

3.3.3 Hyperglycemia contributes to association of activating histone marks at S100A9 and A12 promoters

Using four individual donors, we have analyzed the abundance of epigenetic marks in five regions of S100 gene promoters. Hyperglycemia enhanced increase of activating histone modifications H3K4me1, H3K4me3 and AceH3 was similar at promoters of *S100A9* and *S100A12* in M1 macrophages. Only the level of AceH3 had significantly changed at both *S100A9* and *S100A12* promoters (P = 0.0024 and 0.0004 respectively) (Fig. 19). Thus, histone code at S100 promoters had changed by culture under HG conditions.

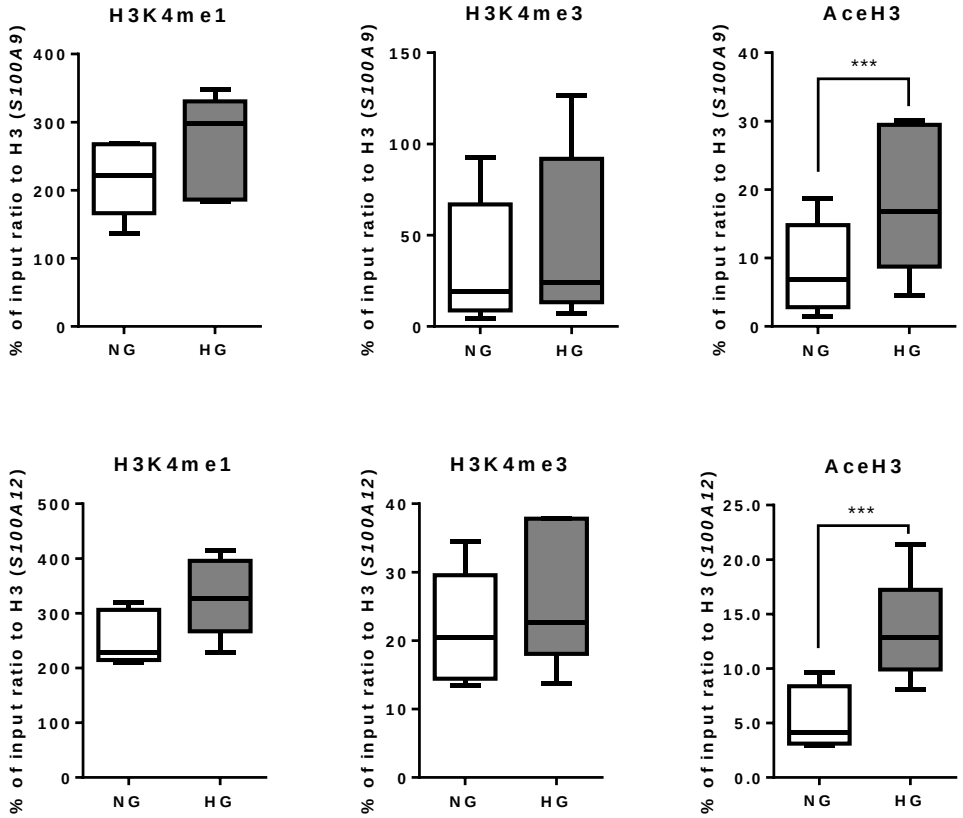

Figure 19. Hyperglycemia enhances activating histone code at promoters of S100A9 and S100A12 in M1 macrophages. Level of histone modifications in *S100A9* (top) and *S100A12* (bottom) promoter regions, average of 5 regions in the promoter, Min to Max plot. Rabbit IgG was used as a negative control for the pull-down. Histone modifications are presented as percent of input DNA and normalized to total H3 (by D2B12 antibody) (n=4).

3.3.4 ChIP analysis of histone code on 5 different regions of S100A9 and S100A12 promoters

Next, we analysed five regions at different distances from the TSS of the promoter to investigate the regions with the most pronounced presence of each activating histone mark and the regions which are most affected by glucose (Fig.20). By two-way ANOVA was determined how two factors i.e. promoter region and glucose influence the abundance of the antibody binding. Association (regardless of glucose) was not the same in the different regions of the S100A9 promoter (H3K4me3, $P < 0.0001$ and AceH3, $P = 0.0137$). The site with highest association of histone modification with the S100A9 promoter H3K4me3 was at the TSS whereas general acetylation has highest binding affinity at 1200 and 1600bp upstream from the TSS. Also promoter regions were identified which were mostly affected by culturing cells under high glucose conditions. General acetylation on the promoter of S100A9 was significantly affected (AceH3, $P = 0.0157$). For the S100A12 promoter the abundance of histone marks did not significantly differ depending on glucose or promoter region.

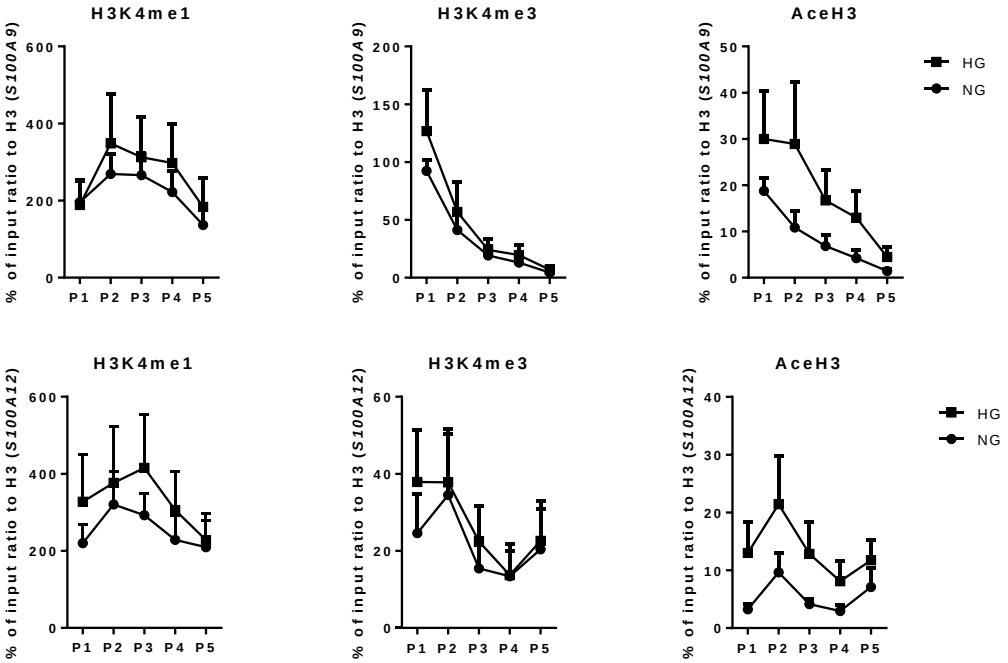

Figure 20. Histone code at 5 single regions in promoters in M1 macrophages. Level of activating histone marks at each single promoter region (P1-P5) of *S100A9* (top) and *S100A12* (bottom). Rabbit IgG was used as a negative control for the pull-down. Histone modifications are presented as percent of input DNA and normalized to total H3 (by D2B12 antibody). Graphs represent mean + SEM (n=4).

3.3.5 Correlation gene expression of S100A9 and S100A12 and histone modifications to their respective promoters

Next, we investigated the correlation of S100A9 and S100A12 glucose-induced changes in gene expression and glucose-induced changes in the presence of the activating histone marks on their respective promoters. Gene expression was increased under hyperglycemic conditions in M1 macrophages in 3 out of 4 donors for both *S100A9* and *S100A12* (Fig. 21). Association of level of changes in the association of activating histone marks correlated negatively with the level of the increase in the gene expression. Donors 1 and 2 which show highest level of gene expression and increase upon culture in HG conditions did not show pronounced epigenetic changes (Fig. 21) whereas donor 3 and 4 respond with increased levels of H3K4me1, H3K4me3 and AceH3. Therefore, fold change increase in gene expression correlated negatively with increase in level of histone mark. On the other side, we observed that total H3, representing the nucleosome density, was reduced under HG conditions in all donors (Fig. 21; Fig. 22).

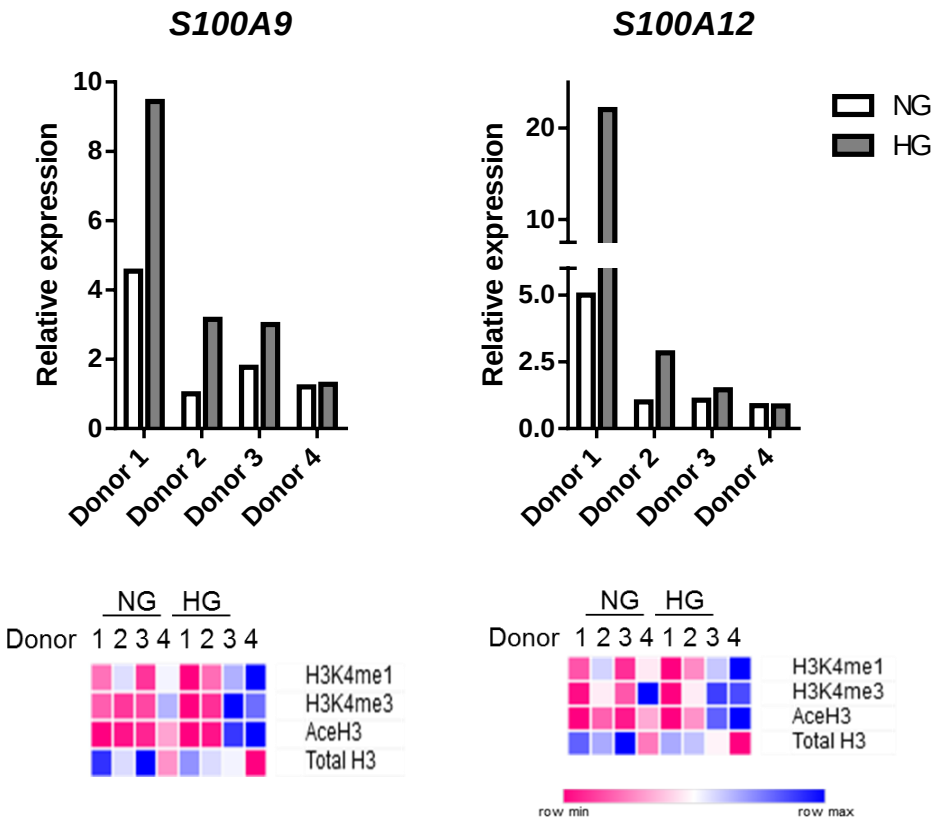

Figure 21. Increase in gene expression is not associated with increased level of activating histone marks in M1 macrophages. mRNA levels of *S100A9* and *S100A12* in M1 macrophages cultured for 6 under NG or HG conditions (n=4) (top). Heatmap of histone modifications at *S100A9* and *S100A12* promoter of the 4 individual donors (bottom).

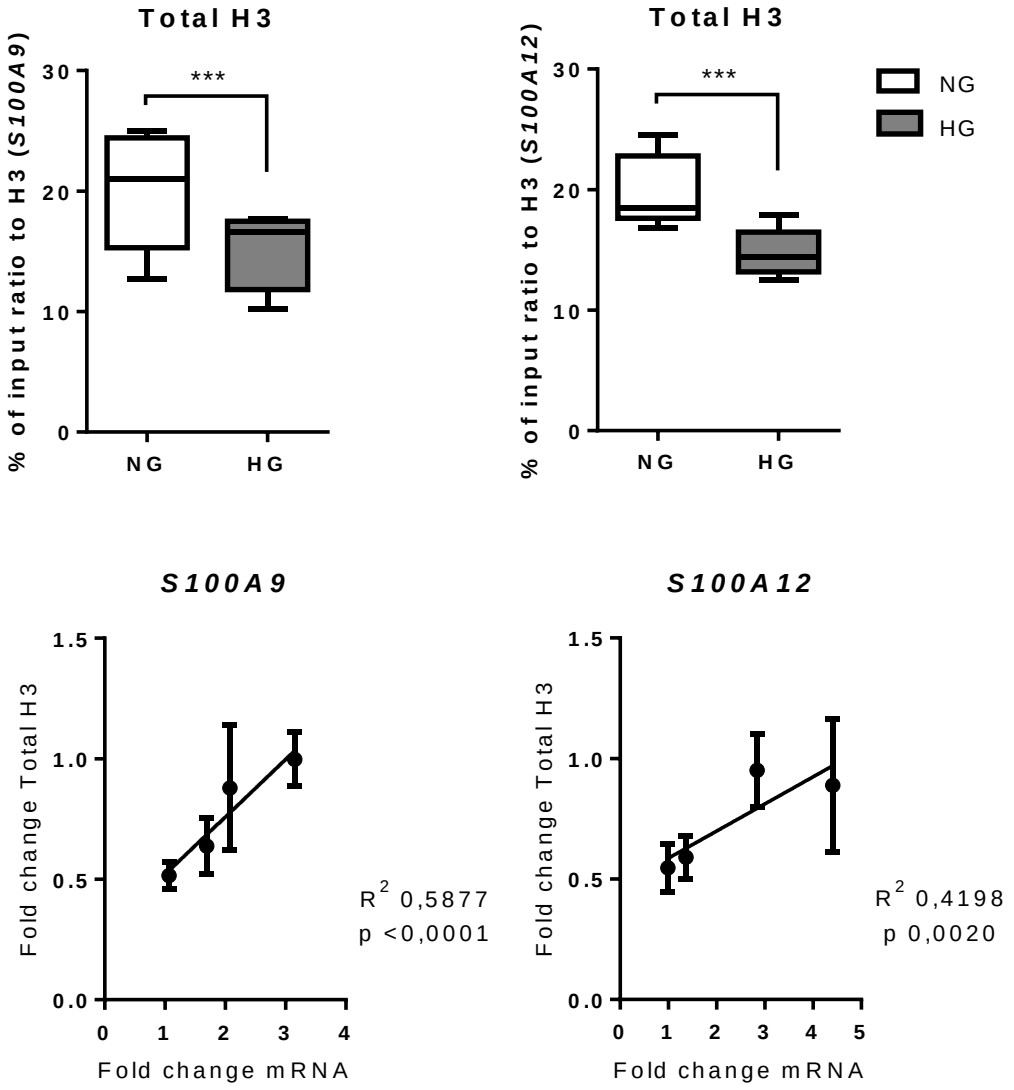

Figure 22. Increase in gene expression correlates with change in total H3 in M1 macrophages. Total endogenous H3 levels on the promoter regions of *S100A9* and *S100A12* average of 5 regions in the promoter (n=4) (top). Linear regression of fold change increase in gene expression (x-axis) with fold change increase of total H3 (y-axis) due to culture under HG conditions (bottom). Stdev presents average of 5 primer regions.

Stronger induction of gene expression by HG then was associated with higher density of nucleosomes i.e. positive correlation of fold change in total H3 with fold change in gene expression for the individual donors (Fig. 22).

Next, the changes in levels of H3 in specific promoter regions were examined. For *S100A9* P2 and P4 region as well as P1 region within *S100A12* promoter, which is the nearest region to the transcription start site, an almost linear correlation was observed between fold change increases in H3 and fold change increase in gene expression (Fig. 23). In summary, high glucose culture enhanced the presence of activation histone marks on average and decreased

the level of total H3. The change in levels of total endogenous H3 is positively correlated to fold change increases in gene expression.

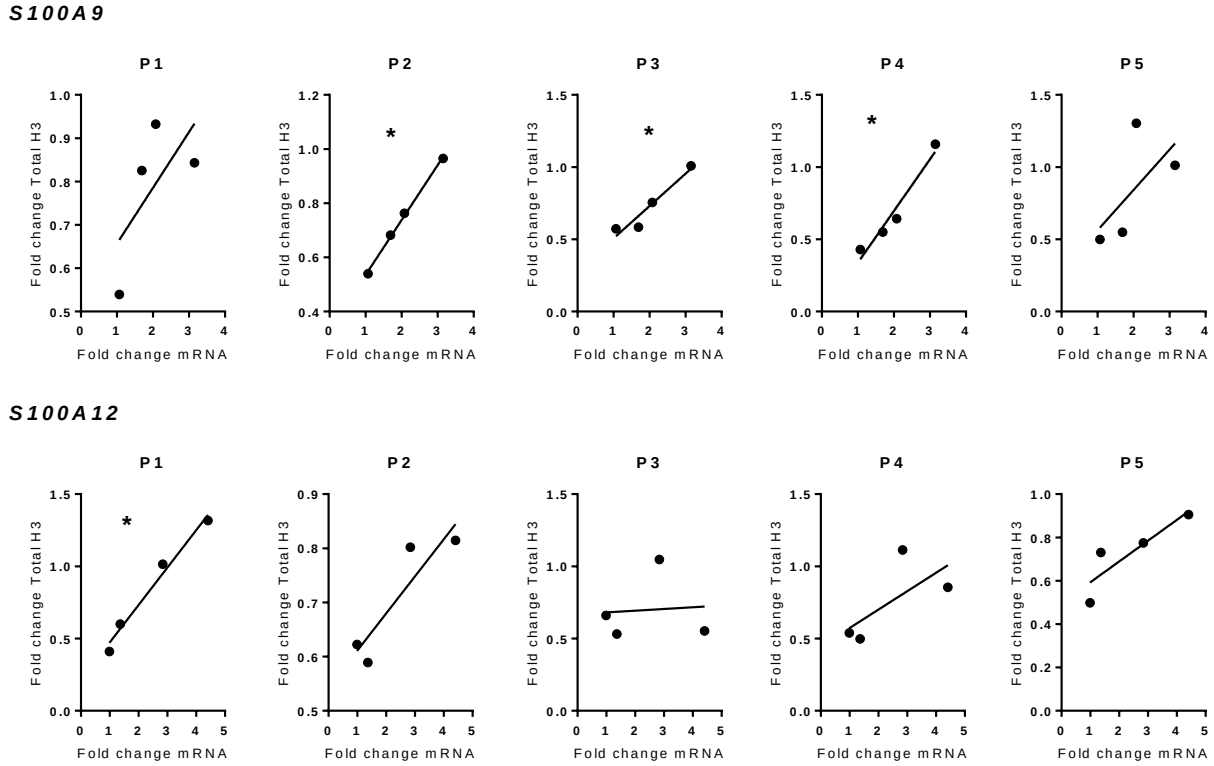

Figure 23. Relation H3 occupancy and gene expression depends on promoter region in M1 macrophages. Linear regression of the histone mark association with fold change increase in gene expression (x-axis) with fold change increase of total H3 (y-axis) by culture under HG conditions. Correlation was shown for 5 single regions in promoters (P1 – P5) of *S100A9* (top) and *S100A12* (bottom). The correlation was considered to be statistically significant in case of *p<0.05 by linear regression analysis.

3.4 Histone modifying enzymes

3.4.1 Inhibition of SET7 affects both S100A9 and S100A12 expression

As hyperglycemia resulted in the enhanced association of activating histone marks H3K4me1, H3K4me3 on promoters of S100A9 and S100A12, our next aim was to identify which histone modifying enzymes is mediating methylation. Histone methyltransferases responsible for H3K4me are the MLL/KMT2 family, SET1A, SET1B, SET7/9, SMYD and PRDM9 where SET7 specifically exhibits monomethylation activity and MLL1/2 and MLL3/4 trimethylation of H3K4 (Khare, Habib et al. 2011). SMYD3 catalyses trimethylation of histone H3K4 and is mostly associated with cancer, but cancer cells share metabolic similarities with immune cells (Andrejeva and Rathmell 2017). SET7 has been shown to be sensor for hyperglycemic

changes in EC (El-Osta, Brasacchio et al. 2008) whereas MLL has been found to be important in macrophages differentiation (Kaikkonen, Spann et al. 2013, Kittan, Allen et al. 2013). We analyzed the regulatory effect of HMTs on transcription of *S100A9* and *–A12* using specific inhibitors; (R)-PFI-2 hydrochloride, a substrate-competitive inhibitor which occupies the substrate peptide binding groove of SETD7 (Barsyte-Lovejoy, Li et al. 2014), EPZ031686 inhibitor for SMYD3 (Mitchell, Boriack-Sjodin et al. 2015) and WDR5 0103 inhibitor of MLL which disrupts WDR5 interaction with MLL and inhibits MLL core complex methyltransferase activity (Senisterra, Wu et al. 2013). The application of the inhibitors did not affect the viability of cells, tested by Alamar blue (Fig. 24).

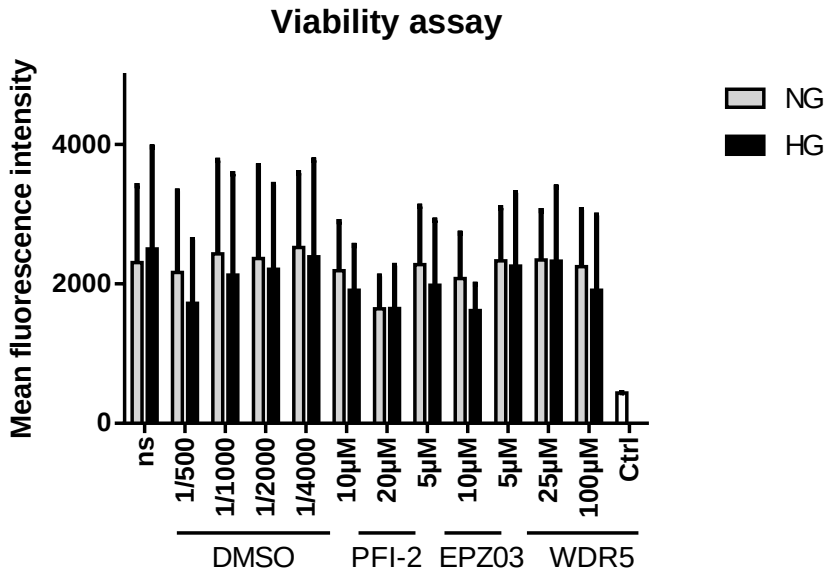

Figure 24. Macrophage viability/metabolic activity after treatment with HMT inhibitors. Following inhibitors were used: PFI-2 hydrochloride, EPZ031686 and/or WDR5 0103. Corresponding concentrations of DMSO were used as vehicle controls. M1 macrophages were cultured for 6 days followed by measurement of metabolic activity using Alamar blue assay. Data present mean ± SD for 6 donors.

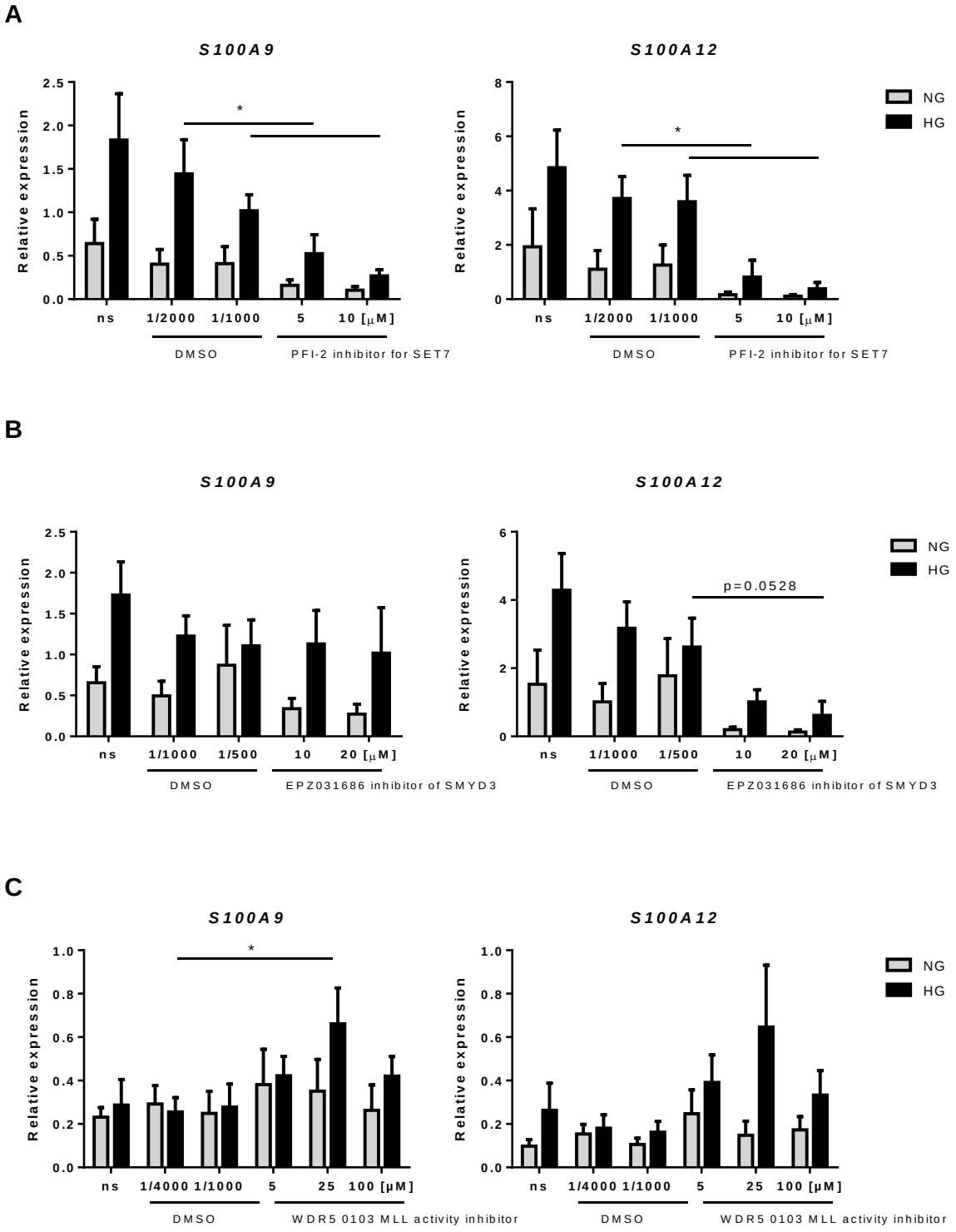

Figure 25. Regulation of S100A9 and S100A12 gene expression by HMTs in M1 macrophages. RT-PCR analysis of the effect of treatment with PFI-2 hydrochloride inhibitor for SET7 in 5 and 10μM concentrations corresponding to 1/2000 and 1/1000 dilutions of DMSO (A), EPZ031686 inhibitor for SMYD3 in 10 and 20μM concentrations corresponding to 1/1000 and 1/500 dilutions of DMSO (B) or WDR5 0103 inhibition of MLL activity in 5, 25 and 100μM concentrations corresponding to negligible, 1/4000 and 1/1000 dilutions of DMSO (C). Data present mean ± SEM normalized to 18SrRNA levels, n=5 *p<0.05, **p<0.01.

In the experiment where PFI-2 inhibitor of SET7 was applied (Fig. 25A), high glucose increased the expression of S100A9 and –A12, but not so significant level, in the absence of inhibitors. It significantly up regulated expression in the macrophages treated with vehicle control for 5µM PFI-2 (P 0.0315 and 0.0290 for both genes respectively). In case of macrophages treated with inhibitor PFI-2 at both concentrations *S100A9*, and S100A12 gene expression was significantly down-regulated compared to its DMSO control in the cells cultured under high glucose conditions.

In the experiment where EPZ03 inhibitor of SMYD3 was applied (Fig. 25B), high glucose highly increased the expression of *S100A9* and *–A12*, but not to a significant level in the absence of inhibitors. Expression of both genes was significant up regulated expression in the vehicle controls (P 0.0238 for *S100A9*) or inhibitor (EPZ03 10µM, P= 0.0472 for *S100A12*). In case of macrophages treated with inhibitor EPZ03 *S100A9* expression did not change. For *S100A12* expression application of EPZ03 abolished the effect of high glucose. This effect of EPZ inhibition was seen in highest concentration and did not reach significance when compared to its vehicle control (P = 0.0529).

In the experiment where WDR5 inhibitor of MLL activity was applied, high glucose highly increased the expression of *S100A9* and *–A12*, but not to a significant level in macrophages in the absence of inhibitors as well as DMSO as a vehicle. Glucose up regulated S100 expression in the macrophages treated with inhibitor (WDR5 25µM P= 0.0187 for *S100A9*). In case of macrophages treated with inhibitor, both *S100A9* and *–A12* expression did increase, which was significant for *S100A9* (WDR5 25µM P= 0.0187). MLL inhibition seemed to work synergistically with glucose (Fig. 25C).

Since the effect was observed both in normal and hyperglycemic conditions, we conclude that HMTs act on the mentioned promoters independent of the influence of glucose (NG vs HG).

3.4.2 Glucose affects SET7 gene expression in M1 macrophages

Histone methyltransferases SET7 has emerged as a key regulatory enzyme in mediating methylation of lysine residues at histone tails and non-histone protein targets (Keating and El-Osta 2013). Also, it has shown to play a role in sustained enrichment of H3K4me1 at the RELA promoter encoding NFκB subunit p65, in primary human and bovine endothelial cells indicating a role in metabolic memory of previous exposure to glucose (El-Osta, Brasacchio et al. 2008). Therefore, we analysed *SET7* expression during macrophage polarisation and under hyperglycemic conditions. We observed that *SET7* expression had not changed in response to glucose or cytokines after one day (Fig. 26). Though after 6 days, when monocytes are maturated into macrophages, we found that SET7 expression is significantly increased, in 4 out of 6 donors for M1 and all donors for M2, compared to M0 macrophages under normal glycemic conditions (M1 P = 0.0049 vs M2 P = 0.0118) as well as hyperglycemic conditions (M1 P=0.0124 vs M2 P=0.0162) (Fig. 26). This indicates that macrophages need *SET7* for activation, as SET7 expression is increased by both pro-inflammatory cytokine IFNγ as well as anti-inflammatory cytokine IL-4. Further we found that glucose modestly but significant affected *SET7* expression in M1 macrophages only (P = 0.0100), suggesting that this gene encoding the histone modifying enzyme, is under metabolic control or affected by glycolysis.

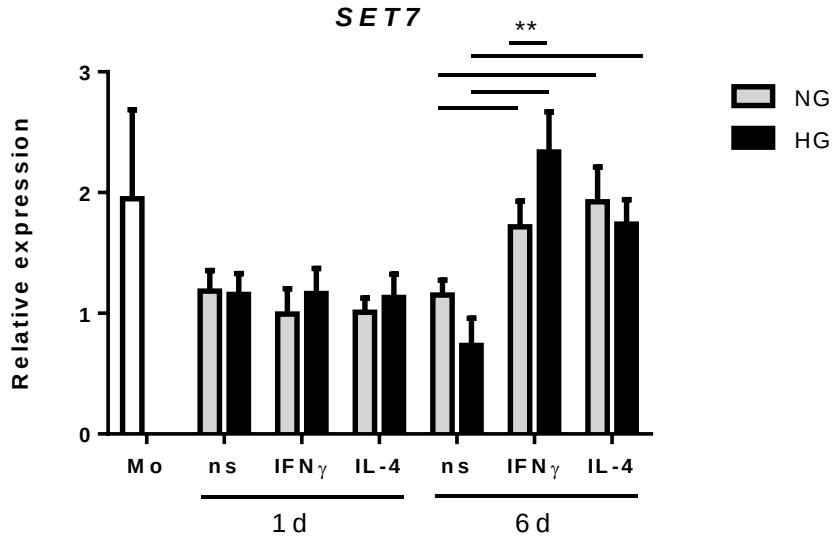

Figure 26. SET7 mRNA expression during differentiation of macrophages. RT-PCR analysis of mRNA expression SET7 in M0, M1 and M2 macrophages cultured for 6 days cultured under normal (NG, 5mM) and high glucose (HG, 25mM) conditions. Data present mean ± SD normalized to 18SrRNA levels. Statistical analysis was found by paired student's t-test, n = 6, *p<0.05, **p<0.01.

3.4.3 Effect of hyperglycemia on the localisation of SET7 in macrophages

Additionally, SET7 was demonstrated to translocate to the nucleus in endothelial cells in response to high glucose (Okabe, Orlowski et al. 2012). the localisation of SET7 was investigated. M0 and M1 macrophages cultured under normal and high glucose conditions of seven individual donors were stained and SET7 protein expression and localisation was analysed by use of confocal microscopy. The appearance of the cells strongly changed by addition of IFNγ, whereas the cells lose their bigger round shaped form, become strongly adherent and stretch out M0 and M1 macrophages all contained large amount of intracellular SET7, and it was localized in the cytoplasm and in the nucleus (Fig. 27). Further, it was observed that IFNγ strongly induces SET7 protein expression after 6d in M1 of all individual donors (Fig. 27). Immunofluorescence imaging of M1 macrophages under normal and high glucose conditions indicate that hyperglycemia enhances the levels of nuclear translocation of SET7 in M1 macrophages (Fig. 28).

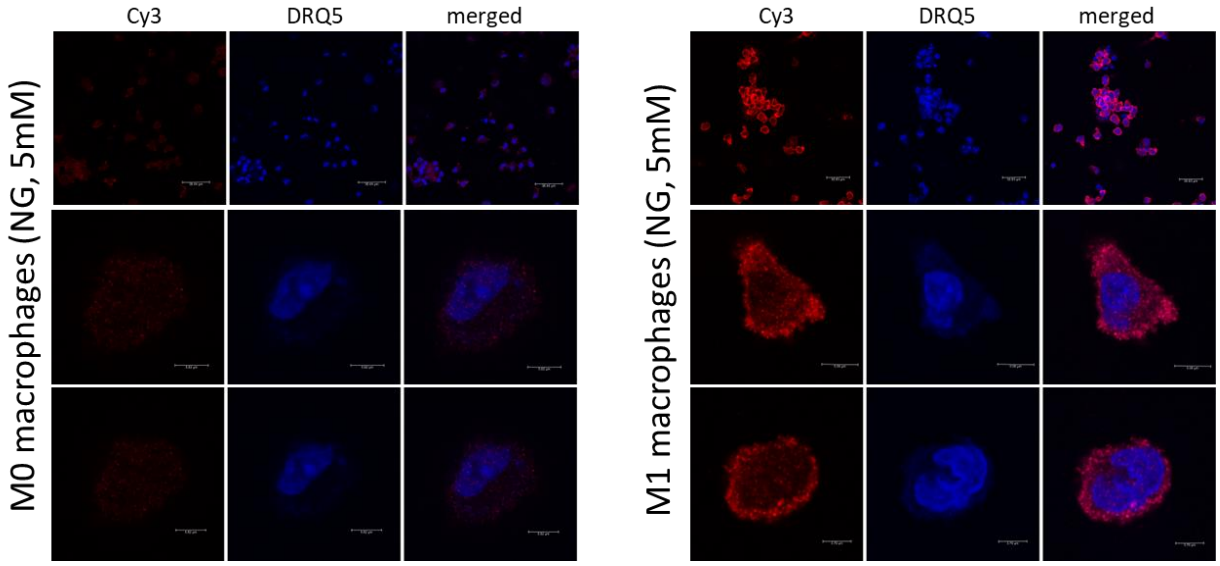

Figure 27. SET7 expression is induced by IFNγ. Immunofluorescence/confocal imaging of SET7 protein expression in $M0_{ns}$ and $M1_{IFN\gamma}$ macrophages cultured for 6 days cultured under normal (NG, 5mM). Cells were stained with primary antibody against SET7 from Rabbit and secondary antibodies were Cy3 donkey anti-rabbit (red). Nuclei were visualised with and DRAQ5 (blue). Purple indicates localisation of SET7 in the nucleus (merging blue and red). Scale bars from top to bottom equal 50, 10 and 10μm.

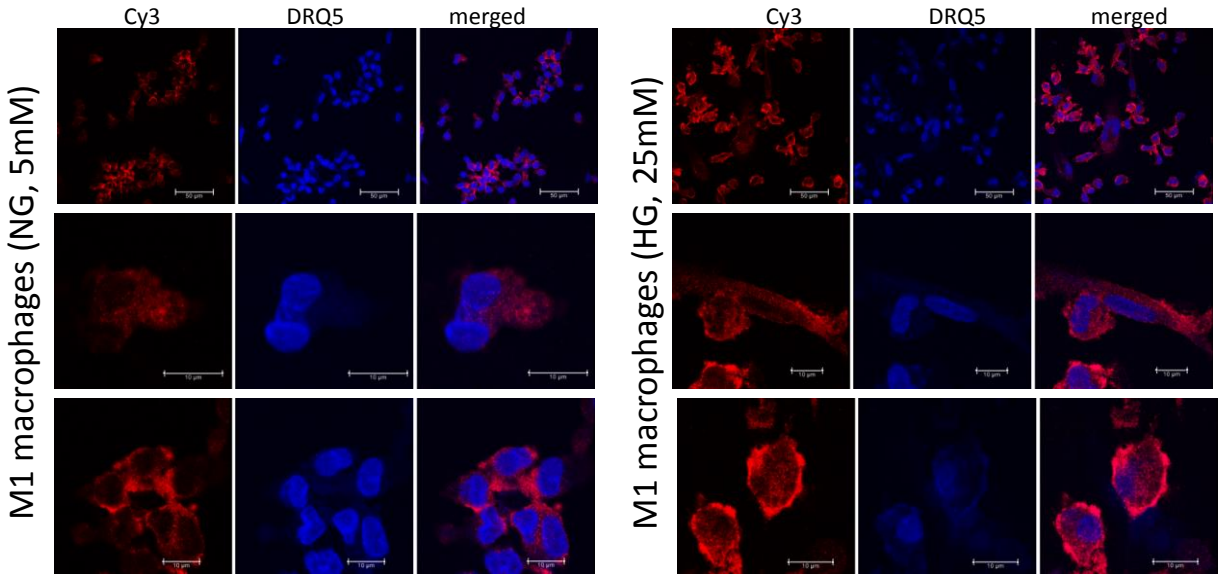

Figure 28. Effect of hyperglycemia on the localisation of SET7 in macrophages. Immunofluorescence/confocal imaging of SET7 protein expression in M1 macrophages cultured for 6 days cultured under normal (NG, 5mM) and high glucose (HG, 25mM) conditions. Cells were stained with primary antibody against SET7 from Rabbit and secondary antibodies were Cy3 donkey anti-rabbit (red). Nuclei were visualised with and DRAQ5 (blue).. Purple indicates localisation of SET7 in the nucleus (merging blue and red). Scale bars from top to bottom equal 50, 10 and 10μm.

3.5 Metabolic memory

3.5.1 S100 gene expression is sustained in transient hyperglycemia

Transient hyperglycemia has been studied in vascular system and in the kidney i.e. endothelial cells (Chen, Wu et al. 2018) and mesengial cells (Yunlei, Qiuling et al. 2018) but not in cells of the innate immune system. We designed a model system for the analysis of hyperglycemic memory in primary human macrophages. After 6 days when the monocytes are differentiated into macrophages, the medium was changed, from containing NG to NG, from containing HG to HG and from containing HG back to NG (transient hyperglycemia). Macrophages from 7 donors were analysed. Higher expression of *S100A9* in HG-HG compared to NG-NG was observed (P = 0.0386) (Fig. 29). The increase was found in 5 out of 7 analysed donors with highest increase for individual donors being 2.8 fold. When the medium was changed back to normal glucose levels higher levels of gene expression compared to cells that were in NG medium continuously were found for 4 out of 7 donors.

For *S100A12*, higher expression was observed in HG-HG compared to NG-NG conditions (P = 0.0056) (Fig. 29). Increased expression levels were found in 5 out of 7 analysed donors with highest levels for individual donors being 8.6 fold. When the medium was changed back to normal glucose higher levels of gene expression compared to cells that were in NG medium continuously (P = 0.0180). The increase was found in 6 out of 7 donors with highest levels of for individual donors being 5.7-fold (Fig. 29).

Five out of 7 donors have higher expression of *IL-1B* in HG-HG medium compared to NG-NG medium, though when the medium was changed back to normal glucose sustained levels of higher gene expression was found only for one donor. All donors had near significant higher expression of *CCR2* in HG-HG compared to NG-NG (P= 0.0775), though higher gene expression levels were found for 4 out of 7 donors CCR2 expression was reduced back to normal in transient hyperglycemia.

Thus, hyperglycemia causes memorable changes of S100 genes expression that last after the glucose concentrations are normalized.

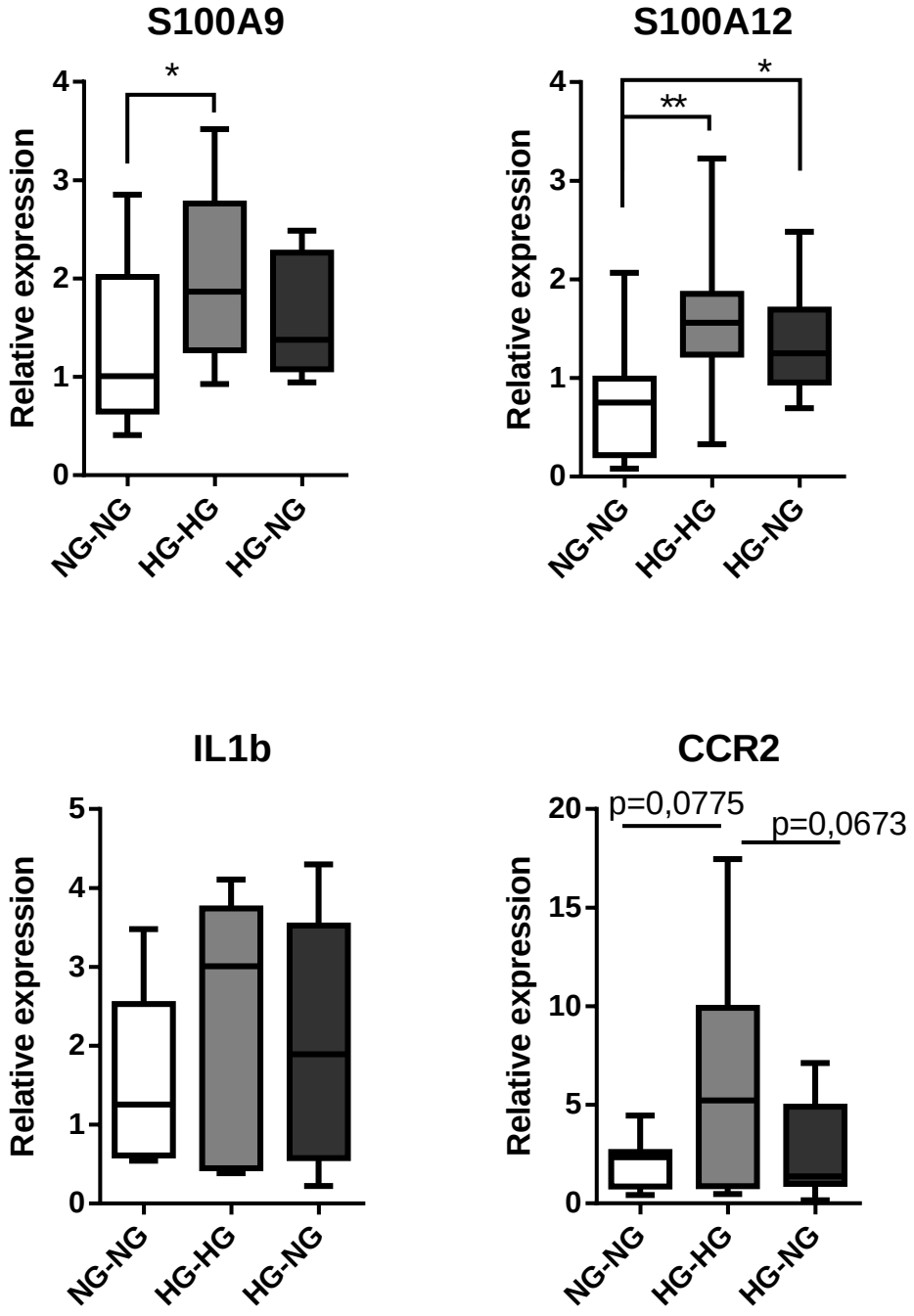

Figure 29. Hyperglycemic memory in macrophages after 12 days. RT-PCR analysis of mRNA expression, from left to right; IL-1β and CCR2 (A) and S100 genes -A9 and S100A12in M1 macrophages, individual patterns (left) and combined in box plots (right). After 6 days medium was changed and the cells were harvested at d12 for analysis. Data present mean ± SD normalized to 18SrRNA levels. Statistical analysis was found by student's t-test. The difference was considered to be statistically significant in case of *p<0.05.

3.5.2 Transient hyperglycemia results in decrease of activating histone marks at promoters of S100A9 and S10012 genes

Next, using four individual donors, we performed ChIP analysis in our memory model with transient hyperglycemia. H3K4me3 as well as AceH3 on the promoter of both *S100A9* and *S100A12* were significantly decreased in cell cultured continuously under HG conditions. This decrease in AceH3 was reversible and not present any more in transient hyperglycemic cells (Fig. 30). H3K4me1 for S100A9 and H3K4me3 for S100A12 were sustained in transient hyperglycemia thereby possibly marking memory. Association of activating histone marks again negatively correlated with the increase in gene expression (data not shown). On the other side, we observed again that total H3 was reduced under HG conditions and this was reversible and not present in transient hyperglycemic cells (Fig.30).

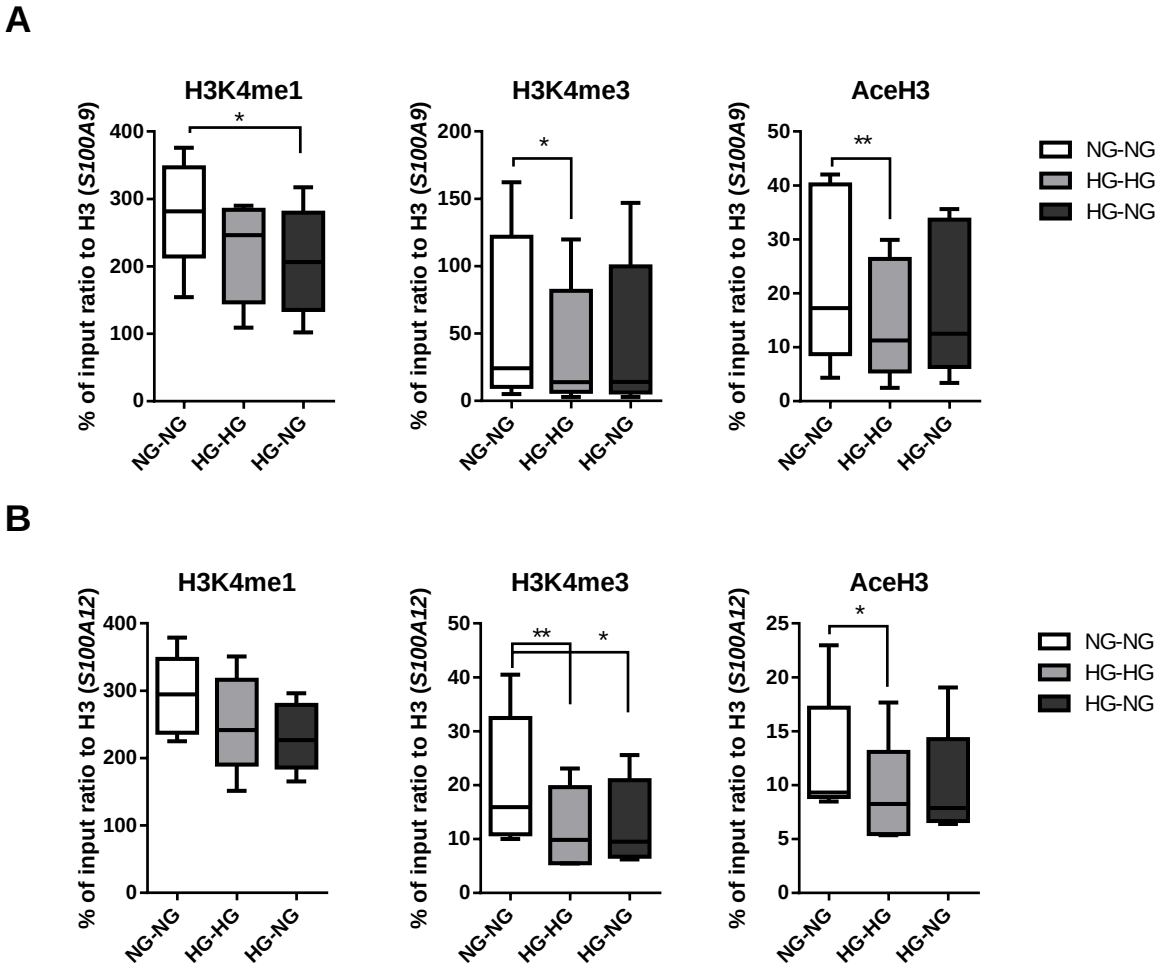

Figure 30. Hyperglycemia decreases activating histone code at promoters of S100A9 and –A12 after transient hyperglycemia. Level of histone modifications and total H3 in S100A9 and –A12 promoter regions, average of 5 regions, Min to Max plot. Rabbit IgG was used as a negative control for the pull-down. Histone modifications are presented as percent of input DNA and normalized to total H3 (by D2B12 antibody) (n=4).

3.5.3 Correlation gene expression and histone code in memory model

Gene expression was increased in M1 macrophages in 3 out of 4 donors for *S100A9* and all donors for *S100A12* in both HG as well as transient glucose vs NG, transient glucose still presenting 26 and 60% of the fold change increase induced by HG for *S100A9* and *–A12* respectively (data not shown). By two-way ANOVA it was determined how two factors i.e. promoter region and glucose influence the association of the histone mark at the promoter. For *S100A9*, the abundance of epigenetic marks, regardless of glucose, was not the same in the different promoter regions (H3K4me1 P = 0.0082, H3K4me3 and AceH3, P < 0.0001). The same held true for the *S100A12* promoter (H3K4me3, P < 0.0001 and AceH3, P = 0.0017). Only H3K4me3 association at the *S100A12* promoter was significantly affected by glucose, regardless of the promoter region (P = 0.0335). Changes in H3 correlated positively with fold change increases in gene expression for *S100A9* in transient hyperglycemia only (Fig. 31). To summarize, presence of activating histone marks on the promoters of *S100A9* and *S100A12* had decreased after 12 days of culture with transient hyperglycemia. AceH3 and total H3 loss was reversible. H3k4me1 for *S100A9* and H3K4me3 for *S100A12* possibly mark metabolic memory.

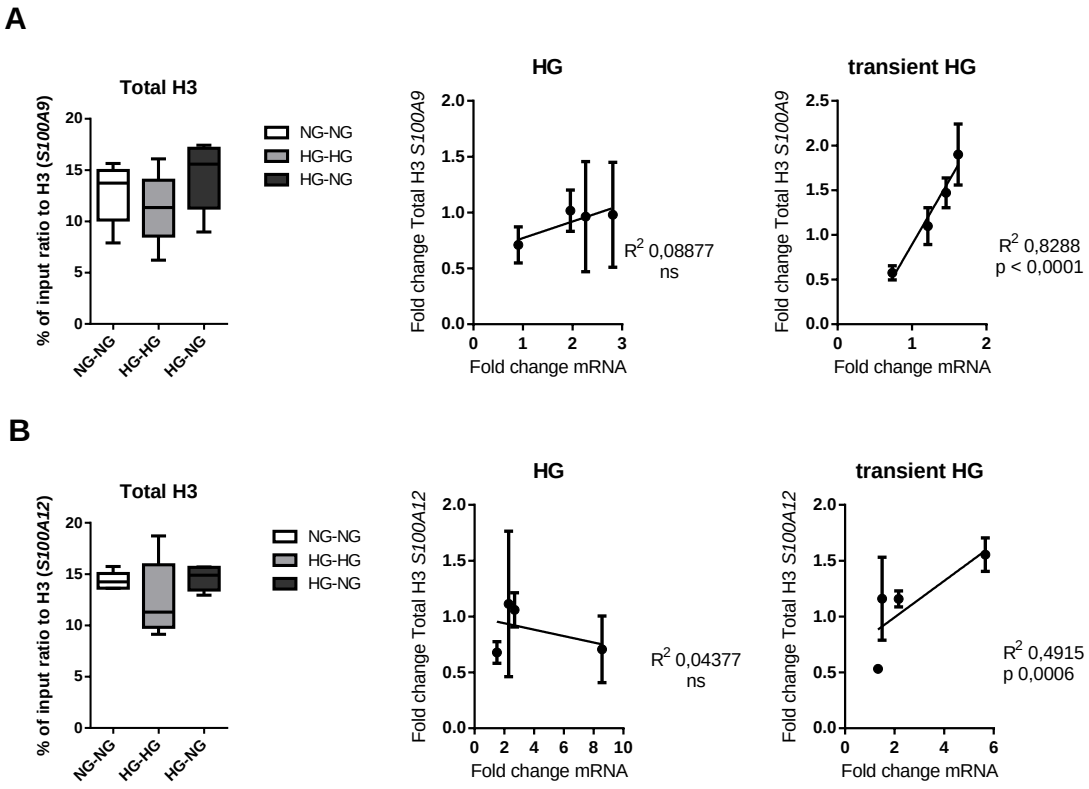

Figure 31. Modifications of histones at promoter regions in transient hyperglycemia. Level of total H3 in *S100A9* (A) and *–A12* (B) promoter regions, average of 5 regions, Min to Max plot and correlation of fold change increase in gene expression with increase of total H3 (n=4).

3.6 Hyperglycemia sensitizes macrophages to exogenous and endogenous factors inducing S100A9 and S100A12 gene expression

To investigate the effect of glucose on the training of macrophages, non-stimulated monocytes cells were cultured under NG and HG conditions and after 6 days they were challenged overnight with TLR-ligands. TLR receptors are known to be up regulated by glucose (unpublished observations of Michael Balduff) and act as receptors to mediate pro-inflammatory involved in M1 macrophage activation during insulin resistance (IR)/metabolic disease (Olefsky and Glass 2010). For example, Palmitic Acid (PA) is a saturated fatty acid with a role in atherogenesis and T2D (Diaf, Khaled et al. 2015). In turn, this could sensitize monocytes/macrophages to be more responsive to a 2nd stimulus by factors associated with diabetes/metabolic disease (van Diepen, Thiem et al. 2016).

We investigated the effect of glucose on the training of macrophages by measuring gene expression of *S100A9* and *S100A12* (Fig. 32). LPS induced expression of both *S100A9, S100A12* compared to non-stimulated controls. We observed that high glucose dramatically increased the expression levels of *S100A9* in response to PA (9.9-fold). *S100A12* was significantly up regulated by glucose in LPS stimulated cells (5.4-fold). Therefore, hyperglycemia works synergistically together with stimulation with TLR-ligands to induce expression of *S100A9* and *S100A12*. This indicates that S100 proteins are sensitive to glucose programming.

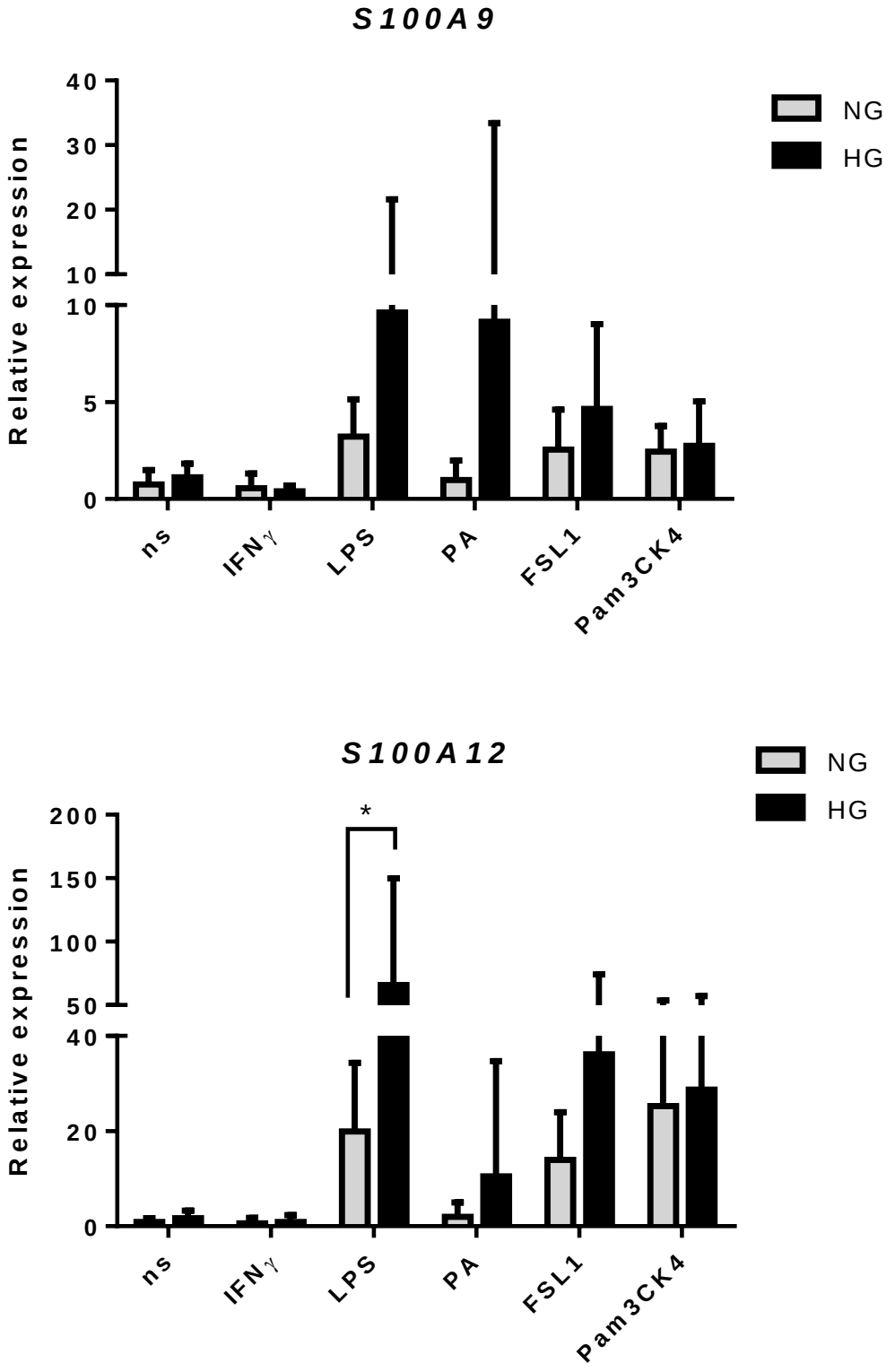

Figure 32. Programming of mature macrophages overnight with cytokines, fatty acids and/or TLR-ligands. RT-PCR analysis of IL-6, IL-10, S100A9, –A12 and IL-1β mRNA expression M0 macrophages cultured for 6 days cultured under normal (NG, 5mM) and high glucose (HG, 25mM) conditions and stimulated overnight with TLR-ligands. Data present mean ± SD normalized to 18SrRNA levels, n = 8. Significance is indicated in the figure by two-way ANOVA followed by Sidak's multiple comparisons test. P-values in the text belonging to this figure are according to student's t-test.

4 DISCUSSION

4.1 Regulation of S100 protein expression in macrophages under NG and HG conditions

Hyperglycemia enhances the expression levels of *S100A9, S100A12* among other genes in macrophages. *S100A9* and *S100A12* were significantly higher expressed in M1 macrophages and lower in M2 macrophages. The expression of S100 mRNA drops during differentiation in all types of macrophages. But on the late stages of differentiation IFNγ again induces S100 gene expression. In addition, HG glucose increases the expression in M1 macrophages after 6 days.

Further, under HG conditions the correlation between S100A9 and S100A12 expression decreased in favour of S100A9. Lorenz et all. described this correlation of protein levels in acute and chronic lung disease (Lorenz, Muhlebach et al. 2008). Increased expression of S100A12 in acute respiratory distress syndrome suggested that S100A12 is more important in the onset of neutrophil influx and less elevated in chronic inflammation, whereas in sputum of cystic fibrosis and COPD patients higher levels of S100A8/A9 expression than S100A12 indicating that chronic infection might be mediated by S100A8/A9 (Lorenz, Muhlebach et al. 2008). We believe the regulation of expression and ratio of the two different genes might provide more insight in the mechanism of inflammation.

Differences in protein expression relate to different donor responses, though on average macrophages contain high levels of intracellular S100 proteins and protein expression had not changed significantly by stimulation with cytokines or culture under high glucose. According to literature, protein levels of S100A8 and –A9 but not mRNA, are increased upon LPS/IFNγ stimulation in macrophages. In this study, cells were stimulated for 24h only (Averill, Barnhart et al. 2011). Our antibody for S100A12 was specific but our antibody for S100A9 showed also the presence of homodimer and heterodimer with S100A8. Variability has been observed for recombinant proteins as well and partly, the presence of monomers might result from the dissociation of homodimers and heterodimers caused by SDS in nonreducing gels (Ryckman, Vandal et al. 2003). In the cell calcium levels are low. But after secretion, in the presence of extracellular calcium the heterodimer complex form tetramers and failure to tetramerize was associated with lack of functional activity (Leukert, Vogl et al. 2006). It was found that this formation of tetramers due to extracellular Ca+ is the auto inhibitory mechanism. The activity of heterodimers released by activated phagocytes at local site of inflammation, are restricted by tetramerization due to which the TLR4/MD2 binding site is

hidden (Vogl, Stratis et al. 2018). However, HG-induced oxidative stress has shown to increase Ca-influx in the cell via TRP-channels (Wuensch, Thilo et al. 2010) but additional effect on intracellular S100 protein levels remains to be tested. Another possible reason for discrepancy between mRNA and protein expression might be additional regulation on the level of translation.

When intracellular levels of protein are high and not secreted more regulation might happen on the level of posttranslational modifications. S100 proteins can undergo different modifications but key seems to be their regulation through oxidative changes on their Cys residues (Lim, Raftery et al. 2009). S100A8 and –A9 are oxidized by peroxide, hypochlorite and NO however S100A12, which lacks Met and Cys residues, is susceptible for changes by oxidative environment (Goyette and Geczy 2011). NO production, mediated by iNOS in activated macrophages, is key in antimicrobial defence (Xue, Yan et al. 2018). Too much oxidative stress might be prevented through S-nitrosylation of thiols by NO (Biswas, Chida et al. 2006). S100A8 and S100A9 were found to be readily S-nitrosylated. But unlike iNOS, LPS and IFNγ stimulation in macrophages did not induce S100A8, therefore when ROS is needed for antimicrobial defence, S100A8 is not produced and in this case does not scavenge NO (Lim, Raftery et al. 2008). This modifications can regulate different functions of S100 proteins (Goyette and Geczy 2011) but also convert short term NF-κB activation or oxidative stress into long-lasting activation of cells during pathological conditions as has been suggested for Nε-carboxymethyllysine(CML)-modification of S100 proteins due to oxidative and carbonyl stress can cause, in inflammatory bowel diseases (Andrassy, Igwe et al. 2006). Mild oxidation can be transient. Reversibility of oxidation reactions occurs through specific reductases e.g. glutathione or Met sulfoxide reductases and peroxiredoxins (Forman, Fukuto et al. 2004). TXNIP (thioredoxin interacting protein) is up regulated by glucose in all types of MF, but highest in M1 macrophages (KM thesis ref). The reductase functions as an important regulator of S-Nitrosylation (Forrester, Seth et al. 2009) and HG-induced TXN mediated inflammasome activation in U937 monocytes (Tseng, Vong et al. 2016).

The secreted levels of S100A9 and S100A12 in our cell culture model was much lower than serum levels identified in diabetic patients (Bouma, Lam-Tse et al. 2004, Nagareddy, Murphy et al. 2013, Ingels, Derese et al. 2015). In healthy individuals they are already 30 times higher and during inflammation local concentrations raise up to 80µg/ml (Frosch, Strey et al. 2000). It seemed that macrophages cannot release the intracellular accumulated S100 protein and might need an addition trigger from the *in vivo* microenvironment to be able to secrete the S100 protein e.g., cytokines, Fatty Acids (FA), AGEs or direct contact with activated

endothelium. Alternatively, S100 proteins have more intracellular functions (Xia, Braunstein et al. 2018).

Secretion of S100 proteins does not follow classical ER/Golgi route but is released after PKC activation through inflammatory stimuli and is energy and calcium dependent (Rammes, Roth et al. 1997). DAMPs are passively released from necrotic cells whereas active release occurs *in vivo* as well as *in vitro* in activated cells i.e. granulocytes. Upon activation by PMA or TNFα, S100A12 translocates from cytoplasm toward the plasma membrane. S100A12 lacks the signal peptide for secretion via ER and the Golgi apparatus though inhibition of protein kinase activity or inhibition of tubulin polymerization blocked S100A12 release (Foell, Wittkowski et al. 2013). For S100A9, secretion is promoted through stimulation with IL-10 and TNFα (Diercks, Hauschildt et al. 2013, Chakraborty, Bjork et al. 2015). Whereas especially IL-10 alone, promoted surface localization and TNF-α was needed for release (Diercks, Hauschildt et al. 2013). S100A9 alone is detected at the surface whereas S100A8/A9 heterodimer co-fractions intracellular with endolysosomes (Chakraborty, Bjork et al. 2015). Diercks et al. suggest that activation of MAPK38 by IL-10 (Lee and Chau 2002) might induce phosphorylation of S100A8/A9 which has shown to promote translocation to the plama membrane (Lominadze, Rane et al. 2005). Phosphorylation of MRP14 is antagonistically regulated by binding of MRP8 and calcium (Vogl, Ludwig et al. 2004). Only the phosphorylated form of S100A9 in the complex can induce proinflammatory cytokine expression and secretion (Schenten, Plançon et al. 2018). Lastly, both release of S100A9 and A12 from PMA-stimulated neutrophils depended on ROS production and K^+ efflux from ATP-sensitive K^+ channels, just like IL-1β (Tardif, et al. 2015). Here S100A12 expression and secretion was very early upon response to PMA, TNFα and LPS respectively (Foell, Wittkowski et al. 2013) and S100A8/A9 peaked after 24 to 48h of stimulation (Diercks, Hauschildt et al. 2013, Chakraborty, Bjork et al. 2015). The increased secretion of S100A9 after 24h depends on few strong responding donors only and might be associated with monocyte adhesion still or be stimulated by endogenous TNF-α release (Moganti, Li et al. 2017) or glucose induced ROS (Tardif, #xe9 et al. 2015, Rendra, Riabov et al. 2019). In our hands, IFNγ did not induce secretion higher than in the unstimulated cells. Similar to one study with murine macrophages, where IFNγ was found to induce S100A8 but not S100A9 expression beside LPS and TNF, and declined slowly over 96h. Monomeric S100A8 was secreted by cells stimulated with IFNγ or TNFα but S100A9 or S100A8/A9 heterodimers were not detected (Xu and Geczy 2000). After 6 days we may measure only accumulation in supernatants, there is no literature on reuptake or autocrine effects. Interestingly IL-4 seems to

have an opposite effect on S100A9 compared to S100A12 release after 6 days. This might be due to anti-inflammatory functions of S100A9 as well and therefore uncontrolled secretion might point to a dysregulation of inflammatory functions (Austermann, Friesenhagen et al. 2014). In general, secretion of S100A9 and S100A12 is not dependent on each other, and depends on agonist as well as cell type (Tardif, Chapeton-Montes et al. 2015).

4.2 S100 expression in diabetic patients

We examined whether S100 genes are higher expressed and therefore relevant in prediabetic and diabetic patients. *S100A9* tend to be higher expressed in T2D whereas *S100A12* was higher expressed in T1D patients but not to a significant level. Other factors *in vivo* may act stronger than glucose e.g. fatty acids, TLR ligands although no correlation between *S100A9* and *S100A12* expression was found with BMI or body weight either. Another possible reason might be effect of the treatment of the patients receive (Rendra, Riabov et al. 2019).

However also in prediabetic individuals we did not find a correlation of *S100A9* and *S100A12* expression with HbA1c. However, as we can see from Fig. 7 though FG levels were not as well as HbA1c levels were not as high as seen in patients. However, similarly to the *in vitro* results, in patient monocytes, S100A9 and S100A12 expression were very tightly correlated in T1D, T2D and healthy controls ($P < 0.0001$ for all three) but not in prediabetic individuals (Table 18).

Monocytes are usually classified into three subtypes based on CD14 and CD16 expression; non-classical monocytes (CD14-, CD16+) and high in classical (CD14+, CD16-) and highest in intermediate monocytes (CD14+, CD16+) (Mukherjee, Kanti Barman et al. 2015). By FACS we did not find significant difference in monocyte populations between controls and T2D. This is according to a study with prediabetic individuals with low prevalence of cardiovascular problems (Fadini, Cappellari et al. 2013). Authors observed no difference in percentages of classical, non-classical and intermediate monocytes. However, there was an increase in CD68 positive (M1 marker) cells which correlated with HbA1c (Fadini, Cappellari et al. 2013). For the association of S100 proteins in diabetic patients with late complications, often plasma levels are measured (Pedersen, Nybo et al. 2014, Dong, Shi et al. 2015). We found that S100A9 was hardly expressed in non-classical monocytes and high in classical and highest in intermediate monocytes. Also, we observed highest absolute increase in S100A9 expression in the intermediate monocytes of T2D compared to healthy controls. Highest expression of S100A9 has been found before in classical monocytes but expression greatly varied between single cells (Yang, Anholts et al. 2018)

In our PBMCs from T2D diabetic patients which were analysed by flow cytometer, we also find S100A9 and S100A12 expression was enhanced. Expression of S100A12 was especially increased in the group with known CVD. S100 proteins have been linked with cardiovascular disease before but often circulating levels were measured (Burke, Kolodgie et al. 2004, Basta, Sironi et al. 2006, Schiopu and Cotoi 2013). Serum and mucosal S100A8/A9 and S100A12 are elevated in patients with inflammatory bowel disease and therefore widely used as diagnosing marker (Leach, Yang et al. 2007). Plasma levels of S100A12 were also related to retinopathy in patients with T2D (Dong, Shi et al. 2015) and circulating soluble RAGE (sRAGE) was found to be inversely correlated with S100A12 protein and correlated to glycemic control in patients with T2D (Basta, Sironi et al. 2006). Two other studies find plasma levels S100A8/A9 positively correlated with diabetic measures of IR, fasting blood glucose and impaired glucose metabolism (Ortega, Sabater et al. 2012) and HbA1c levels (Cotoi, Dunér et al. 2014). And in another study involving T2D patients, the higher concentrations of plasma S100A8/A9 were also associated with obesity, metabolic syndrome and associated but not predict cardiovascular problems i.e. neuropathy, peripheral arterial disease and myocardial ischemia (Pedersen, Nybo et al. 2014). Other clinical and mouse studies on the role of S100A8/A9 in cardiovascular diseases are reviewed (Schiopu and Cotoi 2013).

4.3 Regulation of S100 expression on epigenetic level

Hyperglycemia enhanced increase of activating histone modifications H3K4me1, H3K4me3 and AceH3 was similar at promoters of *S100A9* and *S100A12* in M1 macrophages. The level of AceH3 had significantly increased at both *S100A9* and *S100A12* promoters. Donors responded very heterogenous. In some of them studied epigenetic marks correlated to gene expression changes.

H3K4me1 is known to function as distal mark (Barski, Cuddapah et al. 2007), whereas H3K4me3 is a promoter mark (Dong, Greven et al. 2012). H3K4me1 association was similar over several distances of TSS of S100 promoters whereas the highest association of H3K4me3 and AceH3 are seen near the TSS. The effect of H3K4me3 on transcription was once studied by specifically inducing PRDM9 methyltransferase writing only H3K4me3. Researchers were able to increase H3K4me3 at specific promoter site and thereby up regulate transcription ICAM1, RASSF1a and EpCAM in HEK293T, A549 and A2780 cells (Cano-Rodriguez, Gjaltema et al. 2016). Successful upregulation of transcription however depended on the TSS site being DNA hyper methylated or H3K4me3 not already been enriched (Cano-

Rodriguez, Gjaltema et al. 2016). S100A9 and S100A12 promoter do not contain CpG-islands. Dense DNA-methylation on cytosine's of CpG dinucleotides, predominantly concentrated in CG-islands (CGI) (Deaton and Bird 2011) and low CpG genes have shown to be less predictable (Dong, Greven et al. 2012).

Also in RAW 264.7 macrophage-like cells stimulated with LPS, it has been shown that high and ongoing transcription was marked by either H3K79me2 or H3K36me3 and showed specific enrichment of motifs recognized by the NF-kB and IRF proteins (Soldi, Mari et al. 2017). Therefore, another reason that we did not observe strong association with transcription might be that H3K4me3 and transcriptional initiation are tightly linked but elongation of RNApII afterwards might occur through methyltransferases recognizing H3K36me3 (Li, Carey et al. 2007). H3K36me can function according general mechanism as H3K4me but is usually located in the gene body and specific co-association was found of H3K4me1 with H3K36me2/K36me3. This highlights the importance of location and combination of histone marks (Soldi, Mari et al. 2017).

AceH3 was mostly and significantly affected by glucose or metabolic changes at the average of 4 donors and different promoter regions. As a consequence, this loosens chromatin and less nucleosomes that were cross-linked to DNA, as reflected by our immunoprecipitation for total H3. For half of the donors, it was observed that elements gaining AceH3 starting from lower levels, in concert gain H3K4me1 whereas H3K4me3 remained relatively constant, as was seen before (Saeed, Quintin et al. 2014). BMDM from T1D mice also show increased total HAT activity and decreased HDAC activity relative to control macrophages (Filgueiras, Brandt et al. 2017). H3 contains more sites of acetylation. In yeast, at different histones both hyper- and hypoacetylation correlated to gene transcription, whereas acetylation at specific residues negatively correlates with increased transcription, although this was mostly seen at H4 (Kurdistani, Tavazoie et al. 2004). Unique acetylation patterns at single sites, mediate preferential TF binding and cluster in functional categories of genes (Kurdistani, Tavazoie et al. 2004).

Additional epigenetic mechanisms that regulate expression of these genes include enhancers and might be taken in consideration in further studies. Also, most cited studies refer to genome wide studies or have been performed in cell lines where not individual donor responses and genetic differences play a role.

Cultivation of macrophages in the presence of high glucose culture the level of total H3. The change in levels of total endogenous H3 is positively correlated to fold change increases in gene expression, whereas at some single promoter regions an almost linear correlation was

observed. Nucleosomes exclude TFs from binding the DNA and therefore are general repressors of gene transcription (Mao, Brown et al. 2011). Levels of total H3 unexpectedly positively correlated to fold change increases in the expression of *S100A9* and *S100A12*. The strongest correlation was found for *S100A9*. Therefore, S100A9 transcription seems to be tightly regulated by nucleosome density. The positive effect of nucleosome density in our study is not intuitive and indicates that the general rule of activating and repressing marks is not valid in exceptional cases or acts independently from each other. In one study, where nucleosome density on a specific promoter was manipulated by changing GC content - occupancy increases with GC% of intrinsic DNA sequence -, the lowest GC% also did not correlate to highest output i.e. promoter activity (Parikh and Kim 2013). Nucleosomes are not bound 100% of the time but assemble and disassemble in equilibrium. Positioning is defined by DNA sequence and not changeable, but occupancy varies genome wide and gene specifically. A reduction in nucleosome number therefore can increase the variability of relative occupancy since the histone pool is finite (Celona, Weiner et al. 2011). Relative high occupancy together with high DNA accessibility has been described before and were not necessarily correlating with each other (Mieczkowski, Cook et al. 2016). Authors suggest this might be due to low stability of nucleosomes in regions which are often marked with active chromatin marks i.e. acetylation, but also increased chromatin remodelling can induce an increase in inter-nucleosomal spacing (Mieczkowski, Cook et al. 2016). Nucleosome depletion also increased 15% but not affected expression of 75% genes in yeast switched to glucose medium. These could be genes that are already induced, or the transcriptional activators and repressors may be dominant in gene regulation (Wyrick, Holstege et al. 1999). Activators of transcription are believed to act by recruitment of chromatin remodellers (Harikumar and Meshorer 2015) which promote nucleosome removal (Boeger, Shelansky et al. 2015). Chromatin remodelling complexes such as SWI/SNF complex accommodate single nucleosomes and their action is coupled to ATP hydrolysis which biases the spontaneous unwrapping of the DNA (Becker and Workman 2013, Parikh and Kim 2013, Boeger, Shelansky et al. 2015). At last, one key player in macrophages DNA wrapping is high mobility group box1 (HMGB1). It resides in nucleus but is secreted after LPS/IFNγ stimulus reducing histone content and activating transcription (De Toma, Rossetti et al. 2014). It was found to be sensitive to and activated by exposure to high glucose (Chen, Qiao et al. 2015). Therefore, different mechanisms might play a role in our study though it is clear that histone content is critical in interpreting chromatin organization as it constitutes of an extra layer of epigenetic regulation.

4.4 Manipulation of S100 expression by targeting histone modifying enzymes.

We see the different effects of inhibition of HMTs. Inhibition of SET7 down regulated *S100A9* and *S10012* expression, while SMYD3 inhibition was specific for S100A12 in the same donors. Inhibitions of MLL tend to increase expression increased S100 expression.

The key histone methyltransferase that is activated by hyperglycemia is SET7/9 and writes the H3K4me1 activation marks. SET7 is involved in inflammatory signalling and found to be a co-activator of NF-κB in macrophages. DMSO alone did not change expression of *S100A9* and *S100A12*, however a slight decrease has been seen in all the experiments with HMT inhibitors and especially were PFI-2 was applied. The highest concentration of DMSO used in this study was 0.002%. No cytotoxicity of DMSO though has been found up to 10% in BMDM (Ahn, Kim et al. 2014) and hardly change of gene expression profiles up to 0.5% in human hepatocytes (Sumida, Igarashi et al. 2011). However, DMSO might have anti-inflammatory effects and inhibit cytokine production (Ahn, Kim et al. 2014). Possible mechanisms for the anti-inflammatory properties of DMSO suggested include ROS scavenging (Santos, Figueira-Coelho et al. 2003, Xiang, Zhao et al. 2018), NF-κB inhibition (Chang, Llanes et al. 1999) and intracellular calcium reduction (Santos, Figueira-Coelho et al. 2003). Gene silencing of SET7 attenuated TNF-α induced H3K4me and recruitment of NF-κB p65 to inflammatory gene promoters in THP-1 cells as well as in macrophages from diabetic mice (Li, Reddy et al. 2008). SET7 expression was increased and H3K4me1 on NF-kB p65 promoter was associated with expression of NF-kB-dependent oxidant/inflammatory genes COX2 and iNOS in PBMCs form T2D patients (Paneni, Costantino et al. 2015). However, many also non-histone proteins are regulated by SET7 and its biological outcome depends on the specificity of the TF target (Batista and Helguero 2018). Also, SET7 inhibition by PFI(2) compound depends on SAM availability (Kaniskan, Martini et al. 2017). SET7/9 knockdown attenuated adhesion to TNF-α-treated HUVEC monolayers before (Li et al., 2008). Therefore, SET7 is an inflammatory mediator and glucose sensor.

WDR5 is part of complex that stimulates the catalytic activity of HMTs. This WRAD complex exists separate from MLL enzymes and has additional interactions partners and functions in the cells (van Nuland, Smits et al. 2013). Members of the MLL family show preferential methylation levels and this is according to their localization in the chromatin e.g., SET1A and B are found at promoter and preferential trimethylate whereas MLL3 and 4 localize at enhancer regions as is H3K4me1 (Bochynska, Lüscher-Firzlaff et al. 2018). H3K4me1 at the promoter region is even suggested to induce transcriptional silencing and restrict H3K4me3 reading, in macrophages among other cell types, although it is not clear

whether this is provoked by MLL3/4 or the remaining methylation after demethylase activity (Cheng, Blum et al. 2014, Bochynska, Lüscher-Firzlaff et al. 2018). This could be an explanation for the negative correlation of H3K4me1 with increased gene transcription. The authors also observed that H3K4me1 for a group of acutely inducible genes, was mediated by MLL3/4 and loss of this HMT even promoted stimulus-dependent i.e. LPS induced gene expression without changes in H3K4me3 levels (Cheng, Blum et al. 2014). Then, the function of the modification is largely defined by the effector or reader protein and might explain our observation that MLL inhibition did not reduce but even increased gene expression of S100A9 in high glucose conditions.

Specific recruitment seems more likely to occur through the specific subunits of the MLL protein family members and might be reached by sequence specific TFs (Table 2 in (Bochynska, Lüscher-Firzlaff et al. 2018). MLL proteins possess e.g. CXXC zinc finger domains to bind unmethylated CpG islands as well as an AT-hook region or high mobility group 1 binding motifs - or interaction with chromatin via PHD fingers, bromodomains or WD40 (Bochynska, Lüscher-Firzlaff et al. 2018). The MLL1 and MLL2 complexes both contain the tumour suppressor gene menin. In macrophages enhancer transcription was linked to H3K4 methylation and TLR4 signalling which depended on MLL1, 2/4 and 3 (Kaikkonen, Spann et al. 2013). Also, differentiation of macrophage into M0, M1 and M2 showed specific upregulation of MLL HMTases and KDM6B demethylase in M1 macrophages and regulate CXCL10 expression, which could be blocked using a MLL-Menin inhibitor (Kittan, Allen et al. 2013). Notably, HG induced S100 gene expression and regulation of S100 gene expression by MLL enzymes showed to be synergistic for *S100A9*, pointing out pro-inflammatory activation in cultured monocyte/macrophages by glucose. Inhibiting the menin pathway has been suggested before as diabetes treatment (Jen and Wu 2008).

Expression of SMYD3 is up regulated in M0 and M2 compared to M1 macrophages (Kittan, 2013). SMYD family of proteins contains five members and methylate histones as well as non-histone targets (Spellmon, Holcomb et al. 2015). SMYD2 facilitates H3K36me2 and negatively regulates *TNF* and *IL-6* promoters in macrophages inhibits NF-κB and ERK signalling (Xu, Liu et al. 2015). In addition, trimethylation at H4K20 by SMYD5 represses TLR4 target genes in macrophages through its association with NCoR co-repressor complex (Stender, Pascual et al. 2012). SMYD3 however, despite existing literature does not methylate H3K4 but far more efficiently methylates H4K5 (Van Aller, Reynoird et al. 2012) and is mainly involved in regulation of transcription and signal transduction pathways promoting cancer development (Mazur, Gozani et al. 2016). SMYD3-mediated methylation of MAP3K2

promoted the activation of the Ras/Raf/MEK/ERK signalling module in cancer cell lines (Mazur, Reynoird et al. 2014). In this study we show that SMYD3 has effect on specifically *S100A12* promoter but not on *S100A9*. Signalling by SMYD3 in diabetic conditions has not been addressed.

This indicate that epigenetic target enzymes control the levels of pro-inflammatory factors (S100 proteins) induced by HG. It remains to be studied if reduction of S100 expression by inhibition of these enzymes correlates with reduction of diabetes severity in preclinical models.

4.4 The involvement of metabolic memory in the expression of S100 proteins

In our memory model M1 macrophages were cultured for six days and medium was changed and cells were harvested at day twelve for analysis. Transient hyperglycemia caused memorable changes of S100 genes, especially *S100A12* expression that last when glucose concentrations are normalized. This type of metabolic memory was not observed for other pro-inflammatory factors *CCR2* and *IL1B.*

When consequences of glycemic events are not normalized with normalizing blood glucose, within the duration of protein half-life or cellular turnover and potentially accumulate with repeated events. Combined this is known as the metabolic memory that is caused by diabetes (Hansen, Hansen et al. 2017, Testa, Bonfigli et al. 2017). Endogenous stimuli from the diabetic environment through epigenetic changes could contribute to training of macrophages and this can already occur in the bone marrow (El-Osta 2012, van Diepen, Thiem et al. 2016).

On the epigenetic level, association of H3K4me3, AceH3 as well as total H3 with the promoter of both *S100A9* and *S100A12* were decreased in M1 macrophages cultured continuously under HG conditions for 12 days. H3K4me1 for *S100A9* and H3K4me3 for *S100A12* were sustained in transient hyperglycemia.

After 12 days the epigenetic picture is different compared to 6 days. This could be either effect of medium change or chronic exposure to HG, which probably switches on an negative feedback mechanism that start to inactivate chromatin by a decrease in activating marks on the promoter of pro-inflammatory genes. H3K4me1 for *S100A9* and H3K4me3 for *S100A12* possibly mark metabolic memory. H3K4me1 has been associated with epigenetic memory and/or trained immunity in macrophages before but in opposite manner; it was found that elements that loose the H3K27ac not loose H3K4me1 (Saeed, Quintin et al. 2014). It might be that glucose induced *S100A12* expression is involved in training processes. Enhancers also may provide a mechanism for epigenetic memory based on their responses to different

stimuli. Latent enhancers, after washout of the stimulus, showed a residual sustained H3K4me1 although PU.1 and acetylation were lost which was associated with more rapid and intense induction upon restimulation (Ostuni, Piccolo et al. 2013). Similar, we observed that the change in AceH3 as well as total H3 was reversible and therefore seems to be more dynamic and responsive to metabolic changes. That the changes on gene expression level are not as fast as changes in epigenetic marks could then be a consequence of stabilisation of RNA.

To conclude, memorable changes in S100 gene expression might mediate detrimental effects of chronic hyperglycemia even if glucose levels return to normal range.

4.5 Glucose sensitizes macrophages to the action of exogenous and endogenous pro-inflammatory factors

LPS induced expression of both *S100A9, S100A12* compared to non-stimulated controls. We observed that high glucose dramatically increased the expression levels of *S100A9* in response to PA and of *S100A12* in LPS stimulated cells. Therefore, hyperglycemia works synergistically together with stimulation with TLR-ligands and S100 proteins are sensitive to glucose programming. It has been shown before that high glucose induces a priming effect in macrophages and sensitizes cells towards inflammatory response (Grosick, Alvarado-Vazquez et al. 2018, Pavlou, Lindsay et al. 2018). It might be that due to the fact that glucose directly elevates the expression of TLRs (Dasu, Devaraj et al. 2008). Another possible explanation would be that chromatin on S100 promoters is already opened and the presences of secondary pro-inflammatory mediators dramatically induce the expression of these genes. Probably, both metabolic and epigenetic changes contribute to observed effects at a few levels in this study.

Firstly, since glucose metabolism determines immune cell activation and also long-term training of monocytes via the AKT–mTOR–HIF-1a pathway (Cheng, Quintin et al. 2014) it had been hypothesized that high circulating levels of glucose could program immune cells towards an inflammatory phenotype through increased glucose utilization via glycolysis (van Diepen, Thiem et al. 2016). However, we observed that culture in high glucose conditions did not change glucose uptake of M0 and M1 macrophages (paragraph 3.2.1), and it has been suggested before that increased glucose supply, i.e. increased uptake alone are not sufficient to drive inflammatory activation and atherosclerosis in myeloid cells (Vallerie and Bornfeldt 2015). Instead, overutilization of glucose via glycolytic enzyme pyruvate kinase M2 (PKM2) which phosphorylates STAT3 in turn, has been shown in macrophages of patients with coronary artery disease (Shirai, Nazarewicz et al. 2016). Likewise, in BMDM macrophages

after long term culture under high glucose conditions mitochondrial functions and basal glycolysis were not affected, but cells showed impaired glycolytic capacity i.e. the maximum rate of conversion of glucose to pyruvate or lactate. The glycolytic reserve is an important source of energy in cases of ATP demand. When proinflammatory response depends on glycolysis e.g. NADPH production for ROS and NO, the limited energy supply translates into impaired functions (Pavlou, Lindsay et al. 2018).

Second, several metabolic characteristics of M1 macrophages i.e. ROS, NO and succinate, are important demethylase inhibitors and inhibiting glycolysis or stimulating mitochondrial metabolism reduced the formation of HDAC inhibitor lactate (Baardman, Licht et al. 2015). This might provide a link between metabolism and AceH3 levels in our study.

Third, hyperglycemia-induced ROS and methylglyoxal production has shown do regulate expression of RAGE, S100A8, S100A12, and HMGB1 expression, which was normalized by overexpression of UCP1, SOD2, or GLO1. Loss of GLO1 mimicked the effect of high glucose whereas overexpression of GLO1 normalized the increased binding of NFκB p65 and AP-1 to the respective promoters (Yao and Brownlee 2009), which might be mediated by SET7 (Yang, Huang et al. 2009). At last, overexpression S100A8 and -A9 led to increased IL-10, where TN-α and IL-1β did not change (Yang, Anholts et al. 2018). IL-10 mediates many anti-inflammatory effects in macrophages, but also has a role in metabolic programming; it inhibits glycolytic flux by inhibiting translocation of GLUT1 to the membrane and in LPS-stimulated murine BMDMs (Ip, Hoshi et al. 2017). GLUT1 seems to be the primary rate-limiting glucose transporter for proinflammatory macrophages (Freemerman, Johnson et al. 2014) which expression had not changed (GSE86298 by (Moganti 2017). On the other side we find ARRDC4 together with TXNIP highly up regulated under high glucose conditions. Both are able to inhibit glucose uptake and lactate output in adipocytes and skin fibroblasts (Patwari, Chutkow et al. 2009) and therefore might provide another mechanism by which macrophages regulate glucose metabolism.

To summarize, a strong upregulation of S100 proteins by endogenous and diabetes-relevant ligands in HG glucose conditions suggests that they can be important players in diabetes-related inflammation.

4.6 Conclusion and outlook

Glucose primes macrophages towards increased inflammatory response, whereas hyperglycemia causes memorable changes of S100 genes expression that last when glucose concentrations are normalized. S100 proteins have pleiotropic functions in immune cells.

S100A8 and S100A9 seem to have more protective effects in regulation of inflammation, whereas S100A12 is rather pro-inflammatory (Bowman, Wilk et al. 2010, Goyette and Geczy 2011). Glucose inhibits its down regulation during maturation, and this is accompanied with epigenetic changes at the promoters. HMTs play a role in metabolic induced changes in polarized macrophages. S100A8/A9 is involved in tolerance and negative feedback of inflammation (Austermann, Friesenhagen et al. 2014). Its increase under high glucose conditions seems a protective mechanism of the macrophage to reduce excessive inflammation. A suggested order of events by Schiopu et all. is that traditional cardiovascular risk factors like smoking, dyslipidemia, hyperglycemia and obesity directly or indirectly elevate S100A8/A9 production and stimulate myeloid cell production in the bone marrow (Nagareddy, Murphy et al. 2013) as well as their recruitment to the vessel wall via endothelial activation (Viemann, Strey et al. 2005) and increased expression of integrin's (Eue, Pietz et al. 2000, Bouma, Lam-Tse et al. 2004). Local levels of S100 proteins may be deposited by leukocytes and S-nitrosylation by NO coming from EC may regulate function, but, in turn, regulatory roles of S100A8/A9 is important resolution of inflammation, T cell tolerance, and tissue repair because of its co-dependence on IL-10 for induction and secretion, but also because of oxidant scavenging or ROS regulating capacities (Lim, Raftery et al. 2009).

Individual differences in S100 protein expression in response to hyperglycemia and pro-inflammatory stimuli suggest that S100 proteins can be used to distinguish between responders and non-responders towards hyperglycemia indicating the risks for later vascular complications in diabetes patients. Hyperglycemia can reprogram M1 macrophages via regulation of S100A expression on the epigenetic level. An upregulation of S100 proteins by endogenous and diabetes-relevant ligands in HG glucose conditions suggests that they can be important players in diabetes-related inflammation and their targeting (e.g. using inhibitors of chromatin-modifying enzymes) can reduce inflammation providing a benefit for diabetes patients.

5 SUMMARY

The number of diabetic patients in Europe and world-wide is growing. Diabetes confers to about two-fold higher risk for a wide range of vascular diseases independently from common risk factors such as age, sex, smoking, high blood pressure, and BMI. Lack of insulin (T1D) or lack of insulin responsiveness (T2D) causes metabolic changes such as hyperglycemia (HG) which contributes to the pathology of diabetes. Macrophages are essential regulators of inflammation and play a critical role in diabetic macro- and microvascular complications. Previous work in our laboratory using Affymetrix chip profiling identified that hyperglycemia enhances the expression of several members of the S100 protein family in macrophages. S100A9 and S100A12 are pro-inflammatory molecules that activate endothelial cells. Their elevated levels in the circulation positively correlate with diabetes pathology. However the role of hyperglycemia in the production of S100A9 and A12 by macrophages was not investigated to date. The aims of the study were 1) to investigate the regulation of S100A9 and - S100A12 expression during macrophage differentiation in normal and hyperglycemic conditions and diabetic patients; to examine the effect of hyperglycemia on the histone code on the promoters of *S100A9* and *S100A12* and the involvement of specific histone modifying enzymes; to examine potential hyperglycemic memory for the expression of *S100A9* and *S100A12* in macrophages.

Human primary monocytes-derived macrophages were used and differentiated for 6 day in the presence of IFNγ or IL-4 to generate M1 and M2 macrophages respectively and without cytokines to generate M0 macrophages. Using RT-PCR it was demonstrated that S100A9 and –A12 are highly expressed in M1 macrophages compared to M2. Hyperglycemia increased the expression of S100A9 and S100A12 in M0 but mostly in M1 macrophages, up to 4.4-fold and 9.8-fold for individual donors respectively. Association for activating histone marks with the promoters of these genes was analysed by chromatin immunoprecipitation (ChIP). Hyperglycemia induced the increased association of activating histone marks; H3K4me1, H3K4me3 and general H3Ace with promoters of *S100A9* and *S100A12*. Association correlated negatively with the increase in gene expression. The total H3, representing the nucleosome density, was reduced under HG conditions. The increase in total endogenous H3 positively correlated to the fold change increases in gene expression of *S100A9* and *S100A12*. Histone methyltransferases regulate gene expression in differentiated M1 macrophages. Application of inhibitors of the MLL complex increased S100 gene expression synergistically with glucose. Inhibition of SMYD3 specifically down regulated S100A12 expression.

Inhibition of SET7, the key histone methyltransferase that writes H3K4me1, down regulated both S100A9 and –A12 gene expression. Expression of SET7 and its translocation to the nuclei was increased in M1 macrophages and under high glucose conditions. In a macrophage model were glucose concentrations were changed to normal glucose concentration after 6 days, and gene expression was measured on day 12, memorable changes of S100 genes expression in M1 macrophages were observed. In another model, where macrophages without polarizing factors are cultured in high glucose conditions for 6 days and subsequently stimulated overnight with TLR-ligands, increased expression of S10 protein was identified. *S100A9* had increased in response to stimulation with PA (9.9-fold). *S100A12* was up regulated in LPS stimulation of macrophages (5.4-fold).

Therefore, increased expression of S100 proteins may be indicative for the long-term pro-inflammatory effects of hyperglycemia. S100 proteins are expressed in M1 macrophage and their expression is up regulated in hyperglycemic conditions, whereas histone modifying enzymes SMYD3 and SET7 are involved. Also, histone code might regulate transcription independently from nucleosome density in our study and histone content constitutes of an extra layer of epigenetic regulation. At last, stimulation of hyperglycemia-exposed macrophages by TLR-ligands revealed that S100 proteins are sensitive to glucose macrophages programming.

Individual differences in S100 protein expression in response to hyperglycemia and pro-inflammatory stimuli suggest that S100 proteins can be used to distinguish between responders and non-responders towards hyperglycemia indicating the risks for later vascular complications in diabetes patients. S100 proteins can be considered as a target in chronic inflammatory conditions, and macrophage directed treatments that aim to reprogram M1 macrophages, should take into account the level of induced epigenetic changes.

6 REFERENCES

Abdel-Moneim, A., H. H. Bakery and G. Allam (2018). "The potential pathogenic role of IL-17/Th17 cells in both type 1 and type 2 diabetes mellitus." Biomedicine & Pharmacotherapy **101**: 287-292.
Ahn, H., J. Kim, E.-B. Jeung and G.-S. Lee (2014). "Dimethyl sulfoxide inhibits NLRP3 inflammasome activation." Immunobiology **219**(4): 315-322.
Ajami, B., J. L. Bennett, C. Krieger, W. Tetzlaff and F. M. V. Rossi (2007). "Local self-renewal can sustain CNS microglia maintenance and function throughout adult life." Nature Neuroscience **10**: 1538.
Altmann, C. and M. H. H. Schmidt (2018). "The Role of Microglia in Diabetic Retinopathy: Inflammation, Microvasculature Defects and Neurodegeneration." International journal of molecular sciences **19**(1): 110.
Alvarez, M. M., J. C. Liu, G. Trujillo-de Santiago, B.-H. Cha, A. Vishwakarma, A. M. Ghaemmaghami and A. Khademhosseini (2016). "Delivery strategies to control inflammatory response: Modulating M1–M2 polarization in tissue engineering applications." Journal of Controlled Release **240**: 349-363.
Andrassy, M., J. Igwe, F. Autschbach, C. Volz, A. Remppis, M. F. Neurath, E. Schleicher, P. M. Humpert, T. Wendt, B. Liliensiek, M. Morcos, S. Schiekofer, K. Thiele, J. Chen, R. Kientsch-Engel, A.-M. Schmidt, W. Stremmel, D. M. Stern, H. A. Katus, P. P. Nawroth and A. Bierhaus (2006). "Posttranslationally Modified Proteins as Mediators of Sustained Intestinal Inflammation." The American Journal of Pathology **169**(4): 1223-1237.
Andrejeva, G. and J. C. Rathmell (2017). "Similarities and distinctions of cancer and immune metabolism in inflammation and tumors." Cell metabolism **26**(1): 49-70.
Asmis, R. (2016). "Monocytes and Macrophages: A Fresh Look at Functional and Phenotypic Diversity." Antioxidants & redox signaling **25**(14): 756-757.
Austermann, J., J. Friesenhagen, Selina K. Fassl, T. Ortkras, J. Burgmann, K. Barczyk-Kahlert, E. Faist, S. Zedler, S. Pirr, C. Rohde, C. Müller-Tidow, M. von Köckritz-Blickwede, Constantin S. von Kaisenberg, Stefanie B. Flohé, T. Ulas, Joachim L. Schultze, J. Roth, T. Vogl and D. Viemann (2014). "Alarmins MRP8 and MRP14 Induce Stress Tolerance in Phagocytes under Sterile Inflammatory Conditions." Cell Reports **9**(6): 2112-2123.
Averill, M. M., S. Barnhart, L. Becker, X. Li, J. W. Heinecke, R. C. LeBoeuf, J. A. Hamerman, C. Sorg, C. Kerkhoff and K. E. Bornfeldt (2011). "S100A9 Differentially Modifies Phenotypic States of Neutrophils, Macrophages, and Dendritic Cells." Circulation **123**(11): 1216-1226.
Baardman, J., I. Licht, M. P. d. Winther and J. V. d. Bossche (2015). "Metabolic–epigenetic crosstalk in macrophage activation." Epigenomics **7**(7): 1155-1164.
Bannister, A. J. and T. Kouzarides (2011). "Regulation of chromatin by histone modifications." Cell research **21**(3): 381-395.
Barres, R., J. Yan, B. Egan, J. T. Treebak, M. Rasmussen, T. Fritz, K. Caidahl, A. Krook, D. J. O'Gorman and J. R. Zierath (2012). "Acute exercise remodels promoter methylation in human skeletal muscle." Cell metabolism **15**(3): 405-411.
Barski, A., S. Cuddapah, K. Cui, T.-Y. Roh, D. E. Schones, Z. Wang, G. Wei, I. Chepelev and K. Zhao (2007). "High-resolution profiling of histone methylations in the human genome." Cell **129**(4): 823-837.
Barsyte-Lovejoy, D., F. Li, M. J. Oudhoff, J. H. Tatlock, A. Dong, H. Zeng, H. Wu, S. A. Freeman, M. Schapira and G. A. Senisterra (2014). "(R)-PFI-2 is a potent and selective inhibitor of SETD7 methyltransferase activity in cells." Proceedings of the National Academy of Sciences **111**(35): 12853-12858.

Basta, G., A. M. Sironi, G. Lazzerini, S. Del Turco, E. Buzzigoli, A. Casolaro, A. Natali, E. Ferrannini and A. Gastaldelli (2006). "Circulating Soluble Receptor for Advanced Glycation End Products Is Inversely Associated with Glycemic Control and S100A12 Protein." The Journal of Clinical Endocrinology & Metabolism **91**(11): 4628-4634.
Batista, I. d. A. A. and L. A. Helguero (2018). "Biological processes and signal transduction pathways regulated by the protein methyltransferase SETD7 and their significance in cancer." Signal transduction and targeted therapy **3**: 19-19.
Becker, P. B. and J. L. Workman (2013). "Nucleosome remodeling and epigenetics." Cold Spring Harbor perspectives in biology **5**(9): a017905.
Bernstein, B. E., T. S. Mikkelsen, X. Xie, M. Kamal, D. J. Huebert, J. Cuff, B. Fry, A. Meissner, M. Wernig and K. Plath (2006). "A bivalent chromatin structure marks key developmental genes in embryonic stem cells." Cell **125**(2): 315-326.
Biswas, S., A. S. Chida and I. Rahman (2006). "Redox modifications of protein–thiols: Emerging roles in cell signaling." Biochemical Pharmacology **71**(5): 551-564.
Biswas, S. K., M. Chittezhath, I. N. Shalova and J.-Y. Lim (2012). "Macrophage polarization and plasticity in health and disease." Immunologic Research **53**(1): 11-24.
Biswas, Subhra K. and A. Mantovani (2012). "Orchestration of Metabolism by Macrophages." Cell Metabolism **15**(4): 432-437.
Bochynska, A., J. Lüscher-Firzlaff and B. Lüscher (2018). "Modes of interaction of KMT2 histone H3 lysine 4 methyltransferase/COMPASS complexes with chromatin." Cells **7**(3): 17.
Bode, K. A., K. Schroder, D. A. Hume, T. Ravasi, K. Heeg, M. J. Sweet and A. H. Dalpke (2007). "Histone deacetylase inhibitors decrease Toll- like receptor- mediated activation of proinflammatory gene expression by impairing transcription factor recruitment." Immunology **122**(4): 596-606.
Boeger, H., R. Shelansky, H. Patel and C. R. Brown (2015). "From Structural Variation of Gene Molecules to Chromatin Dynamics and Transcriptional Bursting." Genes **6**(3): 469-483.
Boniakowski, A. E., A. S. Kimball, B. N. Jacobs, S. L. Kunkel and K. A. Gallagher (2017). "Macrophage-Mediated Inflammation in Normal and Diabetic Wound Healing." The Journal of Immunology **199**(1): 17-24.
Bouma, G., J. Coppens, W. K. Lam- Tse, W. Luini, K. Sintnicolaas, W. Levering, S. Sozzani, H. Drexhage and M. Versnel (2005). "An increased MRP8/14 expression and adhesion, but a decreased migration towards proinflammatory chemokines of type 1 diabetes monocytes." Clinical & Experimental Immunology **141**(3): 509-517.
Bouma, G., W. K. Lam-Tse, A. F. Wierenga-Wolf, H. A. Drexhage and M. A. Versnel (2004). "Increased serum levels of MRP-8/14 in type 1 diabetes induce an increased expression of CD11b and an enhanced adhesion of circulating monocytes to fibronectin." Diabetes **53**(8): 1979-1986.
Bouma, G., W. K. Lam-Tse, A. F. Wierenga-Wolf, H. A. Drexhage and M. A. Versnel (2004). "Increased serum levels of MRP-8/14 in type 1 diabetes induce an increased expression of CD11b and an enhanced adhesion of circulating monocytes to fibronectin." Diabetes **53**(8): 1979-1986.
Bourne, R. R., G. A. Stevens, R. A. White, J. L. Smith, S. R. Flaxman, H. Price, J. B. Jonas, J. Keeffe, J. Leasher and K. Naidoo (2013). "Causes of vision loss worldwide, 1990–2010: a systematic analysis." The lancet global health **1**(6): e339-e349.
Bowman, M. H., J. Wilk, A. Heydemann, G. Kim, J. Rehman, J. A. Lodato, J. Raman and E. M. McNally (2010). "S100A12 Mediates Aortic Wall Remodeling and Aortic Aneurysm." Circulation Research **106**(1): 145-154.
Brasacchio, D., J. Okabe, C. Tikellis, A. Balcerczyk, P. George, E. K. Baker, A. C. Calkin, M. Brownlee, M. E. Cooper and A. El-Osta (2009). "Hyperglycemia induces a dynamic cooperativity of histone methylase and demethylase enzymes associated with gene-activating epigenetic marks that coexist on the lysine tail." Diabetes **58**(5): 1229-1236.

Bresnick, A. R., D. J. Weber and D. B. Zimmer (2015). "S100 proteins in cancer." Nature Reviews Cancer **15**: 96.
Burke, A. P., F. D. Kolodgie, A. Zieske, D. R. Fowler, D. K. Weber, P. J. Varghese, A. Farb and R. Virmani (2004). "Morphologic Findings of Coronary Atherosclerotic Plaques in Diabetics." Arteriosclerosis, Thrombosis, and Vascular Biology **24**(7): 1266-1271.
Cairo, G., S. Recalcati, A. Mantovani and M. Locati (2011). "Iron trafficking and metabolism in macrophages: contribution to the polarized phenotype." Trends in Immunology **32**(6): 241-247.
Cano-Rodriguez, D., R. A. F. Gjaltema, L. J. Jilderda, P. Jellema, J. Dokter-Fokkens, M. H. J. Ruiters and M. G. Rots (2016). "Writing of H3K4Me3 overcomes epigenetic silencing in a sustained but context-dependent manner." Nature communications **7**: 12284.
Celona, B., A. Weiner, F. Di Felice, F. M. Mancuso, E. Cesarini, R. L. Rossi, L. Gregory, D. Baban, G. Rossetti, P. Grianti, M. Pagani, T. Bonaldi, J. Ragoussis, N. Friedman, G. Camilloni, M. E. Bianchi and A. Agresti (2011). "Substantial Histone Reduction Modulates Genomewide Nucleosomal Occupancy and Global Transcriptional Output." PLOS Biology **9**(6): e1001086.
Chakraborty, P., P. Bjork, E. Källberg, A. Olsson, M. Riva, M. Mörgelin, D. Liberg, F. Ivars and T. Leanderson (2015). "Vesicular location and transport of S100A8 and S100A9 proteins in monocytoid cells." PloS one **10**(12): e0145217.
Chang, C. K., S. Llanes and W. Schumer (1999). "Inhibitory effect of dimethyl sulfoxide on nuclear factor-κB activation and intercellular adhesion molecule 1 gene expression in septic rats." Journal of Surgical Research **82**(2): 294-299.
Chang, S.-C. and W.-C. V. Yang (2016). "Hyperglycemia, tumorigenesis, and chronic inflammation." Critical Reviews in Oncology/Hematology **108**: 146-153.
Chen, Y., F. Qiao, Y. Zhao, Y. Wang and G. Liu (2015). "HMGB1 is activated in type 2 diabetes mellitus patients and in mesangial cells in response to high glucose." International journal of clinical and experimental pathology **8**(6): 6683-6691.
Cheng, J., R. Blum, C. Bowman, D. Hu, A. Shilatifard, S. Shen and B. D. Dynlacht (2014). "A role for H3K4 monomethylation in gene repression and partitioning of chromatin readers." Molecular cell **53**(6): 979-992.
Cheng, S.-C., J. Quintin, R. A. Cramer, K. M. Shepardson, S. Saeed, V. Kumar, E. J. Giamarellos-Bourboulis, J. H. A. Martens, N. A. Rao, A. Aghajanirefah, G. R. Manjeri, Y. Li, D. C. Ifrim, R. J. W. Arts, B. M. J. W. van der Veer, P. M. T. Deen, C. Logie, L. A. O'Neill, P. Willems, F. L. van de Veerdonk, J. W. M. van der Meer, A. Ng, L. A. B. Joosten, C. Wijmenga, H. G. Stunnenberg, R. J. Xavier and M. G. Netea (2014). "mTOR- and HIF-1α–mediated aerobic glycolysis as metabolic basis for trained immunity." Science **345**(6204): 1250684.
Chistiakov, D. A., V. A. Myasoedova, V. V. Revin, A. N. Orekhov and Y. V. Bobryshev (2018). "The impact of interferon-regulatory factors to macrophage differentiation and polarization into M1 and M2." Immunobiology **223**(1): 101-111.
Collaboration, E. R. F. (2010). "Diabetes mellitus, fasting blood glucose concentration, and risk of vascular disease: a collaborative meta-analysis of 102 prospective studies." The Lancet **375**(9733): 2215-2222.
Cotoi, O. S., P. Dunér, N. Ko, B. Hedblad, J. Nilsson, H. Björkbacka and A. Schiopu (2014). "Plasma S100A8/A9 correlates with blood neutrophil counts, traditional risk factors, and cardiovascular disease in middle-aged healthy individuals." Arteriosclerosis, thrombosis, and vascular biology **34**(1): 202-210.
Dasu, M. R., S. Devaraj, S. Park and I. Jialal (2010). "Increased toll-like receptor (TLR) activation and TLR ligands in recently diagnosed type 2 diabetic subjects." Diabetes care **33**(4): 861-868.

Dasu, M. R., S. Devaraj, L. Zhao, D. H. Hwang and I. Jialal (2008). "High Glucose Induces Toll-Like Receptor Expression in Human Monocytes." Mechanism of Activation **57**(11): 3090-3098.
Dasu, M. R., S. Devaraj, L. Zhao, D. H. Hwang and I. Jialal (2008). "High glucose induces toll-like receptor expression in human monocytes." Diabetes **57**(11): 3090-3098.
De Santa, F., V. Narang, Z. H. Yap, B. K. Tusi, T. Burgold, L. Austenaa, G. Bucci, M. Caganova, S. Notarbartolo, S. Casola, G. Testa, W.-K. Sung, C.-L. Wei and G. Natoli (2009). "Jmjd3 contributes to the control of gene expression in LPS-activated macrophages." The EMBO journal **28**(21): 3341-3352.
De Toma, I., G. Rossetti, S. Zambrano, M. E. Bianchi and A. Agresti (2014). "Nucleosome loss facilitates the chemotactic response of macrophages." Journal of Internal Medicine **276**(5): 454-469.
Deaton, A. M. and A. Bird (2011). "CpG islands and the regulation of transcription." Genes & development **25**(10): 1010-1022.
Diaf, M., M. B. Khaled and F. Sellam (2015). "Correlation between dietary fat intake and atherogenic indices in normal, overweight and obese adults with or without type 2 diabetes." Romanian Journal of Diabetes Nutrition and Metabolic Diseases **22**(4): 347-360.
Diercks, B. P., I. Hauschildt, F. Stäb, H. Wenck, O. Döring and N. Peters (2013). "IL- 10 Promotes Secretion of S100A8/A9 from Human Monocytes Trough an Inclusion in Plasma Membranes." Scandinavian journal of immunology **77**(2): 169-170.
Distel, E., T. J. Barrett, K. Chung, N. M. Girgis, S. Parathath, C. C. Essau, A. J. Murphy, K. J. Moore and E. A. Fisher (2014). "miR33 inhibition overcomes deleterious effects of diabetes mellitus on atherosclerosis plaque regression in mice." Circulation research **115**(9): 759-769.
Donath, M. Y. and S. E. Shoelson (2011). "Type 2 diabetes as an inflammatory disease." Nature Reviews Immunology **11**: 98.
Donato, R., B. R. Cannon, G. Sorci, F. Riuzzi, K. Hsu, D. J. Weber and C. L. Geczy (2013). "Functions of S100 proteins." Current molecular medicine **13**(1): 24-57.
Dong, N., H. Shi, B. Xu and Y. Cai (2015). "Increased plasma S100A12 levels are associated with diabetic retinopathy and prognostic biomarkers of macrovascular events in type 2 diabetic patients." Investigative ophthalmology & visual science **56**(8): 4177-4185.
Dong, N., H. Shi, B. Xu and Y. Cai (2015). "Increased Plasma S100A12 Levels Are Associated With Diabetic Retinopathy and Prognostic Biomarkers of Macrovascular Events in Type 2 Diabetic PatientsAssociation Between Plasma S100A12 Levels and DR." Investigative Ophthalmology & Visual Science **56**(8): 4177-4185.
Dong, X., M. C. Greven, A. Kundaje, S. Djebali, J. B. Brown, C. Cheng, T. R. Gingeras, M. Gerstein, R. Guigó and E. Birney (2012). "Modeling gene expression using chromatin features in various cellular contexts." Genome biology **13**(9): R53.
El-Osta, A. (2012). "Glycemic memory." Curr Opin Lipidol **23**(1): 24-29.
El-Osta, A., D. Brasacchio, D. Yao, A. Pocai, P. L. Jones, R. G. Roeder, M. E. Cooper and M. Brownlee (2008). "Transient high glucose causes persistent epigenetic changes and altered gene expression during subsequent normoglycemia." Journal of Experimental Medicine **205**(10): 2409-2417.
Eue, I., B. Pietz, J. Storck, M. Klempt and C. Sorg (2000). "Transendothelial migration of 27E10+ human monocytes." Int Immunol **12**(11): 1593-1604.
Fadini, G. P., R. Cappellari, M. Mazzucato, C. Agostini, S. V. De Kreutzenberg and A. Avogaro (2013). "Monocyte–macrophage polarization balance in pre-diabetic individuals." Acta diabetologica **50**(6): 977-982.
Fang, H.-Y., R. Hughes, C. Murdoch, S. B. Coffelt, S. K. Biswas, A. L. Harris, R. S. Johnson, H. Z. Imityaz, M. C. Simon, E. Fredlund, F. R. Greten, J. Rius and C. E. Lewis (2009). "Hypoxia-inducible factors 1 and 2 are important transcriptional effectors in primary macrophages experiencing hypoxia." Blood **114**(4): 844-859.

Foell, D., H. Wittkowski, C. Kessel, A. Lüken, T. Weinhage, G. Varga, T. Vogl, T. Wirth, D. Viemann, P. Björk, M. A. D. v. Zoelen, F. Gohar, G. Srikrishna, M. Kraft and J. Roth (2013). "Proinflammatory S100A12 Can Activate Human Monocytes via Toll-like Receptor 4." American Journal of Respiratory and Critical Care Medicine **187**(12): 1324-1334.
Forman, H. J., J. M. Fukuto and M. Torres (2004). "Redox signaling: thiol chemistry defines which reactive oxygen and nitrogen species can act as second messengers." American Journal of Physiology-Cell Physiology **287**(2): C246-C256.
Forrester, M. T., D. Seth, A. Hausladen, C. E. Eyler, M. W. Foster, A. Matsumoto, M. Benhar, H. E. Marshall and J. S. Stamler (2009). "Thioredoxin-interacting Protein (Txnip) Is a Feedback Regulator of S-Nitrosylation." Journal of Biological Chemistry **284**(52): 36160-36166.
Fraternale, A., S. Brundu and M. Magnani (2015). "Polarization and repolarization of macrophages." J Clin Cell Immunol **6**(319): 2-12.
Freemerman, A. J., A. R. Johnson, G. N. Sacks, J. J. Milner, E. L. Kirk, M. A. Troester, A. N. Macintyre, P. Goraksha-Hicks, J. C. Rathmell and L. Makowski (2014). "Metabolic Reprogramming of Macrophages: GLUCOSE TRANSPORTER 1 (GLUT1)-MEDIATED GLUCOSE METABOLISM DRIVES A PROINFLAMMATORY PHENOTYPE." Journal of Biological Chemistry **289**(11): 7884-7896.
Frosch, M., A. Strey, T. Vogl, N. M. Wulffraat, W. Kuis, C. Sunderkötter, E. Harms, C. Sorg and J. Roth (2000). "Myeloid-related proteins 8 and 14 are specifically secreted during interaction of phagocytes and activated endothelium and are useful markers for monitoring disease activity in pauciarticular-onset juvenile rheumatoid arthritis." Arthritis & Rheumatism **43**(3): 628-637.
Gallagher, K. A., A. Joshi, W. F. Carson, M. Schaller, R. Allen, S. Mukerjee, N. Kittan, E. L. Feldman, P. K. Henke, C. Hogaboam, C. F. Burant and S. L. Kunkel (2015). "Epigenetic changes in bone marrow progenitor cells influence the inflammatory phenotype and alter wound healing in type 2 diabetes." Diabetes **64**(4): 1420-1430.
Geissmann, F., S. Gordon, D. A. Hume, A. M. Mowat and G. J. Randolph (2010). "Unravelling mononuclear phagocyte heterogeneity." Nat Rev Immunol **10**(6): 453-460.
Gharib, S. A., R. S. McMahan, W. E. Eddy, M. E. Long, W. C. Parks, M. L. Aitken and A. M. Manicone (2019). "Transcriptional and functional diversity of human macrophage repolarization." Journal of Allergy and Clinical Immunology **143**(4): 1536-1548.
Gillespie, B. W., H. Morgenstern, E. Hedgeman, A. Tilea, N. Scholz, T. Shearon, N. R. Burrows, V. B. Shahinian, J. Yee and L. Plantinga (2015). "Nephrology care prior to end-stage renal disease and outcomes among new ESRD patients in the USA." Clinical kidney journal **8**(6): 772-780.
Ginhoux, F. and S. Jung (2014). "Monocytes and macrophages: developmental pathways and tissue homeostasis." Nature Reviews Immunology **14**: 392.
Goyette, J. and C. L. Geczy (2011). "Inflammation-associated S100 proteins: new mechanisms that regulate function." Amino Acids **41**(4): 821-842.
Greer, E. L. and Y. Shi (2012). "Histone methylation: a dynamic mark in health, disease and inheritance." Nature Reviews Genetics **13**(5): 343.
Grosick, R., P. A. Alvarado-Vazquez, A. R. Messersmith and E. A. Romero-Sandoval (2018). "High glucose induces a priming effect in macrophages and exacerbates the production of pro-inflammatory cytokines after a challenge." Journal of pain research **11**: 1769-1778.
Haldar, M. and K. M. Murphy (2014). "Origin, development, and homeostasis of tissue-resident macrophages." Immunological reviews **262**(1): 25-35.
Hansen, N. W., A. J. Hansen and A. Sams (2017). "The endothelial border to health: Mechanistic evidence of the hyperglycemic culprit of inflammatory disease acceleration." IUBMB life **69**(3): 148-161.

Harikumar, A. and E. Meshorer (2015). "Chromatin remodeling and bivalent histone modifications in embryonic stem cells." EMBO reports **16**(12): 1609-1619.
Helm, O., J. Held-Feindt, H. Schäfer and S. Sebens (2014). "M1 and M2: there is no "good" and "bad"-How macrophages promote malignancy-associated features in tumorigenesis." Oncoimmunology **3**(7): e946818-e946818.
Hoeksema, M. A. and M. P. de Winther (2016). "Epigenetic regulation of monocyte and macrophage function." Antioxidants & redox signaling **25**(14): 758-774.
Huang, S. C.-C., B. Everts, Y. Ivanova, D. O'Sullivan, M. Nascimento, A. M. Smith, W. Beatty, L. Love-Gregory, W. Y. Lam, C. M. O'Neill, C. Yan, H. Du, N. A. Abumrad, J. F. Urban Jr, M. N. Artyomov, E. L. Pearce and E. J. Pearce (2014). "Cell-intrinsic lysosomal lipolysis is essential for alternative activation of macrophages." Nature Immunology **15**: 846.
Ingels, C., I. Derese, P. J. Wouters, G. Van den Berghe and I. Vanhorebeek (2015). "Soluble RAGE and the RAGE ligands HMGB1 and S100A12 in critical illness: impact of glycemic control with insulin and relation with clinical outcome." Shock **43**(2): 109-116.
Ip, W. K. E., N. Hoshi, D. S. Shouval, S. Snapper and R. Medzhitov (2017). "Anti-inflammatory effect of IL-10 mediated by metabolic reprogramming of macrophages." Science **356**(6337): 513-519.
Jeltsch, A. and R. Z. Jurkowska (2014). "New concepts in DNA methylation." Trends in biochemical sciences **39**(7): 310-318.
Jen, P. H. S. and C. H. Wu (2008). "Echo duration selectivity of the bat varies with pulse-echo amplitude difference." Neuroreport **19**(3): 373-377.
Jha, Abhishek K., Stanley C.-C. Huang, A. Sergushichev, V. Lampropoulou, Y. Ivanova, E. Loginicheva, K. Chmielewski, Kelly M. Stewart, J. Ashall, B. Everts, Edward J. Pearce, Edward M. Driggers and Maxim N. Artyomov (2015). "Network Integration of Parallel Metabolic and Transcriptional Data Reveals Metabolic Modules that Regulate Macrophage Polarization." Immunity **42**(3): 419-430.
Jia, C., H. Chen, M. Wei, X. Chen, Y. Zhang, L. Cao, P. Yuan, F. Wang, G. Yang and J. Ma (2017). "Gold nanoparticle-based miR155 antagonist macrophage delivery restores the cardiac function in ovariectomized diabetic mouse model." International journal of nanomedicine **12**: 4963.
Jin, Y., A. Sharma, C. Carey, D. Hopkins, X. Wang, D. G. Robertson, B. Bode, S. W. Anderson, J. C. Reed and R. D. Steed (2013). "The expression of inflammatory genes is upregulated in peripheral blood of patients with type 1 diabetes." Diabetes Care **36**(9): 2794-2802.
Kaikkonen, M. U., N. J. Spann, S. Heinz, C. E. Romanoski, K. A. Allison, J. D. Stender, H. B. Chun, D. F. Tough, R. K. Prinjha and C. Benner (2013). "Remodeling of the enhancer landscape during macrophage activation is coupled to enhancer transcription." Molecular cell **51**(3): 310-325.
Kaniskan, H. U. m., M. L. Martini and J. Jin (2017). "Inhibitors of protein methyltransferases and demethylases." Chemical reviews **118**(3): 989-1068.
Kapellos, T. S. and A. J. Iqbal (2016). "Epigenetic control of macrophage polarisation and soluble mediator gene expression during inflammation." Mediators of inflammation **2016**.
Kapellos, T. S. and A. J. Iqbal (2016). "Epigenetic Control of Macrophage Polarisation and Soluble Mediator Gene Expression during Inflammation." Mediators of Inflammation **2016**: 15.
Keating, S. and A. El-Osta (2013). "Transcriptional regulation by the Set7 lysine methyltransferase." Epigenetics **8**(4): 361-372.
Khare, S. P., F. Habib, R. Sharma, N. Gadewal, S. Gupta and S. Galande (2011). "HIstome—a relational knowledgebase of human histone proteins and histone modifying enzymes." Nucleic acids research **40**(D1): D337-D342.

Kirchner, H., M. E. Osler, A. Krook and J. R. Zierath (2013). "Epigenetic flexibility in metabolic regulation: disease cause and prevention?" Trends in cell biology **23**(5): 203-209.
Kittan, N. A., R. M. Allen, A. Dhaliwal, K. A. Cavassani, M. Schaller, K. A. Gallagher, W. F. Carson IV, S. Mukherjee, J. Grembecka and T. Cierpicki (2013). "Cytokine induced phenotypic and epigenetic signatures are key to establishing specific macrophage phenotypes." PloS one **8**(10): e78045.
Klug, M., S. Schmidhofer, C. Gebhard, R. Andreesen and M. Rehli (2013). "5-Hydroxymethylcytosine is an essential intermediate of active DNA demethylation processes in primary human monocytes." Genome biology **14**(5): R46.
Kopan, C., T. Tucker, M. Alexander, M. R. Mohammadi, E. J. Pone and J. R. T. Lakey (2018). "Approaches in Immunotherapy, Regenerative Medicine, and Bioengineering for Type 1 Diabetes." Frontiers in Immunology **9**(1354).
Kurdistani, S. K., S. Tavazoie and M. Grunstein (2004). "Mapping Global Histone Acetylation Patterns to Gene Expression." Cell **117**(6): 721-733.
Kzhyshkowska, J., A. Gratchev, J.-H. Martens, O. Pervushina, S. Mamidi, S. Johansson, K. Schledzewski, B. Hansen, X. He and J. Tang (2004). "Stabilin-1 localizes to endosomes and the trans-Golgi network in human macrophages and interacts with GGA adaptors." Journal of leukocyte biology **76**(6): 1151-1161.
Leach, S. T., Z. Yang, I. Messina, C. Song, C. L. Geczy, A. M. Cunningham and A. S. Day (2007). "Serum and mucosal S100 proteins, calprotectin (S100A8/S100A9) and S100A12, are elevated at diagnosis in children with inflammatory bowel disease." Scandinavian journal of gastroenterology **42**(11): 1321-1331.
Lee, T.-S. and L.-Y. Chau (2002). "Heme oxygenase-1 mediates the anti-inflammatory effect of interleukin-10 in mice." Nature medicine **8**(3): 240.
Li, B., M. Carey and J. L. Workman (2007). "The Role of Chromatin during Transcription." Cell **128**(4): 707-719.
Li, L., T. Sawamura and G. Renier (2004). "Glucose Enhances Human Macrophage LOX-1 Expression." Circulation research **94**(7): 892-901.
Li, Y., M. A. Reddy, F. Miao, N. Shanmugam, J.-K. Yee, D. Hawkins, B. Ren and R. Natarajan (2008). "Role of the histone H3 lysine 4 methyltransferase, SET7/9, in the regulation of NF-κB-dependent inflammatory genes relevance to diabetes and inflammation." Journal of Biological Chemistry **283**(39): 26771-26781.
Lim, S. Y., M. Raftery, H. Cai, K. Hsu, W. X. Yan, H.-L. Hseih, R. N. Watts, D. Richardson, S. Thomas, M. Perry and C. L. Geczy (2008). "S-Nitrosylated S100A8: Novel Anti-Inflammatory Properties." The Journal of Immunology **181**(8): 5627-5636.
Lim, S. Y., M. J. Raftery, J. Goyette, K. Hsu and C. L. Geczy (2009). "Oxidative modifications of S100 proteins: functional regulation by redox." Journal of Leukocyte Biology **86**(3): 577-587.
Liu, Y., Y. O. Olanrewaju, Y. Zheng, H. Hashimoto, R. M. Blumenthal, X. Zhang and X. Cheng (2014). "Structural basis for Klf4 recognition of methylated DNA." Nucleic acids research **42**(8): 4859-4867.
Lominadze, G., M. J. Rane, M. Merchant, J. Cai, R. A. Ward and K. R. McLeish (2005). "Myeloid-related protein-14 is a p38 MAPK substrate in human neutrophils." The Journal of Immunology **174**(11): 7257-7267.
Lorenz, E., M. S. Muhlebach, P. A. Tessier, N. E. Alexis, R. Duncan Hite, M. C. Seeds, D. B. Peden and W. Meredith (2008). "Different expression ratio of S100A8/A9 and S100A12 in acute and chronic lung diseases." Respiratory medicine **102**(4): 567-573.
Lorenz, E., M. S. Muhlebach, P. A. Tessier, N. E. Alexis, R. D. Hite, M. C. Seeds, D. B. Peden and W. Meredith (2008). "Different expression ratio of S100A8/A9 and S100A12 in acute and chronic lung diseases." Respiratory medicine **102**(4): 567-573.

Loscalzo, J. and D. E. Handy (2014). "Epigenetic modifications: basic mechanisms and role in cardiovascular disease (2013 Grover Conference series)." Pulmonary circulation **4**(2): 169-174.
Lu, L., S. McCurdy, S. Huang, X. Zhu, K. Peplowska, M. Tiirikainen, W. A. Boisvert and L. X. Garmire (2016). "Time Series miRNA-mRNA integrated analysis reveals critical miRNAs and targets in macrophage polarization." Scientific reports **6**: 37446.
Mac-Marcjanek, K., A. Zieleniak, M. Zurawska-Klis, K. Cypryk, L. Wozniak and M. Wojcik (2018). "Expression Profile of Diabetes-Related Genes Associated with Leukocyte Sirtuin 1 Overexpression in Gestational Diabetes." International journal of molecular sciences **19**(12): 3826.
Mao, C., C. R. Brown, J. Griesenbeck and H. Boeger (2011). "Occlusion of regulatory sequences by promoter nucleosomes in vivo." PloS one **6**(3): e17521-e17521.
Martinez, F. O., S. Gordon, M. Locati and A. Mantovani (2006). "Transcriptional Profiling of the Human Monocyte-to-Macrophage Differentiation and Polarization: New Molecules and Patterns of Gene Expression." The Journal of Immunology **177**(10): 7303-7311.
Mathers, C. D. and D. Loncar (2006). "Projections of global mortality and burden of disease from 2002 to 2030." PLoS medicine **3**(11): e442.
Mazur, P. K., O. Gozani, J. Sage and N. Reynoird (2016). "Novel insights into the oncogenic function of the SMYD3 lysine methyltransferase." Translational cancer research **5**(3): 330.
Mazur, P. K., N. Reynoird, P. Khatri, P. W. Jansen, A. W. Wilkinson, S. Liu, O. Barbash, G. S. Van Aller, M. Huddleston and D. Dhanak (2014). "SMYD3 links lysine methylation of MAP3K2 to Ras-driven cancer." Nature **510**(7504): 283.
Mieczkowski, J., A. Cook, S. K. Bowman, B. Mueller, B. H. Alver, S. Kundu, A. M. Deaton, J. A. Urban, E. Larschan, P. J. Park, R. E. Kingston and M. Y. Tolstorukov (2016). "MNase titration reveals differences between nucleosome occupancy and chromatin accessibility." Nature Communications **7**: 11485.
Mitchell, L. H., P. A. Boriack-Sjodin, S. Smith, M. Thomenius, N. Rioux, M. Munchhof, J. E. Mills, C. Klaus, J. Totman and T. V. Riera (2015). "Novel oxindole sulfonamides and sulfamides: EPZ031686, the first orally bioavailable small molecule SMYD3 inhibitor." ACS medicinal chemistry letters **7**(2): 134-138.
Moganti, K. (2017). "Effect of hyperglycaemia on the activation and epigenetic programming of primary human macrophages ".
Moganti, K., F. Li, C. Schmuttermaier, S. Riemann, H. Klüter, A. Gratchev, M. C. Harmsen and J. Kzhyshkowska (2016). "Hyperglycemia induces mixed M1/M2 cytokine profile in primary human monocyte-derived macrophages." Immunobiology.
Moganti, K., F. Li, C. Schmuttermaier, S. Riemann, H. Klüter, A. Gratchev, M. C. Harmsen and J. Kzhyshkowska (2017). "Hyperglycemia induces mixed M1/M2 cytokine profile in primary human monocyte-derived macrophages." Immunobiology **222**(10): 952-959.
Morris, K. V. (2009). "RNA-directed transcriptional gene silencing and activation in human cells." Oligonucleotides **19**(4): 299-305.
Mukherjee, R., P. Kanti Barman, P. Kumar Thatoi, R. Tripathy, B. Kumar Das and B. Ravindran (2015). "Non-Classical monocytes display inflammatory features: Validation in Sepsis and Systemic Lupus Erythematous." Scientific reports **5**: 13886-13886.
Murata, Y., T. Shimamura and J. Hamuro (2002). "The polarization of Th1/Th2 balance is dependent on the intracellular thiol redox status of macrophages due to the distinctive cytokine production." International Immunology **14**(2): 201-212.
Murray, P. J. (2017). "Macrophage Polarization." Annual Review of Physiology **79**(1): 541-566.
Nagareddy, P. R., A. J. Murphy, R. A. Stirzaker, Y. Hu, S. Yu, R. G. Miller, B. Ramkhelawon, E. Distel, M. Westerterp and L.-S. Huang (2013). "Hyperglycemia promotes myelopoiesis and impairs the resolution of atherosclerosis." Cell metabolism **17**(5): 695-708.

Naito, Y., T. Takagi and Y. Higashimura (2014). "Heme oxygenase-1 and anti-inflammatory M2 macrophages." Archives of Biochemistry and Biophysics **564**: 83-88.
Nandy, D., R. Janardhanan, D. Mukhopadhyay and A. Basu (2011). "Effect of hyperglycemia on human monocyte activation." Journal of Investigative Medicine **59**(4): 661-667.
Netea, M. G. (2013). "Training innate immunity: the changing concept of immunological memory in innate host defence." European Journal of Clinical Investigation **43**(8): 881-884.
O'Neill, L. A. J. and E. J. Pearce (2016). "Immunometabolism governs dendritic cell and macrophage function." The Journal of experimental medicine **213**(1): 15-23.
O'Neill, Luke A. J. (2015). "A Broken Krebs Cycle in Macrophages." Immunity **42**(3): 393-394.
O'Neill, L. A. J. and E. J. Pearce (2016). "Immunometabolism governs dendritic cell and macrophage function." The Journal of Experimental Medicine **213**(1): 15-23.
Odegaard, J. I. and A. Chawla (2011). "Alternative Macrophage Activation and Metabolism." Annual Review of Pathology: Mechanisms of Disease **6**(1): 275-297.
Okabe, J., C. Orlowski, A. Balcerczyk, C. Tikellis, M. C. Thomas, M. E. Cooper and A. El-Osta (2012). "Distinguishing Hyperglycemic Changes by Set7 in Vascular Endothelial Cells." Circulation Research **110**(8): 1067-1076.
Okabe, Y. and R. Medzhitov (2015). "Tissue biology perspective on macrophages." Nature Immunology **17**: 9.
Olefsky, J. M. and C. K. Glass (2010). "Macrophages, inflammation, and insulin resistance." Annual review of physiology **72**: 219-246.
Orkin, S. H. and L. I. Zon (2008). "Hematopoiesis: An Evolving Paradigm for Stem Cell Biology." Cell **132**(4): 631-644.
Ortega, F. J., M. Sabater, J. M. Moreno-Navarrete, N. Pueyo, P. Botas, E. Delgado, W. Ricart, G. Frühbeck and J. M. Fernández-Real (2012). "Serum and urinary concentrations of calprotectin as markers of insulin resistance and type 2 diabetes." European journal of endocrinology **167**(4): 569-578.
Ostuni, R., V. Piccolo, I. Barozzi, S. Polletti, A. Termanini, S. Bonifacio, A. Curina, E. Prosperini, S. Ghisletti and G. Natoli (2013). "Latent enhancers activated by stimulation in differentiated cells." Cell **152**(1): 157-171.
Pan, B., G. Liu, Z. Jiang and D. Zheng (2015). "Regulation of Renal Fibrosis by Macrophage Polarization." Cellular Physiology and Biochemistry **35**(3): 1062-1069.
Paneni, F., S. Costantino, R. Battista, L. Castello, G. Capretti, S. Chiandotto, G. Scavone, A. Villano, D. Pitocco and G. Lanza (2015). "Adverse epigenetic signatures by histone methyltransferase Set7 contribute to vascular dysfunction in patients with type 2 diabetes mellitus." Circulation: Cardiovascular Genetics **8**(1): 150-158.
Parikh, R. Y. and H. D. Kim (2013). "The Effect of an Intervening Promoter Nucleosome on Gene Expression." PLOS ONE **8**(5): e63072.
Patwari, P., W. A. Chutkow, K. Cummings, V. L. R. M. Verstraeten, J. Lammerding, E. R. Schreiter and R. T. Lee (2009). "Thioredoxin-independent Regulation of Metabolism by the α-Arrestin Proteins." Journal of Biological Chemistry **284**(37): 24996-25003.
Pavlou, S., J. Lindsay, R. Ingram, H. Xu and M. Chen (2018). "Sustained high glucose exposure sensitizes macrophage responses to cytokine stimuli but reduces their phagocytic activity." BMC Immunology **19**(1): 24.
Pedersen, L., M. Nybo, M. K. Poulsen, J. E. Henriksen, J. Dahl and L. M. Rasmussen (2014). "Plasma calprotectin and its association with cardiovascular disease manifestations, obesity and the metabolic syndrome in type 2 diabetes mellitus patients." BMC Cardiovascular Disorders **14**(1): 196.
Rammes, A., J. Roth, M. Goebeler, M. Klempt, M. Hartmann and C. Sorg (1997). "Myeloid-related protein (MRP) 8 and MRP14, calcium-binding proteins of the S100 family, are

secreted by activated monocytes via a novel, tubulin-dependent pathway." Journal of Biological Chemistry **272**(14): 9496-9502.
Reichard, P. (1995). "Are there any glycemic thresholds for the serious microvascular diabetic complications?" Journal of diabetes and its complications **9**(1): 25-30.
Reinhardt, K., D. Foell, T. Vogl, M. Mezger, H. Wittkowski, F. Fend, B. Federmann, C. Gille, T. Feuchtinger, P. Lang, R. Handgretinger, W. Andreas Bethge and U. Holzer (2014). "Monocyte-Induced Development of Th17 Cells and the Release of S100 Proteins Are Involved in the Pathogenesis of Graft-versus-Host Disease." The Journal of Immunology **193**(7): 3355-3365.
Rendra, E., V. Riabov, D. M. Mossel, T. Sevastyanova, M. C. Harmsen and J. Kzhyshkowska (2019). "Reactive oxygen species (ROS) in macrophage activation and function in diabetes." Immunobiology **224**(2): 242-253.
Rieger, M. A. and T. Schroeder (2012). "Hematopoiesis." Cold Spring Harbor Perspectives in Biology **4**(12).
Rothbart, S. B. and B. D. Strahl (2014). "Interpreting the language of histone and DNA modifications." Biochimica et Biophysica Acta (BBA) - Gene Regulatory Mechanisms **1839**(8): 627-643.
Rothbart, S. B. and B. D. Strahl (2014). "Interpreting the language of histone and DNA modifications." Biochimica et Biophysica Acta (BBA)-Gene Regulatory Mechanisms **1839**(8): 627-643.
Roy, S. (2016). "miRNA in Macrophage Development and Function." Antioxid Redox Signal **25**(15): 795-804.
Saeed, S., J. Quintin, H. H. Kerstens, N. A. Rao, A. Aghajanirefah, F. Matarese, S.-C. Cheng, J. Ratter, K. Berentsen and M. A. van der Ent (2014). "Epigenetic programming of monocyte-to-macrophage differentiation and trained innate immunity." Science **345**(6204): 1251086.
Saeed, S., J. Quintin, H. H. D. Kerstens, N. A. Rao, A. Aghajanirefah, F. Matarese, S.-C. Cheng, J. Ratter, K. Berentsen, M. A. van der Ent, N. Sharifi, E. M. Janssen-Megens, M. Ter Huurne, A. Mandoli, T. van Schaik, A. Ng, F. Burden, K. Downes, M. Frontini, V. Kumar, E. J. Giamarellos-Bourboulis, W. H. Ouwehand, J. W. M. van der Meer, L. A. B. Joosten, C. Wijmenga, J. H. A. Martens, R. J. Xavier, C. Logie, M. G. Netea and H. G. Stunnenberg (2014). "Epigenetic programming of monocyte-to-macrophage differentiation and trained innate immunity." Science **345**(6204): 1251086.
Saha, S., I. N. Shalova and S. K. Biswas (2017). "Metabolic regulation of macrophage phenotype and function." Immunological Reviews **280**(1): 102-111.
Sandireddy, R., V. G. Yerra, A. Areti, P. Komirishetty and A. Kumar (2014). "Neuroinflammation and Oxidative Stress in Diabetic Neuropathy: Futuristic Strategies Based on These Targets." International Journal of Endocrinology **2014**: 10.
Santos, N. C., J. Figueira-Coelho, J. Martins-Silva and C. Saldanha (2003). "Multidisciplinary utilization of dimethyl sulfoxide: pharmacological, cellular, and molecular aspects." Biochemical pharmacology **65**(7): 1035-1041.
Schenten, V., S. Plançon, N. Jung, J. Hann, J.-L. Bueb, S. Bréchard, E. J. Tschirhart and F. Tolle (2018). "secretion of the Phosphorylated Form of s100a9 from neutrophils is essential for the Proinflammatory Functions of extracellular s100a8/a9." Frontiers in immunology **9**: 447.
Schiopu, A. and O. S. Cotoi (2013). "S100A8 and S100A9: DAMPs at the crossroads between innate immunity, traditional risk factors, and cardiovascular disease." Mediators of inflammation **2013**.
Senisterra, G., H. Wu, A. Allali-Hassani, G. A. Wasney, D. Barsyte-Lovejoy, L. Dombrovski, A. Dong, K. T. Nguyen, D. Smil and Y. Bolshan (2013). "Small-molecule inhibition of MLL activity by disruption of its interaction with WDR5." Biochemical Journal **449**(1): 151-159.

Shirai, T., R. R. Nazarewicz, B. B. Wallis, R. E. Yanes, R. Watanabe, M. Hilhorst, L. Tian, D. G. Harrison, J. C. Giacomini, T. L. Assimes, J. J. Goronzy and C. M. Weyand (2016). "The glycolytic enzyme PKM2 bridges metabolic and inflammatory dysfunction in coronary artery disease." The Journal of Experimental Medicine **213**(3): 337-354.
Sica, A. and A. Mantovani (2012). "Macrophage plasticity and polarization: in vivo veritas." The Journal of clinical investigation **122**(3): 787-795.
Soares, M. P. and I. Hamza (2016). "Macrophages and Iron Metabolism." Immunity **44**(3): 492-504.
Soldi, M., T. Mari, L. Nicosia, D. Musiani, G. Sigismondo, A. Cuomo, G. Pavesi and T. Bonaldi (2017). "Chromatin proteomics reveals novel combinatorial histone modification signatures that mark distinct subpopulations of macrophage enhancers." Nucleic acids research **45**(21): 12195-12213.
Spellmon, N., J. Holcomb, L. Trescott, N. Sirinupong and Z. Yang (2015). "Structure and function of SET and MYND domain-containing proteins." International journal of molecular sciences **16**(1): 1406-1428.
Stender, J. D., G. Pascual, W. Liu, M. U. Kaikkonen, K. Do, N. J. Spann, M. Boutros, N. Perrimon, M. G. Rosenfeld and C. K. Glass (2012). "Control of proinflammatory gene programs by regulated trimethylation and demethylation of histone H4K20." Molecular cell **48**(1): 28-38.
Sumida, K., Y. Igarashi, N. Toritsuka, T. Matsushita, K. Abe-Tomizawa, M. Aoki, T. Urushidani, H. Yamada and Y. Ohno (2011). "Effects of DMSO on gene expression in human and rat hepatocytes." Human & experimental toxicology **30**(10): 1701-1709.
Tardif, M., #xe9, l. R., J. A. Chapeton-Montes, A. Posvandzic, Pag, #xe9, N. , C. Gilbert and P. A. Tessier (2015). "Secretion of S100A8, S100A9, and S100A12 by Neutrophils Involves Reactive Oxygen Species and Potassium Efflux." Journal of Immunology Research **2015**: 16.
Tardif, M. R., J. A. Chapeton-Montes, A. Posvandzic, N. Pagé, C. Gilbert and P. A. Tessier (2015). "Secretion of S100A8, S100A9, and S100A12 by Neutrophils Involves Reactive Oxygen Species and Potassium Efflux." Journal of immunology research **2015**: 296149-296149.
Tarique, A. A., J. Logan, E. Thomas, P. G. Holt, P. D. Sly and E. Fantino (2015). "Phenotypic, Functional, and Plasticity Features of Classical and Alternatively Activated Human Macrophages." American Journal of Respiratory Cell and Molecular Biology **53**(5): 676-688.
Tesch, G. H. (2010). "Macrophages and Diabetic Nephropathy." Seminars in Nephrology **30**(3): 290-301.
Testa, R., A. R. Bonfigli, F. Prattichizzo, L. La Sala, V. De Nigris and A. Ceriello (2017). "The "Metabolic Memory" Theory and the Early Treatment of Hyperglycemia in Prevention of Diabetic Complications." Nutrients **9**(5): 437.
Thangavel, J., S. Samanta, S. Rajasingh, B. Barani, Y.-T. Xuan, B. Dawn and J. Rajasingh (2015). "Epigenetic modifiers reduce inflammation and modulate macrophage phenotype during endotoxemia-induced acute lung injury." J Cell Sci: jcs. 170258.
The Emerging Risk Factors, C. (2010). "Diabetes mellitus, fasting blood glucose concentration, and risk of vascular disease: a collaborative meta-analysis of 102 prospective studies." The Lancet **375**(9733): 2215-2222.
Torres-Castro, I., Ú. D. Arroyo-Camarena, C. P. Martínez-Reyes, A. Y. Gómez-Arauz, Y. Dueñas-Andrade, J. Hernández-Ruiz, Y. L. Béjar, V. Zaga-Clavellina, J. Morales-Montor and L. I. Terrazas (2016). "Human monocytes and macrophages undergo M1-type inflammatory polarization in response to high levels of glucose." Immunology letters **176**: 81-89.
Tseng, H. H. L., C. T. Vong, Y. W. Kwan, S. M.-Y. Lee and M. P. M. Hoi (2016). "TRPM2 regulates TXNIP-mediated NLRP3 inflammasome activation via interaction with p47 phox under high glucose in human monocytic cells." Scientific Reports **6**: 35016.

Vallerie, S. N. and K. E. Bornfeldt (2015). "Metabolic Flexibility and Dysfunction in Cardiovascular Cells." Arteriosclerosis, Thrombosis, and Vascular Biology **35**(9): e37-e42.
Van Aller, G. S., N. Reynoird, O. Barbash, M. Huddleston, S. Liu, A.-F. Zmoos, P. McDevitt, R. Sinnamon, B. Le and G. Mas (2012). "Smyd3 regulates cancer cell phenotypes and catalyzes histone H4 lysine 5 methylation." Epigenetics **7**(4): 340-343.
van der Wijst, M. G., M. Venkiteswaran, H. Chen, G.-L. Xu, T. Plösch and M. G. Rots (2015). "Local chromatin microenvironment determines DNMT activity: from DNA methyltransferase to DNA demethylase or DNA dehydroxymethylase." Epigenetics **10**(8): 671-676.
van Diepen, J. A., K. Thiem, R. Stienstra, N. P. Riksen, C. J. Tack and M. G. Netea (2016). "Diabetes propels the risk for cardiovascular disease: sweet monocytes becoming aggressive?" Cellular and molecular life sciences : CMLS **73**(24): 4675-4684.
van Nuland, R., A. H. Smits, P. Pallaki, P. W. Jansen, M. Vermeulen and H. M. Timmers (2013). "Quantitative dissection and stoichiometry determination of the human SET1/MLL histone methyltransferase complexes." Molecular and cellular biology **33**(10): 2067-2077.
Van den Bossche, J., J. Baardman, Natasja A. Otto, S. van der Velden, Annette E. Neele, Susan M. van den Berg, R. Luque-Martin, H.-J. Chen, Marieke C. S. Boshuizen, M. Ahmed, Marten A. Hoeksema, Alex F. de Vos and Menno P. J. de Winther (2016). "Mitochondrial Dysfunction Prevents Repolarization of Inflammatory Macrophages." Cell Reports **17**(3): 684-696.
Viemann, D., A. Strey, A. Janning, K. Jurk, K. Klimmek, T. Vogl, K. Hirono, F. Ichida, D. Foell, B. Kehrel, V. Gerke, C. Sorg and J. Roth (2005). "Myeloid-related proteins 8 and 14 induce a specific inflammatory response in human microvascular endothelial cells." Blood **105**(7): 2955-2962.
Vogl, T., A. L. Gharibyan and L. A. Morozova-Roche (2012). "Pro-inflammatory S100A8 and S100A9 proteins: self-assembly into multifunctional native and amyloid complexes." International journal of molecular sciences **13**(3): 2893-2917.
Vogl, T., S. Ludwig, M. Goebeler, A. Strey, I. S. Thorey, R. Reichelt, D. Foell, V. Gerke, M. P. Manitz and W. Nacken (2004). "MRP8 and MRP14 control microtubule reorganization during transendothelial migration of phagocytes." blood **104**(13): 4260-4268.
Wallner, S., C. Schröder, E. Leitão, T. Berulava, C. Haak, D. Beißer, S. Rahmann, A. S. Richter, T. Manke and U. Bönisch (2016). "Epigenetic dynamics of monocyte-to-macrophage differentiation." Epigenetics & Chromatin **9**(1): 33.
Wei, Y., J. Corbalán-Campos, R. Gurung, L. Natarelli, M. Zhu, N. Exner, F. Erhard, F. Greulich, C. Geißler and N. H. Uhlenhaut (2018). "Dicer in Macrophages Prevents Atherosclerosis by Promoting Mitochondrial Oxidative Metabolism." Circulation: CIRCULATIONAHA. 117.031589.
Wyrick, J. J., F. C. P. Holstege, E. G. Jennings, H. C. Causton, D. Shore, M. Grunstein, E. S. Lander and R. A. Young (1999). "Chromosomal landscape of nucleosome-dependent gene expression and silencing in yeast." Nature **402**(6760): 418-421.
Xia, C., Z. Braunstein, A. C. Toomey, J. Zhong and X. Rao (2018). "S100 Proteins As an Important Regulator of Macrophage Inflammation." Frontiers in Immunology **8**(1908).
Xiang, Y., M.-m. Zhao, S. Sun, X.-L. Guo, Q. Wang, S.-A. Li, W.-H. Lee and Y. Zhang (2018). "A high concentration of DMSO activates caspase-1 by increasing the cell membrane permeability of potassium." Cytotechnology **70**(1): 313-320.
Xu, G., G. Liu, S. Xiong, H. Liu, X. Chen and B. Zheng (2015). "The histone methyltransferase Smyd2 is a negative regulator of macrophage activation by suppressing interleukin 6 (IL-6) and tumor necrosis factor α (TNF-α) production." Journal of Biological Chemistry **290**(9): 5414-5423.
Xu, K. and C. L. Geczy (2000). "IFN-γ and TNF Regulate Macrophage Expression of the Chemotactic S100 Protein S100A8." The Journal of Immunology **164**(9): 4916-4923.

Xue, Q., Y. Yan, R. Zhang and H. Xiong (2018). "Regulation of iNOS on Immune Cells and Its Role in Diseases." International journal of molecular sciences **19**(12): 3805.
Yang, J., J. Anholts, U. Kolbe, J. Stegehuis-Kamp, F. Claas and M. Eikmans (2018). "Calcium-Binding Proteins S100A8 and S100A9: Investigation of Their Immune Regulatory Effect in Myeloid Cells." International journal of molecular sciences **19**(7): 1833.
Yang, J., J. Anholts, U. Kolbe, J. A. Stegehuis-Kamp, F. H. J. Claas and M. Eikmans (2018). "Calcium-Binding Proteins S100A8 and S100A9: Investigation of Their Immune Regulatory Effect in Myeloid Cells." International Journal of Molecular Sciences **19**(7): 1833.
Yang, X., X. Wang, D. Liu, L. Yu, B. Xue and H. Shi (2014). "Epigenetic regulation of macrophage polarization by DNA methyltransferase 3b." Molecular endocrinology **28**(4): 565-574.
Yang, X. D., B. Huang, M. Li, A. Lamb, N. L. Kelleher and L. F. Chen (2009). "Negative regulation of NF- κB action by Set9- mediated lysine methylation of the RelA subunit." The EMBO Journal **28**(8): 1055-1066.
Yao, D. and M. Brownlee (2009). "Hyperglycemia-induced reactive oxygen species increase expression of RAGE and RAGE ligands." Diabetes.
Yona, S., K.-W. Kim, Y. Wolf, A. Mildner, D. Varol, M. Breker, D. Strauss-Ayali, S. Viukov, M. Guilliams, A. Misharin, David A. Hume, H. Perlman, B. Malissen, E. Zelzer and S. Jung (2013). "Fate Mapping Reveals Origins and Dynamics of Monocytes and Tissue Macrophages under Homeostasis." Immunity **38**(1): 79-91.
Zheng, Q. F., H. M. Wang, Z. F. Wang, J. Y. Liu, Q. Zhang, L. Zhang, Y. H. Lu, H. You and G. H. Jin (2017). "Reprogramming of histone methylation controls the differentiation of monocytes into macrophages." The FEBS Journal **284**(9): 1309-1323.

7 CURRICULUM VITAE

Name	Dieuwertje Marije Mossel
Date of birth	15.05.1990
Place of birth	Groningen, NL
Nationality	NL

Education:

2016-2019	PhD project: *Mechanism of hyperglycemic control of histone code in metabolic inflammation and microvascular complications* Institute of Transfusion Medicine and Immunology, Heidelberg University, Germany
2011-2014	Master Biomedical Sciences Master research project 1: *Non-homeostatic regulation of energy balance* Centre for Behaviour and Neurosciences Master research project 2: *Adipose Derived Stem Cells for cardiac functional improvement after Myocardial Infarction* Departments of Pathology and Medical Biology, UMCG University of Groningen, Groningen, the Netherlands
2008-2012	Bachelor Life Science and Technology Major Biomedical Sciences Minor theology University of Groningen, Groningen, the Netherlands

Papers published:

Rendra E1, Riabov V2, Mossel DM3, Sevastyanova T2, Harmsen MC4, Kzhyshkowska J5. Reactive oxygen species (ROS) in macrophage activation and function in diabetes. Immunobiology. 2019 Mar;224(2):242-253

8 ACKNOWLEDGEMENTS

I am very grateful to my principal investigators, Prof. Dr. J. Kzhyshkowska (Mannheim) and Prof. Dr. Marco Harmsen (UMCG Groningen, NL) for granting me the opportunity to do my PhD at the University of Heidelberg and for their guidance and supervision through the entire period.

I particularly express my gratitude to Prof. Dr. med. Harald Klüter director of Department of Transfusion Medicine and Immunology for his kindness and professional accessibility.

I greatly value the past and present group members of AG Prof. Dr. J. Kzhyshkowska whom I had the pleasure of working together with; Shuiping Yin, Julia Michel, Dandan Xu, Alexander Gudima and Tatyana Sevastyanova, Vladimir Riabov and Tengfei Liu for their friendship and amazing help in interpretation and analysis of experimental data. I also thank acknowledge Dr. Riabov for proofreading my thesis. Moreover, I thank Dr. Kondaiah Moganti for giving me a great introduction into the project and elaborating this project together. Lastly, I thank Christina Schmuttermaier for technical assistance and caring for group atmosphere.

Likewise, I owe thanks to members of AG Prof. Dr. K. Bieback. Prof. Bieback for her role in the DIAMICOM board as well as advices and support. For Agnese Fiori and Adriana Crigna Torres, it has been a joy to go together through this phase in life and I wish you many blessings and great jobs afterwards. I thank Stefanie Uhlig, and Susanne Evers-Hornung for their technical assistances and generously sharing equipment and resources.

I appreciate Julio Corderes (AG Dobreva) and his wife for inviting me at their home and advice on the analysis of the epigenetic part of the project. Also, I thank Hélène Willer, Erika and Eleonora Scaccia for sharing their office with me and their sunny and attentive presence during the last months writing.

I greatly value Dr. Marianne Rots UMCG, Groningen, NL for giving me the chance to try new techniques in Groningen during the summer of 2017 and sharing her epigenetic expertise. At the same time, I thank Dr. Flemming from the Department of Internal Medicine, University of Heidelberg, Heidelberg, Germany for providing me with patient samples and advise on the flow cytometry experiments.

I acknowledge DFG GRK 1874: “DIAMICOM” together with Prof. Jens Kroll and Prof. Hammes for checking the milestones of the project, for theoretical and methodological advices and organizing the trips.

I am grateful for the friends I made and church family I got in Germany, for their prayers and community. I thank Donald Fonko for his encouragements and for always pointing to Jesus. Most of all, I am thankful for my family for their constant support and encouragement. For being the stable home base and joy in my life.